Stony Brook University

Metal Complexes for Structural Modeling of Active Sites of Metalloenzymes Relevant to Gas Catalysis

A Dissertation Presented

by

Soumya Bhattacharya

to

The Graduate School

in Partial Fulfillment of the

Requirements

for the Degree of

Doctor of Philosophy

in

Chemistry

Stony Brook University

August 2014

Stony Brook University

The Graduate School

Soumya Bhattacharya

We, the dissertation committee for the above candidate for the

Doctor of Philosophy degree, hereby recommend

acceptance of this dissertation.

Stephen A. Koch – Dissertation Advisor
Professor, Chemistry

Joseph W. Lauher - Chairperson of Defense
Professor, Chemistry

Andreas Mayr – Third Member
Professor, Chemistry

Jianfeng Jiang – Outside Member
Associate Professor of Chemistry, Yeshiva University

This dissertation is accepted by the Graduate School

Charles Taber
Dean of the Graduate School

Abstract of the Dissertation

Metal Complexes for Structural Modeling of Active Sites of Metalloenzymes Relevant to Gas Catalysis

by

Soumya Bhattacharya

Doctor of Philosophy

in

Chemistry

Stony Brook University

2014

Sulfur rich metal coordinated active sites is a prominent feature of many metalloenzymes (hydrogenase, nitrogenase, carbon monoxide dehydrogenase) involved in catalytically producing and/or absorbing helpful and/or toxic gases. As the mechanism of gas production and/or absorption heavily depends on the structural intricacies, biomimetic modelling of the active sites is of paramount importance to understand the structure–function relationship. It has been established that the small molecule models with steric bulk of the thiols at the *ortho*- position of dreivatized benzenethiols can provide the stability.

Millar and Koch were pioneers in introducing a series of *ortho*-steric benzene thiols and achieving stabilization of high oxidation state first row transition metal complexes. Fe^{3+} & Co^{3+} complexes and Fe_4S_4 tertamer with 2,4,6-triisopropyl-benzenethiol are the highlights. Following the idea of increasing the steric bulk, this thesis will present a new compound - 2,4,6-

tricyclohexylbenzenethiol, and attempted synthesis and characterization of monomeric and tetrameric metal complexes with it.

Dithiols such as ethanedithiol (edt) and 1,2-benzenedithiol (bdt) have been extensively used for synthesizing models due to their simplicity in structure. While edt lacks the required steric bulk, bdt is a non-innocent ligand influencing electrochemical properties of the complexes. To combat these difficulties, a new class of dithiol was introduced by Michelle Millar and Stephen Koch – norbornanedithiol - a conformationally fixed alkane dithiol. Metal complexes with Fe^{2+}, Co^{2+}, Ni^{2+} & Pt^{2+} will be discussed. Hydrogen bonding of the solvent molecules to the thiolates and the implications of such observation will be presented.

Fe-Ni hydrogenases are responsible for converting H_2 gas to H^+. This class of enzyme contains a bimetallic active site. In our effort to mimic the structure, we have crystallographically characterized Fe-Ni bimetallic compounds with bridged thiolates and intermetallic distance of ~3Å as found in the wild type from *Desulfovibrio gigas*. An extensive IR study of the reaction and the compounds will be presented.

Dedicated to

Parents

Late Mrs. Swapna Bhattacharya (Mother)

&

Mr. Sukumar Bhattacharya (Father)

Table of Contents

List of Figures

List of Tables

List of Schemes

Acknowledgments

A Ph.D. degree is a significant milestone in the career of an individual. The effort that goes into such an endeavor is rarely accomplished without the sustenance of few supporting figures around one.

First and foremost, I would like to take this opportunity to express my gratitude to my mentor – Prof. Millar – a scientist par excellence and a truly inspirational personality. It is an unforeseen tragedy that I lost her during the course of my Ph.D. dissertation period.

My heartfelt thanks goes to Prof. Stephen A. Koch, who graciously accepted me in his research group and help me realize my dream of receiving a Ph.D. degree. Words will never be enough to express my appreciation for his mentorship. A big recognition goes to my committee members – Prof. Joseph Lauher (Chairperson), Prof. Frank Fowler (3rd member), Prof. Andreas Mayr (3rd member substitute) and Dr. Jianfeng Jiang (Outside member) – for their professional help and encouragement. I would like to thank Prof. Lauher especially for his mentorship in my teaching assignments.

The research group members of the Millar & Koch groups – Dr. Daniel Amarante, Dr. Lu Gan, Su'aad Zaman, David Spritzer, Anthony Pesiri – have not only been coworkers but friends as well. The scientific discussions or the philosophical debates we had are all a part of a treasured memory. Just want to let you know that you guys made the best work environment in the laboratory one can hope for.

My friends at Stony Brook University and beyond are all been a great support throughout this period of ups and downs. I would like to specially mention Neeraj, Shivam, Tanaya, Ashish, Divya, Kunal, Alok, Vishal. You guys were just awesome.

Family is always the greatest support one can get in any stage of or situation in life. My family has always been there for me through the thick and thin of this arduous journey. My mother – Late Mrs. Swapna Bhattacharya – has always inspired me in science being a physics major herself. She has and will always be my first and foremost mentor in science. It is my great misfortune that I she could not see me receiving my Ph.D. My father – Mr. Sukumar Bhattacharya – is my greatest teacher in discipline and perseverance. No words can express my gratitude my first and best friend – my brother Sattam. You are the best brother one can ever get. Your care and support is truly appreciated. The new members of my family – my sister-in-law Nabamita & my cute, little nephew Shlok – are just the perfect addition to the family.

Last but not the least, I want to thank the Almighty, who blessed me with no bounds.

Date: 28th July 2014 **Soumya Bhattacharya**

Chapter 1:

Structural Modelling of Iron – Nickel Hydrogenase Enzyme

1.1 Introduction

1.1.1 General Background

Hydrogen gas (H_2) is often termed as "the fuel of the future". The actual realization of this concept relies heavily on how much progress can be made regarding generation, storage and transportation of H_2. Small-scale hydrogen utilization is pretty advanced, but not realistic. In fuel cells, H_2 can be effectively used but the use of platinum group metals as catalysts severely hinders mass application.

Electrochemically viewed, the two electron reduction potential for proton at neutral pH (pH = 7) and natural abundance of H_2 ($p_{H_2} = 10^{-7}$atm) is approximately −208 mV. If there is a higher partial pressure of H_2 (1 atm), the value decreases further (−414 mV). Among the natural systems, cytochrome C_3 (−290 mV) and NAD^+/NAD (−320 mV) are in the range to utilize the hydrogen for substrate reduction.[1] Hydrogenase enzymes bring to us the strong reducing power of H_2 by harnessing it in kinetically useful ways for the reduction of various substrates. There are three major classes of the hydrogenases (Figure 1.1): (a) [NiFe] hydrogenases – majorly a catalyst for uptake of $H_2(g)$; (b) [FeFe] hydrogenases – involved in catalysis of $H_2(g)$ production from protons; (c) [Fe] hydrogenases- utilizes $H_2(g)$ to reduce $CO_2(g)$ to $CH_4(g)$.[2,3]

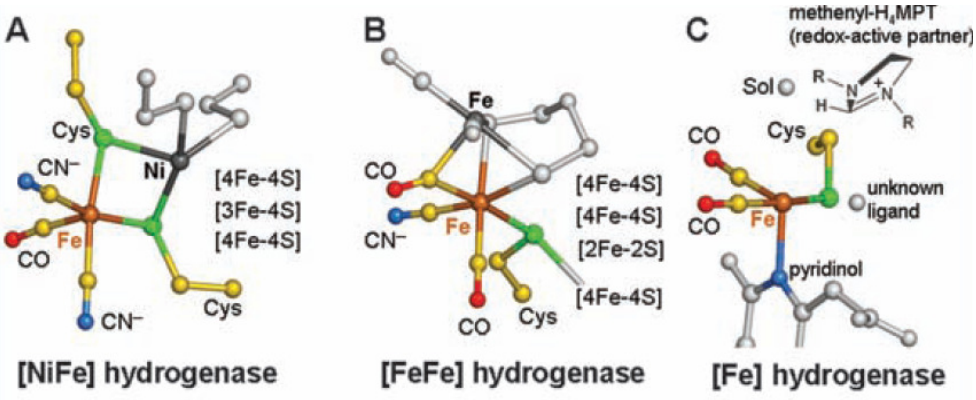

Figure 1.1: Different type of Hydrogenases[4]

Hydrogenases are the class of enzymes that catalyze the simplest reversible reaction of formation and consumption of dihydrogen (Eq. 1.1). So, the hydrogenases can either act as catalysts to produce H_2 gas by acting as 'electron sinks' or have the power to form protons from gaseous H_2.

$$2H^+ + 2e^- \rightleftharpoons H_2(g) \qquad \textbf{(Eq. 1.1)}$$

These enzymes are also capable of converting *para* hydrogen (anti-parallel nuclear spins) to *ortho* hydrogens (parallel nuclear spins) (Eq. 1.2). H_{a+} and H_{b+} come from H_2 and H_2O respectively.

$$\text{Hydrogenase} + H_2\,(\uparrow\downarrow) + H_{b+} \longrightarrow \text{Hydrogenase} + H_2\,(\uparrow\uparrow) + H_{a+} \qquad \textbf{(Eq. 1.2)}$$

On the other hand, in D_2O medium, such a conversion was not observed but the production of HD exceeded that of D_2 (Eq. 1.3). This fact points towards heterolytic splitting of the H_2 molecule into hydron (H^+) and hydride (H^-) (Eq. 1.4). Two sequential pathways (Eq. 1.5 – 1.8) are possible for increased production of HD(*g*) than $D_2(g)$.[5]

$$D^+ + D^- \longrightarrow D_2(g) \qquad \textbf{(Eq. 1.3)}$$

$$H_2(g) \longrightarrow H^+ + H^- \qquad \textbf{(Eq. 1.4)}$$

Pathway I

$H^+ + D_2O(\ell) \longrightarrow HOD(\ell) + D^+$ **(Eq. 1.5)**

$D^+ + H^- \longrightarrow HD(g)$ **(Eq. 1.6)**

Pathway II

$H^- + D_2O(\ell) \longrightarrow HOD(\ell) + D^-$ **(Eq. 1.7)**

$D^- + H^+ \longrightarrow HD(g)$ **(Eq. 1.8)**

H_2 is not only being seen as the fuel of the future but at present, it is one of the most important commercial chemicals to be used by various industries. The different processes requiring H_2 are catalytic hydrogenation in the chemical industries, treatment of crude oil to remove sulfur (dehydrosulfurizaton) and nitrogen (hydrodenitrogenation), and use in Haber's process to produce ammonia for fertilizer industries.[6] Not only is H_2 essential for the chemical industries, it is also a very important component of the prokaryotic organisms found in aquatic system, both under and away from sunlight – biological consumption/production of H_2 (Figure 1.2). The propensities of hydrogen to get oxidized increases as the reactions take place under anaerobic condition away from sunlight.[3]

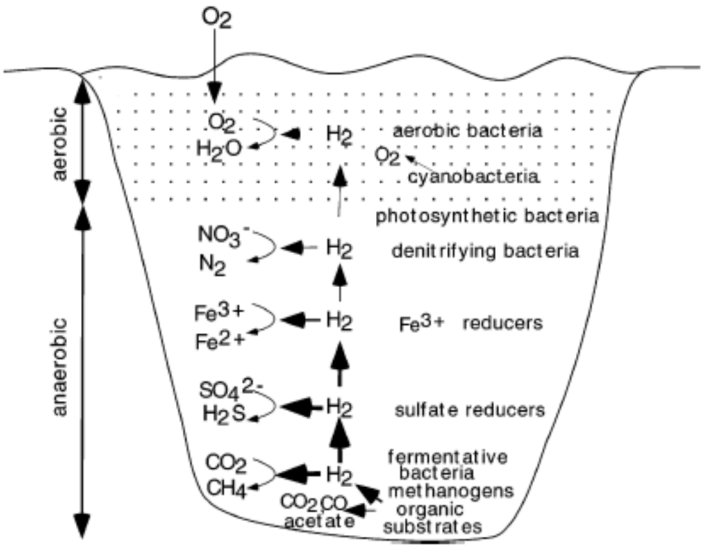

Figure 1.2: Biological consumption/production of H_2[3]

Structural characterization of the hydrogenases from several species (*Desulfovibrio gigas*, *Desulfomicrobium bactalum*, *Desulfovibrio vulgaris*, *Desulfovibrio desulfurican*, *Clostridium pasteurianum*) shows that the common unit of all of them is $Fe(CO)_x$. It is

believed to be central to the biological hydrogen catalysis. In most of the cases where the enzyme structure has been crystallographically determined, it can be seen that the active sites are almost always buried deep inside the polypeptide backbone of the metalloenzyme. This alludes to the fact that different pathways/channels exist for both electron and gas transfer between the surface of the enzyme and the active site. Also, the effect of small molecules such as O_2, CO, NO are of great concern when biomimetic H_2 production is in question.[2]

Another noteworthy structural feature of the hydrogenases is the presence of CN^- ligands on the Fe-center. Experimentally it has been proved that CO ligands do not bind to Fe(II) centers when weak-field N-donor ligands (α-diimines) are attached. But CO binding is very facile when strong-field P-donor ligands (diphosphines) are coordinating ligands on Fe(II). In the hydrogenases enzymes, the Fe(II) centers purposefully binds strongly to CO ligands. Hence, these centers need to maintain a hyperfine balance between electrophilic character to bind CO and heterolytically cleave H_2. CN^- ligands are known to be one of the most strong-field ligands that can assist in maintaining the low-spin configuration of Fe(II) redox state through the entire catalytic cycle involving ligation changes for the proper functioning of the enzyme. Another reason for employing such a strong-field ligand could be to lower the electrochemical potential for H_2 production.[6]

With the exception of the formerly iron-free hydrogenase or Hmd, both [NiFe]- and [FeFe]-hydrogenases have bimetallic active sites. These are very flexible, both in terms of stereochemistry and reactivity. The metal-metal bonds (when interatomic distance < 3.0 Å) have been proved basic enough to be protonated. The ligands connected to the active site; CO, H^- (hydride), ^-SR (thiolate); can alternate between being bridging and terminal

while retaining the binuclearity. The *trans* configuration of CO and H_2 (bridging mode) could favor the heterolysis of the latter. This is important in relevance to [NiFe]-hydrogenases or the uptake hydrogenases.[6]

Subsequent to the structural characterization of the [NiFe] hydrogenase from *Desulfovibrio gigas*, [FeFe] hydrogenase from *Clostridium pasteurianum* and [Fe]only hydrogenase from some hydrogenotrophic archaea, hosts of biomimetic models were synthesized. Also, H^+/H_2 reduction/uptake studies were performed with them to determine the kinetics of reaction and mechanism of the reversibility.

1.1.2 [NiFe]-Hydrogenase Structural Models

Since the discovery of [NiFe]-hydrogenases[7], spectroscopic evidences suggested various structures for the enzyme active site.[8,9] X-ray crystallography of the active site extracted from bacteria *Desulfovibrio*(*D.*) *gigas* indicated the presence of Ni-atom in a distorted square-planar tetrathiolate (cysteine thiolates) environment alongside another unknown metal component, which was determined to be Fe-atom based on EXAFS studies.[10,11] A more recent X-ray study confirms the presence of Fe-atom with two CN^- and one CO ligands in a μ_2-S(cysteine) bridging environment alongside Ni-atoms (Figure 1.3).[12] The CN^- ligands are in a *cis*- fashion. The unknown metal component has been predicted to be oxygen based radical or radical anion ligands (^-OH, ^-OOH, O^{2-}).

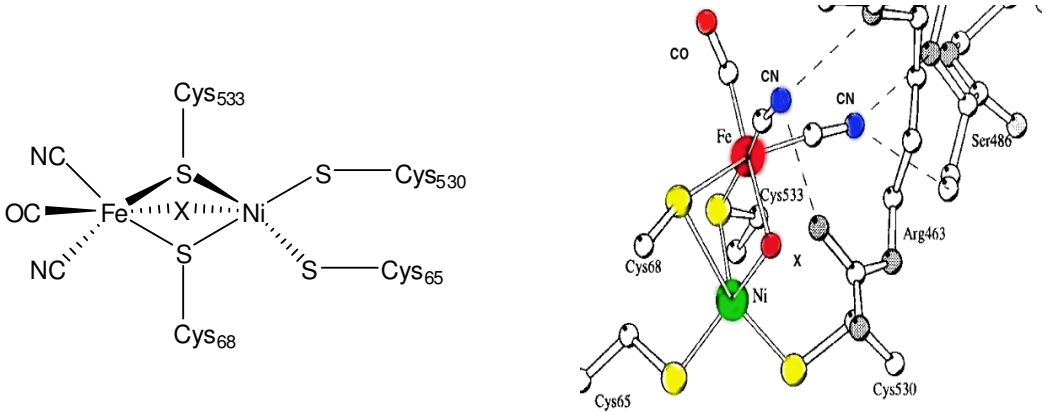

Figure 1.3: Structure of the Active Site of [NiFe]-Hydrogenase[12,13]

To understand the mechanism of dihydrogen uptake and subsequent steps of electron transfer reaction, structural modeling of the active site of [NiFe]-hydrogenase has gained considerable momentum in the recent years. Structural models addressing only the Fe^{II}-center with CO/CN- ligands or the Ni^{II}-center with dithiolate environment with N and/or P ligands are plenty. Some robust models involving dimeric compounds are also available. Upon investigation of the catalytic cycle, Ni^{III}-center was discovered. To achieve the unusual oxidation state, electron-rich ligands such as thiolates with thioethers or amines or amides were used. The primary synthetic challenge was the bonding of two different metal centers, namely iron and nickel. The difficulty was overcome by using amine-thiolate[14-16] or thiolether-thiolate[17-19] ligands. The amine (Figure 1.4A) or the thioether (Figure 1.4B) groups are often separated from the thiol groups in the compound by a chain of two C-atoms. These structural models have shown the Fe^{II}-Ni^{II} intermetallic distance to be close to 3 Å leading to metal-metal interaction, which is also supported by magnetic susceptibility and cyclic voltammetry studies.[20] Another class of structural models included diphenylphosphoethane (dppe) ligands on the Ni-atom or both Ni- and Fe-atoms (Figure 1.4C).[16,19] Predominantly, the unready states of the Fe^{II}-Ni^{II} dimer, involved in the catalysis, have been structurally characterized by chemical synthesis.[9,16,19,20]

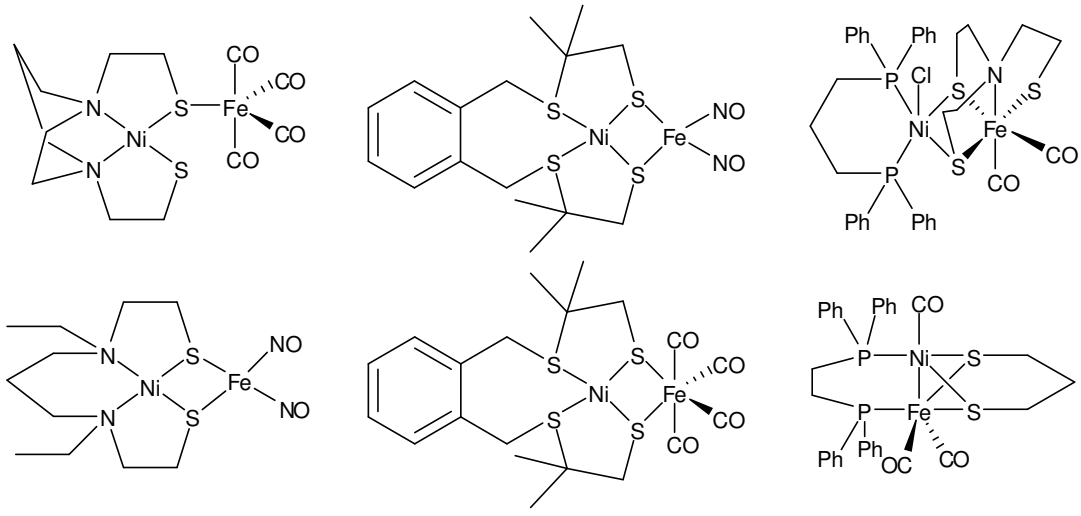

Figure 1.4: Structural models with (A) amine thiolate ligands[14,21] (B) thioether and thiolate ligands[17], (C) with dppe ligands[22]

Models with Ni-atom with four S-atoms coordinated to it and Fe-atom with both CO and CN^- ligands have been reported but the compounds were anionic (Figure 1.5A).[23] The neutral compound, with the Fe^{II}-center with both the CN^- and CO ligands, has the Ni^{II}-atom in an environment of two S- and two P-atoms (Figure 1.5B).[24]

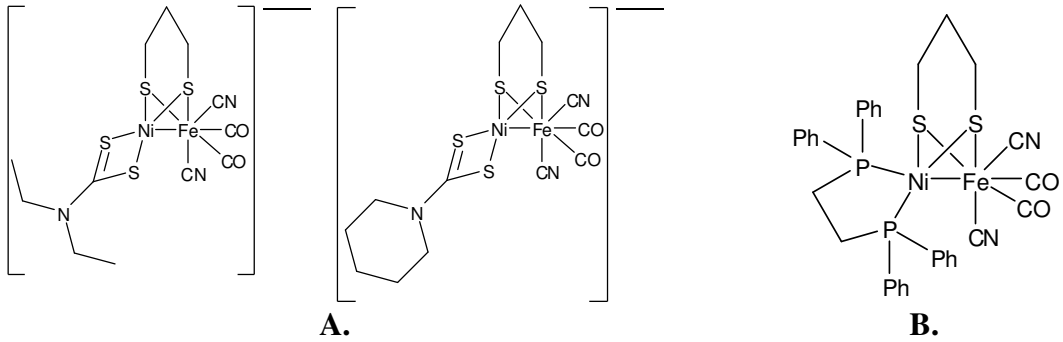

Figure 1.5: (A) Anionic models with Ni^{II}-atom having four S-atoms and $[Fe^{II}(CO)_2(CN)_2]$ center[23] and (B) Neutral model with dppe and $[Fe^{II}(CO)_2(CN)_2]$ center[24]

1.2 Aim of the Project

In this work, ligands with amine or amide or thioether and thiol groups separated by two C-atoms and the Fe-precursor with both CO and CN^- ligands were employed (Figure 1.6).

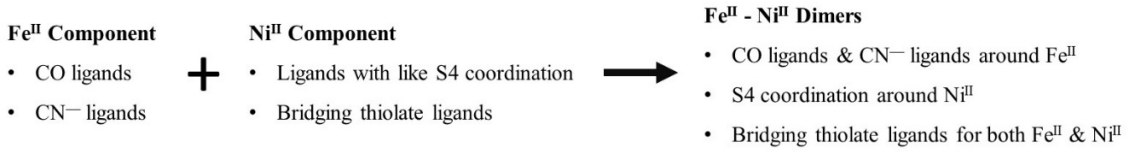

Figure 1.6: General Scheme of Synthetic Approach to Fe^{II}-Ni^{II} Dimers

1.3 Experimental

1.3.1 General Remarks

All the manipulations were carried out under nitrogen unless and otherwise noted. Solvents were distilled according to literature procedures [diethyl ether (Et_2O) over Na/benzophenone, dichloromethane (CH_2Cl_2) over P_2O_5, methanol (CH_3OH) over Mg/I_2], and stored under nitrogen. Dimethylformamide (DMF), potassium cyanide (KCN), tetraethylammonium cyanide (Et_4NCN), chloroethanol, sodium hydroxide (NaOH), N^1,N^3-diethylpropane-1,3-diamine, 1,4-diazepane, thiirane, methyl thioglycolate (Sigma Aldrich) were used as received without further purification. $H_2(S4)$[25], $H_2(N2S2)$[26], $H_2(N2S2')$[27], $H_2(N2S2O2)$[28], $Ni^{II}(S4)$[15], $Ni^{II}(N2S2)$[15], $Ni^{II}(N2S2')$[15], $Ni^{II}(N2S2O2)$[28], $Fe^{II}(CO)_4I_2$[24] and $K[Fe^{II}(CO)_3(CN)_2I]$[24] were synthesized according to published methods. ^1H & ^{13}C NMR spectra were recorded on a Brüker 300 MHz instrument in $CDCl_3$ and standardized with residual solvent peak at 7.26 ppm and 77.23 ppm respectively. IR spectra were collected on a Thermo Fisher Scientific Nicolet iS10 using CaF_2 cell with 1.0 mm pathlength. Wherever applicable, X-ray quality crystals were grown from suitable solvents using appropriate techniques.

1.3.2 Synthesis of $Fe^{II}(CO)_4I_2$

The compound was synthesized according to literature procedure.[24] A solution of I_2 (25.99 g, 0.102 moles) in 60 mL of dry diethyl ether was added dropwise into a solution of $Fe^0(CO)_5$ (20.86 g, 0.106 moles) in 30 mL of dry diethyl ether at 0°C during 30 minutes After addition of iodine reaction mixture was stirred for another 3 h at 0°C and the solvent was removed by rotary–evaporation. The solid red-brown product was dried under vacuum

for 20 minutes and stored at –20°C. Yield 40.3 g, 94%. IR (hexane) ν_{CO} = 2062, 2085 and 2130 cm^{-1}.

1.3.3 Synthesis of *fac*–K[$Fe^{II}(CN)_2(CO)_3I$]

The compound was synthesized according to literature procedure.[24] All the manipulations were performed in air and in absence of light. To a solution of $Fe^{II}(CO)_4I_2$ (5 g, 0.012 moles) in 100 mL of methanol was added KCN (1.72 g, 0.0264 moles). The mixture was stirred overnight at room temperature. A black precipitate was filtered off and the solvent was removed using a rotary evaporator resulting in a dark red solid, which was dissolved in minimum amount of absolute ethanol (~20 mL). The suspension was centrifuged for ten minutes to remove any potassium iodide. The dark red solution was decanted and the solvent was removed *in vacuo*. IR (CH_3OH) ν_{CO} = 2064 and 2103 cm^{-1}; ν_{CN} = 2145 and 2133 cm^{-1}.

1.3.4 Synthesis of *trans*,*cis*–[$(CN)_2(CO)_2Fe^{II}$][$Ni^{II}(S4)$]

To a stirred solution of K[$Fe^{II}(CN)_2(CO)_3I$] (79 mg, 0.222 mmol) in 50 mL of methanol was added Ni^{II}(S4) (63 mg, 0.222 mmol) in the dark. The mixture was allowed to stir for three hours. A light yellow precipitate was observed and was filtered off using a closed frit packed with celite. The solvent was removed *in vacuo*. The resulting dark red product was purified with minimum amount of CH_2Cl_2 and stirred for two hours. The suspension was filtered using a closed frit packed with celite. The solvent was removed to afford a dark red–brown solid. Yield: 85 mg, 54%. Crystals were grown by vapor diffusion using CH_2Cl_2/Et_2O at –20°C. IR (CH_2Cl_2): ν_{CO} = 2057 and 2011 cm^{-1}; ν_{CN} = 2119 and 2099 cm^{-1}.

1.3.5 Synthesis of *trans*,*cis*-[$(CN)_2(CO)_2Fe^{II}$][Ni^{II}(N2S2)]

To a stirred solution of K[$Fe^{II}(CN)_2(CO)_3I$] (79 mg, 0.222 mmol) in 50 mL of methanol was added Ni^{II}(N2S2) (64 mg, 0.222 mmol) in the dark. The mixture was allowed to stir for overnight. The filtrate was removed *in vacuo* resulting in a dark red product, which was extracted with minimum amount of CH_2Cl_2. Layering the solution with Et_2O afforded a dark red–brown solid. Yield: 61 mg, 74%. Crystals were grown by vapor diffusion using CH_2Cl_2/Et_2O at –20°C. IR (CH_2Cl_2): ν_{CO} = 2052 and 2005 cm^{-1}; ν_{CN} = 2115 and 2112 cm^{-1}.

1.3.6 Synthesis of *trans*,*cis*-[$(CN)_2(CO)_2Fe^{II}$][Ni^{II}(N2S2')]

To a stirred solution of K[$Fe^{II}(CN)_2(CO)_3I$] (100 mg, 0.281 mmol) in 50 mL of methanol was added Ni^{II}(N2S2') (62 mg, 0.222 mmol) in the dark. The mixture was allowed to reflux for overnight. The filtrate was removed *in vacuo* resulting in a dark red product, which was extracted with minimum amount of CH_2Cl_2. Layering the solution with Et_2O afforded a dark red–brown solid. Yield: 63 mg, 60%. IR (CH_2Cl_2): ν_{CO} = 2007 and 2055 cm^{-1}; ν_{CN} = 2100 and 2118 cm^{-1}.

1.3.7 Synthesis of *trans*,*cis*-[$(CN)_2(CO)_2Fe^{II}$][Ni^{II}(N2S2O2)]

To a stirred solution of K[$Fe^{II}(CN)_2(CO)_3I$] (179 mg, 0.5 mmol) in 50 mL of methanol was added Ni^{II}(N2S2O2) (203 mg, 0.5 mmol) in the dark. The mixture was allowed to reflux for overnight. The filtrate was removed *in vacuo* resulting in a dark red product, which was extracted with minimum amount of CH_2Cl_2. Layering the solution with Et_2O afforded a dark red–brown solid. Yield: 110 mg, 32%. IR (CH_2Cl_2): ν_{CO} = 1976 and 2021 (2033 sh) cm^{-1}; ν_{CN} = 2093 and 2117 (sh) cm^{-1}.

1.3.8 X-Ray Crystallography

A red–brown plate crystal measuring $0.40 \times 0.20 \times 0.10$ mm^3 was mounted using a nylon loop and centered on the X–ray beam at 100 K. Crystals were grown by vapor diffusion of methylene chloride and diethyl ether at –20^{o}C. Crystals were grown within one week. The data reduction was done using CryAlisPro and the structure refinement was done with SHELXL–97 (Sheldrick)[29]. All the non–hydrogen atoms were located by Direct Methods and were refined anisotopically by a full–matrix least–squares method. The positions of the remaining hydrogen atoms were calculated.

1.4 Results and Discussion

1.4.1 Synthesis of the Metal Complexes

The redox reaction between $Fe^0(CO)_5$ and I_2 was performed under anaerobic conditions in a solution of diethyl ether (Scheme 1.1). The desired product $[Fe^{II}(CO)_4I_2]$ was stored at –20°C; however, the compound is stable at room temperature for a long period of time. $Fe^{II}(CO)_4I_2$, has been shown to polymerize at room temperature under long exposure to air where the iodide act as bridging ligands.[30] Synthesis of *fac*–$[Fe^{II}(CN)_2(CO)_3I]^-$ was performed in the dark under aerobic conditions (Scheme 1.1). A black precipitate, which may be a polymer, was observed and filtered to result in a dark red solution. The side product, potassium iodide, can be removed by treatment with ethanol and subsequent centrifugation of the mixture. Removing the solvent of the supernatant *in vacuo* gives a red–orange solid, which is potassium salt of *fac*–$[Fe^{II}(CN)_2(CO)_3I]^-$. The product is thermodynamically or photochemically unstable and so stored at –20°C. The black precipitate formed in the synthesis of the potassium salt of *fac*–$[Fe^{II}(CN)_2(CO)_3I]^-$ is insoluble in a wide range of solvents including strong acids or strong bases. This leads to the assumption that the product is polymeric in nature. The thiol ligands (Scheme 1.2) Ni^{II}-precursors (Scheme 1.3) were synthesized according to literature procedures and the yields were comparable. Ni^{II}(S4) and Ni^{II}(N2S2O2) are air-sensitive compounds whereas, Ni^{II}(N2S2) and Ni^{II}(N2S2') can be stored under air. None of the compounds are heat or light sensitive. ^{1}H NMR and UV-Vis spectroscopic techniques were employed to check purity of the compounds, as described in the literature.[27,28,31]

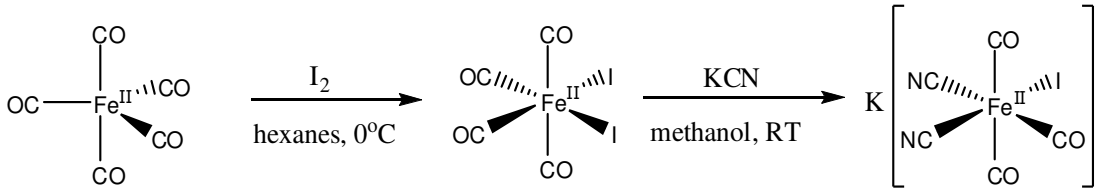

$Fe^0(CO)_5$ $Fe^{II}(CO)_4I_2$ $K[Fe^{II}(CO)_3(CN)_2I]$

Scheme 1.1: Synthesis of Precursor Fe^{II}-Compounds[24,30]

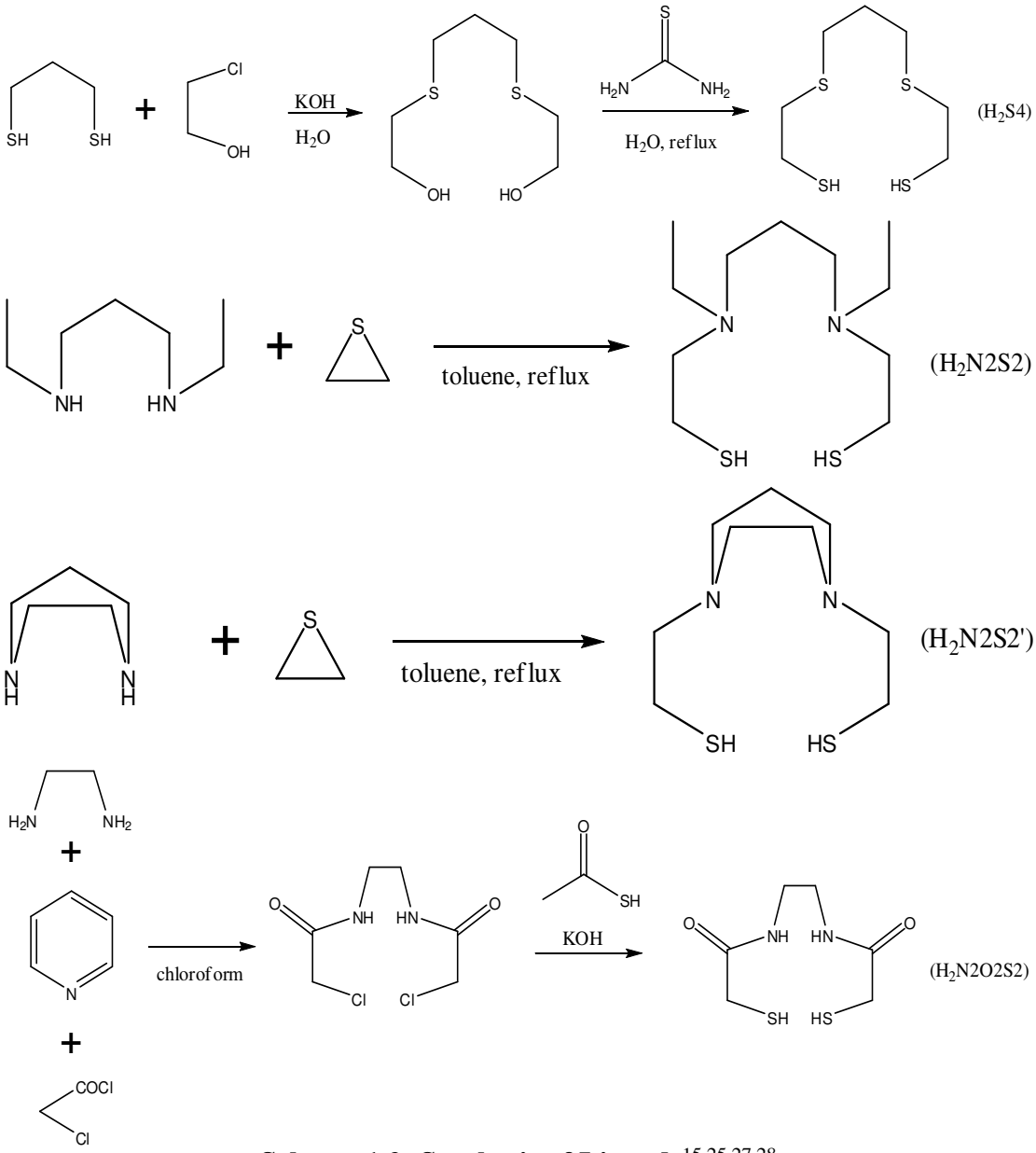

Scheme 1.2: Synthesis of Ligands[15,25,27,28]

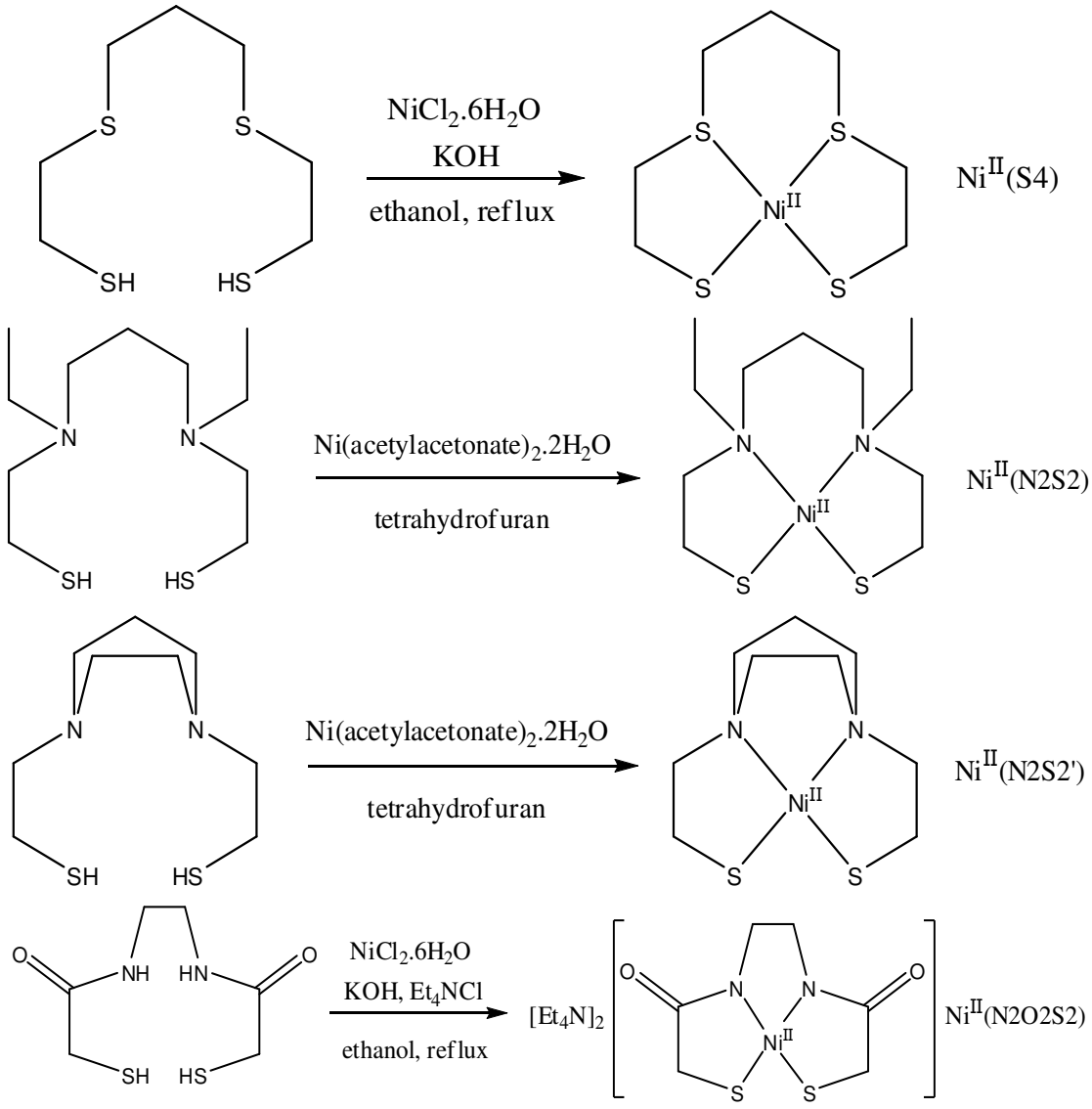

Scheme 1.3: Synthesis of Precursor Ni^{II}-Complexes[15,28]

Equivalent amounts of both the metal precursors in a suitable solvent under dark and anaerobic conditions were reacted to synthesize the Fe^{II} – Ni^{II} dimers. For more sterically encumbered aminothiols, reflux temperature was required (Scheme 1.4). The solubility of the Fe^{II} – Ni^{II} dimers in CH_2Cl_2 facilitates easy separation of the product from the starting material and by-product (KI) of the reaction. The iodide ligand is an excellent leaving group. The thiolate ligands, coupled with their bridging tendencies, were very good rational choice for displacing the iodide ligand; thus forming the bimetallic compounds.

The exact nature of the methylene chloride insoluble product from the reaction of $Ni^{II}S4$ compound is yet to be ascertained, but a thorough solubility test over a vast range of solvents (methanol, ethanol, isopropanol, diethyl ether, tetrahydrofuran, dioxan, acetonitrile, chloroform, dimethylsulfoxide, dimethylformamide) under both room temperature and refluxing conditions indicate polymeric property. Under reflux condition in dimethylsulfoxide and dimethylformamide the residue dissolved with a change in color from orange-yellow to deep red, presumably undergoing decomposition or solvolysis. The reason for the formation of polymers can be attributed to the bridging capability of the thiolate ligands. With Ni-atom in a tetra-sulfur environment like $[Ni(edt)_2]^{2-}$ (edt = ethanedithiolate), polymerization is facilitated due to lack of any steric factor.[32-36] With Ni^{II}(N2S2), Ni^{II}(N2S2'), Ni^{II}(N2S2O2) as the starting compounds, no polymeric products were observed. All the dimeric compounds were recrystallized by layering methylene chloride solutions with almost non-polar diethyl ether. With the exception of the dimer from Ni^{II}(N2S2O2), all the other compounds were neutral. All the reactions were monitored by IR spectra to ascertain completion.

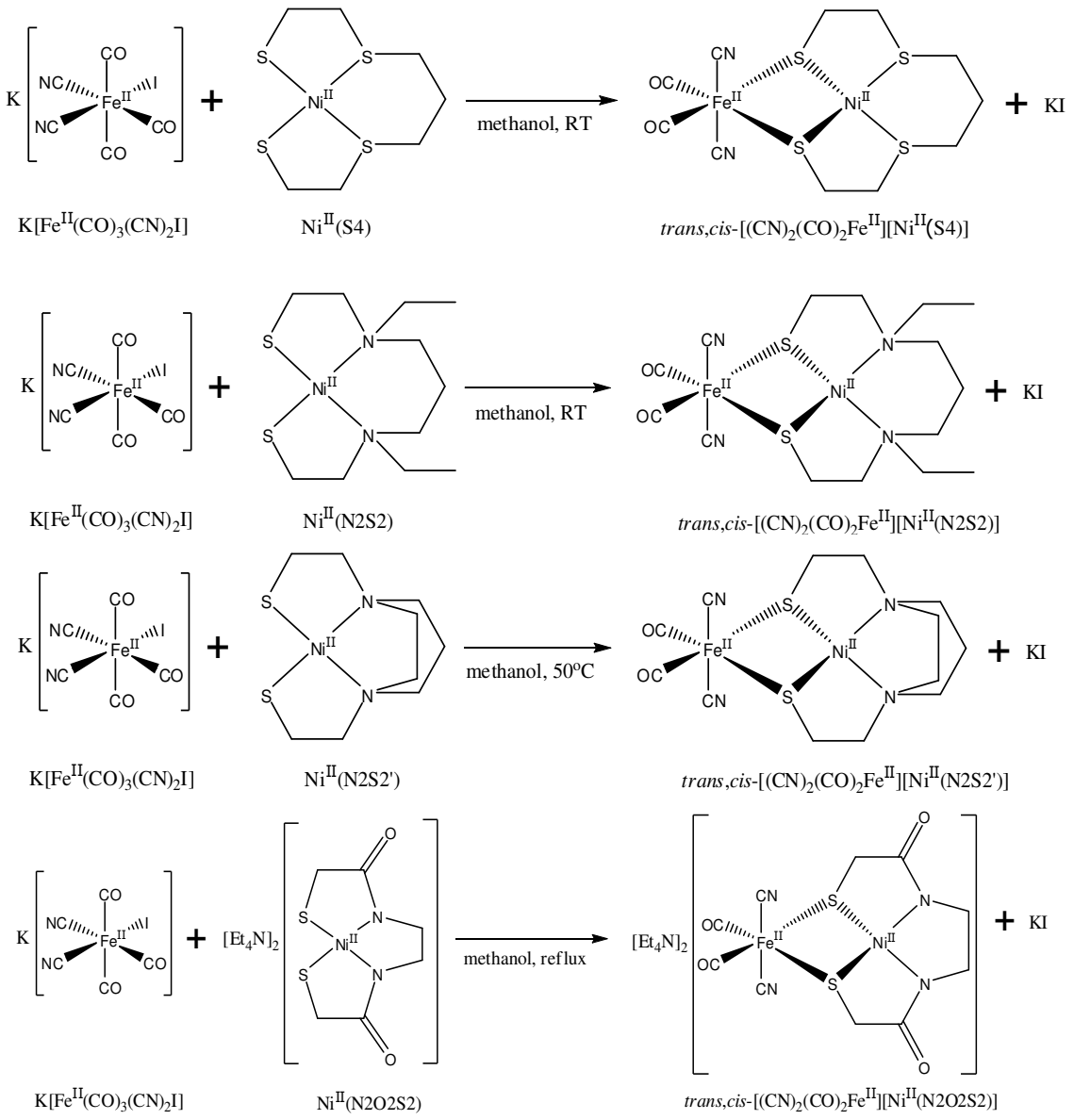

Scheme 1.4: Synthesis of Fe^{II} – Ni^{II} Dimers (1-1 – 1-4)

1.4.2 IR Study of the Metal Complexes

The peaks at 2090 cm^{-1} and 2071 cm^{-1} for $Fe^{II}(CO)_4I_2$ correspond to a *cis*-arrangement of two CO ligands on the Fe^{II}-center. The *trans*-effect of a σ-donor, such as the iodide ligands, is responsible for the peak positions of the two *cis*-CO ligands. The peak at 2136 cm^{-1} corresponds to *trans*- arrangement of two CO ligands on the Fe^{II}-center for the $Fe(CO)_4I_2$. The sharp peak at 2103 cm^{-1} and a broad peak at 2066 cm^{-1} with a shoulder

correspond to a facial arrangement of CO ligands on the Fe^{II}-center in the potassium salt of *fac*–$[Fe^{II}(CN)_2(CO)_3I]^-$. The peaks at 2133 and 2145 cm^{-1} are due to the presence of the two *cis*-CN^- ligands on the Fe^{II}-center (Figure 1.7).[24,37-39]

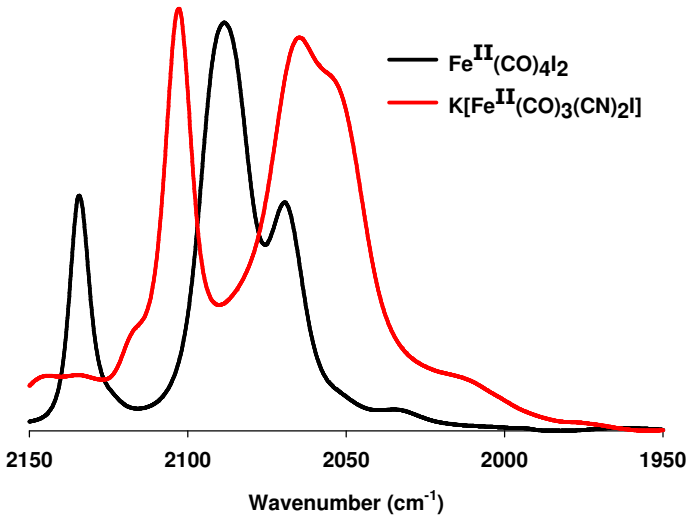

Figure 1.7: IR spectra of the Fe^{II}-precursors[24]

The IR spectra of the Fe^{II} – Ni^{II} dimers in methylene chloride (Figure 1.8) show two CO ligand peaks in the region between 1950 and 2080 cm^{-1}, indicating that the ligands are in a *cis*- orientation. The two peaks in the region between 2100 cm^{-1} and 2150 cm^{-1} were assigned as the CN^- peaks, pointing that the cyanides could also be in the *cis*-orientation, which was proved wrong by x-ray studies. (Table 1.1) The loss of the *fac* carbonyl peaks in the IR spectrum shows a loss of one CO ligand. The two sharp peaks corresponding to the CO region for the same ligands on the Fe^{II}-atom in each of the Fe^{II}-Ni^{II} dimers show that they are in a *cis*- fashion. The carbonyl peaks are red shifted from the *fac*–$[Fe^{II}(CN)_2(CO)_3I]^-$ spectrum due to the presence of the sulfur on the dithiolate ligands. Thiolates are better σ–donors than iodide and CO, which results in increase in electron density on the metal. The effect is strengthening of the π–backbonding with the

carbonyl but weakening of the C≡O bond strength. Comparing to the IR of the native enzyme (*D. gigas*) in its unready state[26,40,41], the Fe^{II}-Ni^{II} dimers show the CO peaks in the same region. For *trans*,*cis*-$[Et_4N]_2[(CO)_2(CN)_2Fe^{II}][Ni^{II}N2O2S2]$ the CO peaks suffer further red-shift, as compared to $Ni^{II}S4$, $Ni^{II}N2S2$ and $Ni^{II}N2S2'$, because the Ni^{II}-center carries a net negative charge. This increases electron density on Fe^{II} center causing an increase in π-donating effect to the 2π* orbitals of the CO resulting in red shift of CO peaks. For all of the Fe^{II}-Ni^{II} dimers, there are two CN^- peaks in the region 2100 – 2125 cm^{-1} indicating an inequivalency of the two CN^- ligands on the Fe^{II}-center in the dimer. X-ray structure of *trans*,*cis*-$[(CN)_2(CO)_2Fe^{II}][Ni^{II}(N2S2)]$ reveals the two ligands to be in different chemical environment leading to two peak intensities in the IR spectrum.[40]

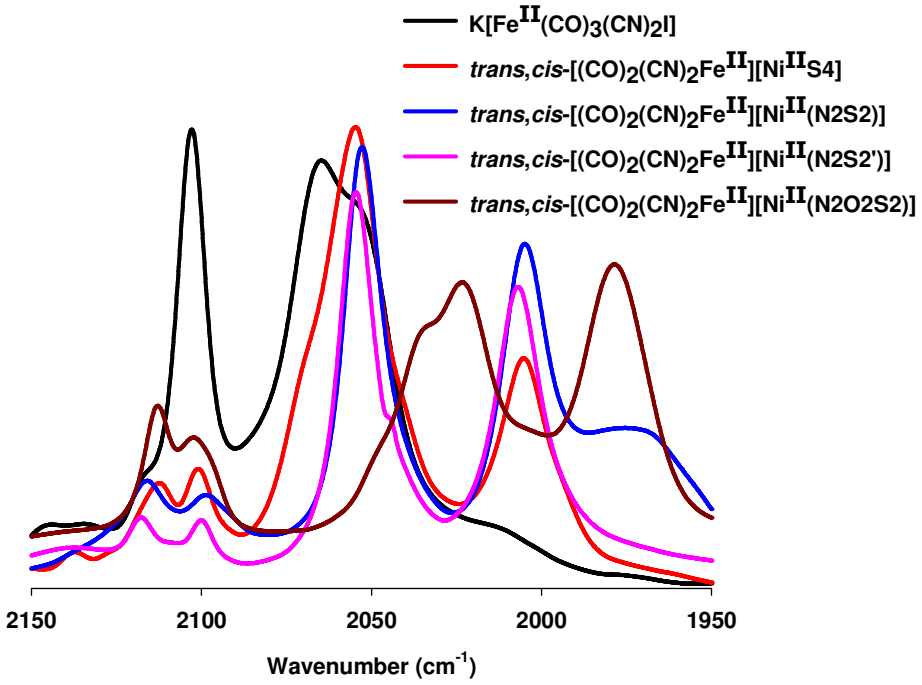

Figure 1.8: IR spectra of Fe^{II}-Ni^{II} Dimers in methylene chloride

Table 1.1: IR Data of Fe^{II}-Ni^{II} Dimers

Compd.	*trans*,*cis*-$[(CO)_2(CN)_2Fe^{II}]$ $[Ni^{II}(S4)]$	*trans*,*cis*-$[(CO)_2(CN)_2Fe^{II}]$ $[Ni^{II}(N2S2)]$	*trans*,*cis*-$[(CO)_2(CN)_2Fe^{II}]$ $[Ni^{II}(N2S2')]$	*trans*,*cis*-$[(CO)_2(CN)_2Fe^{II}]$ $[Ni^{II}(N2O2S2)]$
CO peaks	2005	2005	2007	1976
(cm^{-1})	2057	2052	2055	2021 (2033 sh)
CN^- peaks	2101	2100	2100	2099
(cm^{-1})	2112	2116	2118	2109

The IR (KBr pellet) spectrum of the orange–yellow precipitate isolated while using Ni^{II}(S4) indicates the presence of carbonyls (2052 and 2005 cm^{-1}) and cyanides (2112 and 2120 cm^{-1}) (Figure 1.9). As mentioned earlier, the solubility tests performed point to a polymeric product.

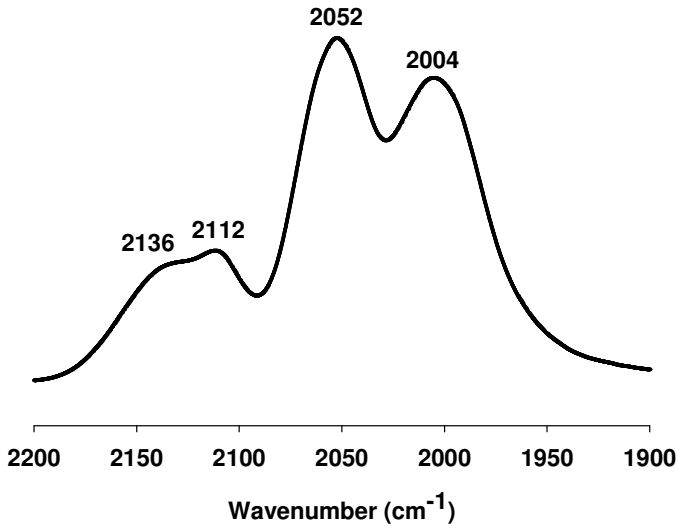

Figure 1.9: IR spectrum (KBr) of orange-yellow precipitate from the synthesis of *trans*,*cis*-$[(CO)_2(CN)_2Fe^{II}][Ni^{II}(S4)]$[42]

1.4.3 X-ray Crystallography Study of the Metal Complexes

For the Ni^{II}-center of the Fe^{II}-Ni^{II} dimers, Ni^{II}(S4), Ni^{II}(N2S2), Ni^{II}(N2S2'), Ni^{II}(N2O2S2) were used for which the crystal structures have been reported earlier. All these compounds show a slightly distorted square planar environment around the Ni^{II}-center. The terminal thiolate ligands in each case can bridge with $Fe^{II}(CO)_x(CN)_y$ moieties.

IR studies indicated two *cis* CO & CN^- ligands. X-ray crystal structure shows that the CO ligands are indeed *cis* but the CN^- ligands are *trans* to each other (Figure 1.20 & 1.21). The NiX2S2 plane [X = N(Et)/S] is not coplanar with Fe(CO)2S2 plane. This makes the two CN^- ligands symmetrically inequivalent and that results in two peaks in the IR spectrum. Both the *trans*,*cis*-$[(CN)_2(CO)_2Fe^{II}][Ni^{II}(S4)]$ and *trans*,*cis*–$[(CN)_2(CO)_2Fe^{II}][Ni^{II}(N2S2)]$ compounds have a crystallographically imposed mirror plane.

Table 1.2: Crystallographic Parameters for Fe^{II}-Ni^{II} Dimers

Compound	*trans*,*cis*-$[(CN)_2(CO)_2Fe^{II}][Ni^{II}(S4)]$	*trans*,*cis*-$[(CN)_2(CO)_2Fe^{II}][Ni^{II}(N2S2)]$
Empirical Formula	$C_{12}H_{14}FeN_2NiO_2S_4$	$C_{15}H_{24}FeN_4NiO_2S_2$
Formula Weight	461.1	471.1
Crystal System	Triclinic	Monoclinic
Space Group	*P*–1	$P2_1/n$
a (Å)	7.8344(5)	9.480(5)
b (Å)	10.2131(6)	19.713(5)
c (Å)	13.0208(8)	10.539(5)
α (°)	76.188(5)	90.0
β (°)	78.263(5)	91.884(5)
γ (°)	73.029(5)	90.0
Z	2	4
Cell Volume ($Å^3$)	957.57(10)	1968.5(15)
Crystal Color	red	red
Crystal Dimensions (mm)	0.2 x 0.15 x 0.15	0.4 x 0.2 x 0.1
Crystal Morphology	prism	prism
Calc. Density (g cm^{-3})	1.60	1.59
F_{000}	468	976
μ (mm^{-1})	2.180	1.921
R_{obs}	0.1161	0.0739
Temperature (K)	100(2)	100(0)
θ range (°)	2.91 – 29.6	2.94 – 29.5
Radiation (Mo Kα)	07107	0.7107

The detail structural discussion about *trans*,*cis*-$[(CN)_2(CO)_2Fe^{II}][Ni^{II}(S4)]$ is presented elsewhere.[42]

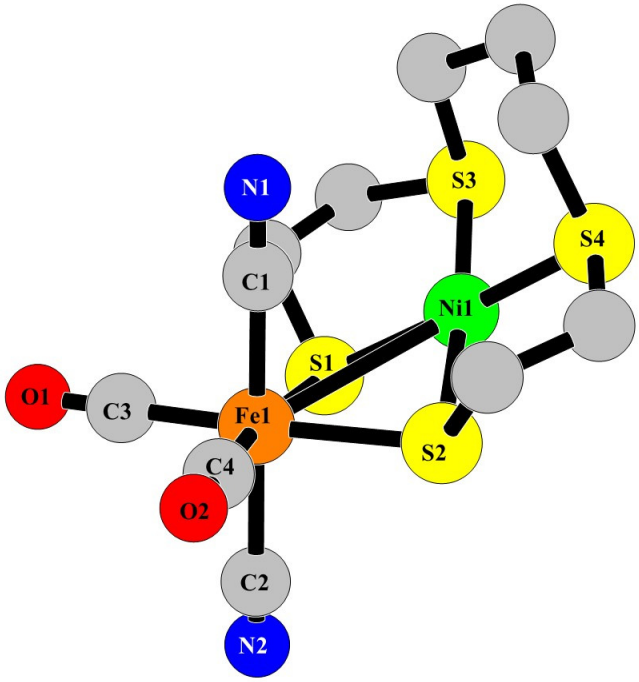

Figure 1.10: Structure of *trans*,*cis*-[$(CN)_2(CO)_2Fe^{II}$][$Ni^{II}(S4)$][42]
[H-atoms omitted for clarity]

Table 1.3: Selected Crystallographic Data for *trans*,*cis*-[$(CN)_2(CO)_2Fe^{II}$][$Ni^{II}(S4)$][42]

Bond Distances (Å)		Bond Angles (°)	
Fe(1) – C(1)	1.963(5)	C(1) – Fe(1) – C(2)	177.8(3)
Fe(1) – C(2)	1.869(8)	C(1) – Fe(1) – C(3)	91.7(2)
Fe(1) – C(3)	1.787(6)	C(1) – Fe(1) – S(1)	90.87(2)
Fe(1) – C(4)	1.786(5)	C(1) – Fe(1) – S(2)	91.88(2)
Fe(1) – S(1)	2.3295(2)	C(3) – Fe(1) – S(1)	172.0(2)
Fe(1) – S(2)	2.3365(2)	C(3) – Fe(1) – S(2)	94.26(2)
C(1) – N(1)	1.116(6)	C(4) – Fe(1) – S(1)	92.67(2)
C(1) – N(2)	1.243(1)	C(4) – Fe(1) – S(2)	172.77(2)
C(3) – O(1)	1.134(7)	S(1) – Fe(1) – S(2)	78.13(5)
C(4) – O(2)	1.129(6)	S(1) – Ni(1) – S(2)	85.22(5)
Ni(1) – S(1)	2.1723(2)	S(1) – Ni(1) – S(3)	91.80(6)
Ni(1) – S(2)	2.1710(2)	S(1) – Ni(1) – S(4)	174.30(6)
Ni(1) – S(3)	2.1907(2)	S(2) – Ni(1) – S(3)	175.07(6)
Ni(1) – S(4)	2.1914(2)	S(2) – Ni(1) – S(4)	91.58(6)
		S(3) – Ni(1) – S(4)	91.06(6)

Compared to the Ni^{II}(N2S2) complex, in *trans*,*cis*-[$(CN)_2(CO)_2Fe^{II}$][Ni^{II}(N2S2)], the Ni – N and Ni – S bond distances increase slightly. With the S-atoms bridging between the Ni^{II}-center and the Fe^{II}-center, the bond strength decreases as the bond lengths increase. The wild type enzyme isolated from *D. gigas* contains only one CN^- ligand, whereas the models presented here contain two. To distinguish between the CO & CN^- ligands, the Fe^{II}-C(Y) [Y = N/O] bond distances were used. The N2S2 plane is titlted towards one of the CN^- ligands. The N-atom of that CN^- ligand is far away (5.128 Å) from Ni^{II}-center to form any coordination.

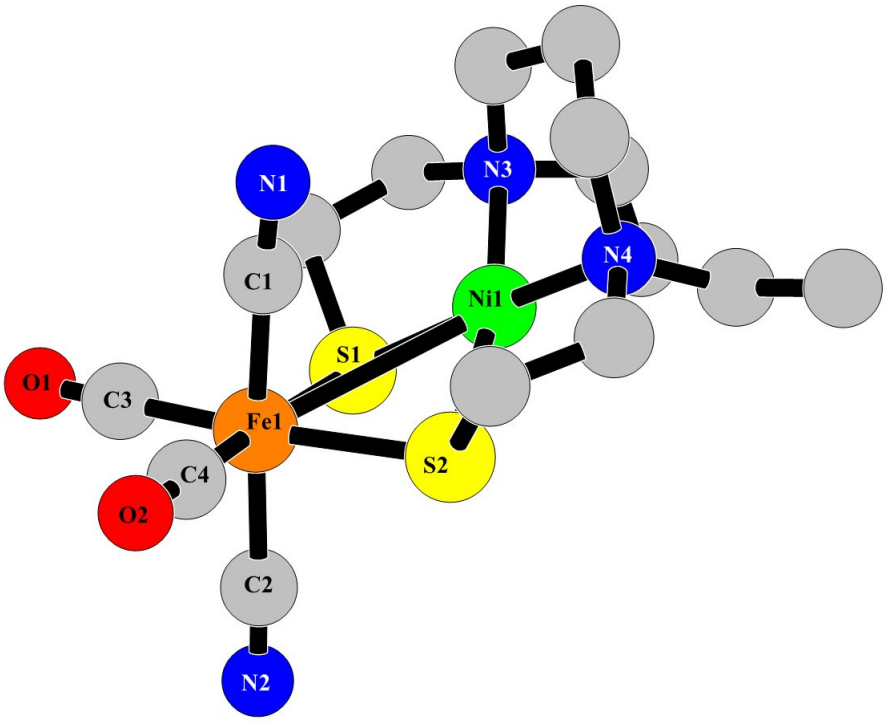

Figure 1.11: Structure of *trans*,*cis*-[$(CN)_2(CO)_2Fe^{II}$][Ni^{II}(N2S2)]
[H-atoms omitted for clarity]

Table 1.4: Selected Crystallographic Data for *trans,cis*–[$(CN)_2(CO)_2Fe^{II}$][Ni^{II}(N2S2)]

Bond Distances (Å)		Bond Angles (°)	
Fe(1) – C(1)	1.9220(6)	C(1) – Fe(1) – C(2)	174.75(3)
Fe(1) – C(2)	1.9359(6)	C(1) – Fe(1) – C(3)	93.40(3)
Fe(1) – C(3)	1.7995(7)	C(1) – Fe(1) – S(1)	92.09(2)
Fe(1) – C(4)	1.7701(8)	C(1) – Fe(1) – S(2)	88.71(2)
Fe(1) – S(1)	2.3045(2)	C(3) – Fe(1) – S(1)	90.01(2)
Fe(1) – S(2)	2.3045(2)	C(3) – Fe(1) – S(2)	166.66(2)
C(1) – N(1)	1.1609(8)	C(4) – Fe(1) – S(1)	176.15(4)
C(2) – N(2)	1.1442(8)	C(4) – Fe(1) – S(2)	99.42(4)
C(3) – O(1)	1.1535(1)	S(1) – Fe(1) – S(2)	76.73(7)
C(4) – O(2)	1.1230(8)	S(1) – Ni(1) – S(2)	82.38(6)
Ni(1) – S(1)	2.1649(2)	S(1) – Ni(1) – N(3)	88.90(2)
Ni(1) – S(2)	2.1789(2)	S(1) – Ni(1) – N(4)	170.94(2)
Ni(1) – N(3)	2.0113(6)	S(2) – Ni(1) – N(3)	168.51(2)
Ni(1) – N(4)	2.0089(4)	S(2) – Ni(1) – N(4)	89.36(2)
Ni(1) – N(1)	3.501(3)	Fe(1) – S(1) – Ni(1)	90.073(6)
Ni(1) – N(2)	5.128(6)	Fe(1) – S(2) – Ni(1)	89.724(3)

Comparing the two structures namely *trans,cis*-[$(CO)_2(CN)_2Fe^{II}$][Ni^{II}(S4)] and *trans,cis*- [$(CO)_2(CN)_2Fe^{II}$][Ni^{II}(N2S2)] with other synthetic models and wild type enzyme (Table 1.4), it can be seen that the Fe^{II} – S, Ni^{II} – S and Fe^{II} – Ni^{II} bond distances are in the same range. With the exception of the structure with dppe ligand, all the other structures show planar arrangement of Fe^{II}(S)2Ni^{II} fragment.

Table 1.5: Comparison of Selected Crystallographic Data of Synthetic Analogues of [NiFe]-Hydrogenase and Oxidized form of *D. gigas* and *D. fructosovorans*

Compound	Fe – Ni	Fe – S – Ni	Fe – S (bridge)	Ni – S (bridge)
D. gigas	2.9	73.7°	2.2	2.6
D. fructosovorans	2.9	No Data	2.4	2.4
trans,cis-[$(CO)_2(CN)_2Fe^{II}$(μ–pdt)$Ni^{II}(S_2CNEt_2)]^-$	3.059	84.43°	2.337	2.213
trans,cis [$(CO)_2(CN)_2Fe^{II}$(μ–pdt)Ni^{II}(dppe)]	2.809	50.06°	2.341	2.219
trans,cis-[$(CO)_2(CN)_2Fe^{II}$][Ni^{II}(S4)]	3.133	88.06°	2.333	2.172
trans,cis-[$(CO)_2(CN)_2Fe^{II}$][Ni^{II}(N2S2)]	3.164	89.90°	2.305	2.172

1.5 Conclusions & Future Work

Fe^{II}-Ni^{II} dimers closely resembling the active site of [NiFe] hydrogenase, been synthesized and characterized structurally. With the exception of one compound, in this work, all the compounds are neutral. This type of compounds can be synthesized using *fac*–$[Fe^{II}(CN)_2(CO)_3I]^-$ with a deprotonate thiolate in the form of a Ni^{II}–complex. Characterization of the Fe^{II}-Ni^{II} dimers were done by IR spectroscopy and X–ray crystallography. The IR studies of the Fe^{II}-Ni^{II} dimers showed a red shift in the carbonyl and cyanide stretching frequencies of *fac*–$[Fe^{II}(CN)_2(CO)_3I]^-$. It is caused by increased σ–donation affecting the π–backbonding of the carbonyl ligands and σ–bonding of the cyanide ligands.

The X-ray structures of *trans,cis*-$[(CO)_2(CN)_2Fe^{II}][Ni^{II}(S4)]$ and *trans,cis*-$[(CO)_2(CN)_2Fe^{II}][Ni^{II}(N2S2)]$ confirmed dimeric complexes with iron having an octahedral geometry while the nickel was square planar. The neutral complex *trans,cis*-$[(CO)_2(CN)_2Fe^{II}][Ni^{II}(S4)]$ is the first to be structurally characterized that models the [NiFe]-hydrogenase having all the key components. Catalytic studies need to be investigated to show if this complex truly models the enzyme active site.

1.6 References

(1) Heinekey, D. M. *J. Organomet. Chem.* **2009**, *694*, 2671.

(2) Fontecilla-Camps, J. C.; Volveda, A.; Cavazza, C.; Nicolet, Y. *Chem. Rev.* **2007**, *107*, 4273.

(3) Vignais, P. M.; Billoud, B. *Chem. Rev.* **2007**, *107*, 4206.

(4) Shima, S.; Pilak, P.; Vogt, S.; Schick, M.; Stagni, M. S.; Meyer-Klaucke, W.; Warkentin, E.; Thauer, R. K.; Ermler, U. *Science* **2008**, *321*, 572.

(5) Frey, M. *ChemBioChem* **2002**, *3*, 153.

(6) Kubas, G. J. *Chem. Rev.* **2007**, *107*, 4152.

(7) Thauer, R. K. *Microbiol.* **1998**, *144*, 2377.

(8) Yoshida, K.-i.; Kimura, H. *Biochim. Biophys. Acta.* **1985**, *842*, 62.

(9) Darensbourg, M. Y.; Lyon, E. J.; Smee, J. J. *Coord. Chem. Rev.* **2000**, *206-207*, 533.

(10) Volveda, A.; Marie-Helenw, C.; Piras, C.; Hatchikian, E. C.; Frey, M.; Fontecilla-Camps, J. C. *Nature* **1995**, *373*, 580.

(11) Volveda, A.; Garcin, E.; Piras, C.; De Lacey, A. L.; Fernandez, V. M.; Hatchikian, E. C.; Frey, M.; Fontecilla-Camps, J. C. *J. Am. Chem. Soc.* **1996**, *118*, 12989.

(12) Ogata, H.; Hirota, H.; Nakahara, N.; Komori, K.; Shibata, S.; Kato, K.; Kano, K.; Higuchi, Y. *Structure* **2005**, *13*, 1635.

(13) Nicolet, Y.; Piras, C.; Legrand, P.; Hatchikian, E. C.; Fontecilla-Camps, J. C. *Structure* **1999**, *7*, 13.

(14) Osterloh, F.; Saak, W.; Haase, D.; Pohl, S. *Chem. Commun.* **1997**, 979.

(15) Osterloh, F.; Saak, W.; Pohl, S. *J. Am. Chem. Soc.* **1997**, *119*, 5648.

(16) Marr, A. C.; Spencer, D. J. E.; Schroder, M. *Coord. Chem. Rev.* **2001**, *219-221*, 1055.

(17) Verhagen, J. A. W.; Lutz, M.; Spek, A. L.; Bouwman, E. *Eur. J. Inorg. Chem.* **2003**, 3968.

(18) Wang, Q.; Barclay, J. E.; Blake, A. J.; Davies, E. S.; Evans, D. J.; Marr, A. C.; McInnes, E. J. L.; McMaster, J.; Wilson, C.; Schroder, M. *Chem. Eur. J.* **2004**, *10*, 3384.

(19) Bouwman, E.; Reedijk, J. *Coord. Chem. Rev.* **2005**, *249*, 1555.

(20) Tard, C.; Pickett, C. J. *Chem. Rev.* **2009**, *109*, 2245.

(21) Lai, C.-H.; Reibenspies, J. H.; Darensbourg, M. Y. *Angew. Chem. Int. Ed.* **1996**, *35*, 2390.

(22) Zhu, W.; Marr, A. C.; Wang, Q.; Neese, F.; Spencer, D. J. E.; Blake, A. J.; Cooke, P. A.; Wilson, C.; Schroder, M. *Proc. Natl. Acad. Sci.* **2005**, *102*, 18280.

(23) Li, Z.; Ohki, Y.; Tatsumi, K. *J. Am. Chem. Soc.* **2005**, *127*, 8950.

(24) Jiang, J.; Maruani, M.; Solaimanzadeh, J.; Lo, W.; Koch, S. A.; Millar, M. M. *Inorg. Chem.* **2009**, *48*, 6359.

(25) Buter, J.; Kellogg, R. M. *Org. Synth. Coll.* **1993**, *8*, 150.

(26) de Lacey, A. L.; Hatchikian, E. C.; Volveda, A.; Frey, M.; Fontecilla-Camps, J. C.; Fernandez, V. M. *J. Am. Chem. Soc.* **1997**, *119*, 7181.

(27) Smee, J. J.; Miller, M. L.; Grapperhaus, C. A.; Reibenspies, J. H.; Darensbourg, M. Y. *Inorg. Chem.* **2001**, *40*, 3601.

(28) Kruger, H. J.; Peng, G.; Holm, R. H. *Inorg. Chem.* **1991**, *30*, 734.

(29) Farrugia, L. J. *J. Appl. Cryst.* **2012**, *45*, 849.

(30) Hieber, W.; Wirsching, A. *Z. Annorg. Allgem. Chem.* **1940**, *245*, 35.

(31) Roundhill, D. M. *Inorg. Chem.* **1980**, *19*, 557.

(32) Herskovitz, T.; DePamphilis, B. V.; Gillum, W. O.; Holm, R. H. *Inorg. Chem.* **1975**, *14*, 1426.

(33) Mukherjee, R. N.; Rao, C. P.; Holm, R. H. *Inorg. Chem.* **1986**, *25*, 2979.

(34) Rao, C. P.; Dorfman, J. R.; Holm, R. H. *Inorg. Chem.* **1986**, *25*, 428.

(35) Snyder, B. S.; Rao, C. P.; Holm, R. H. *Aust. J. Chem.* **1986**, *39*, 963.

(36) Baidya, N.; Mascharak, P. K.; Stephan, D. W.; Campagna, C. F. *Inorg. Chim. Acta.* **1990**, *177*, 233.

(37) Jiang, J.; Acunzo, A.; Koch, S. A. *J. Am. Chem. Soc.* **2001**, *123*, 12109.

(38) Jiang, J.; Koch, S. A. *Angew. Chem. Int. Ed.* **2001**, *40*, 2629.

(39) Jiang, J.; Koch, S. A. *Inorg. Chem.* **2002**, *41*, 158.

(40) Nakamoto, K. *In Infrared and Raman Spectroscopy of Inorganic and Coordination Compounds*; John Wiley & Sons: New York, **1986**.

(41) Van Der Spek, T. M.; Arendsen, A. F.; Happe, R. P.; Yun, S.; Bagley, K. A.; Stufkens, D. J.; R.;, H. W.; Albracht, S. P. J. *Eur. J. Biochem.* **1996**, *237*, 629.

(42) Amarante, D., Stony Brook Unversity, **2011**.

Chapter 2:

Structural Modelling of Metal – Thiolate Units i) Monomeric ii) Tetrameric using 2,4,6-Tricyclohexyl-benzenethiol

2.1 Introduction

2.1.1 General Background

The primary interest in metal thiolate chemistry stems from the isolation of various Fe-S centers found in bacteria.[1] The structural variation ranges from monomeric center to tetrameric center alongside other variations (Figure 2.1).

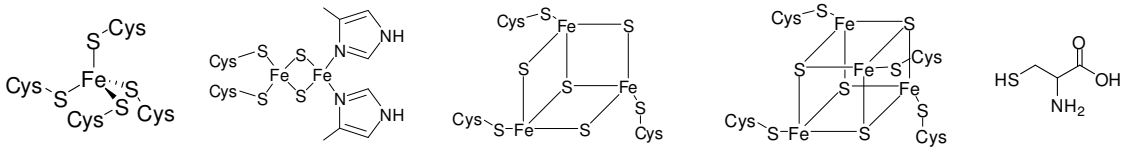

Figure 2.1: Different Types of Fe-S Clusters

2.1.2 Monomeric Metal Thiolate Chemistry

Prior to x-ray crystallographic studies, the Fe-S proteins were thought to have a labile sulfur in combination with cysteinyl sulfur in a persulfide linkage.[2] Following the crystal structure of the Rubredoxins from anaerobic bacteria (*Desulfovibrio desulfaricans*, *Desulfovibrio vulgaris* & *Clostridium pasteurianum*), it was found that the Fe-center is linked to four cysteinyl sulfur atoms in a tetrahedral (or distorted) fashion (Figure. 2.2)[3] The Fe-S bonds are chemically identical in the sense that all of them are from the cysteine

residue. They are almost equal in length except for the fourth one and only one of the six angles differ considerably from the ideal tetrahedral angle.[4]

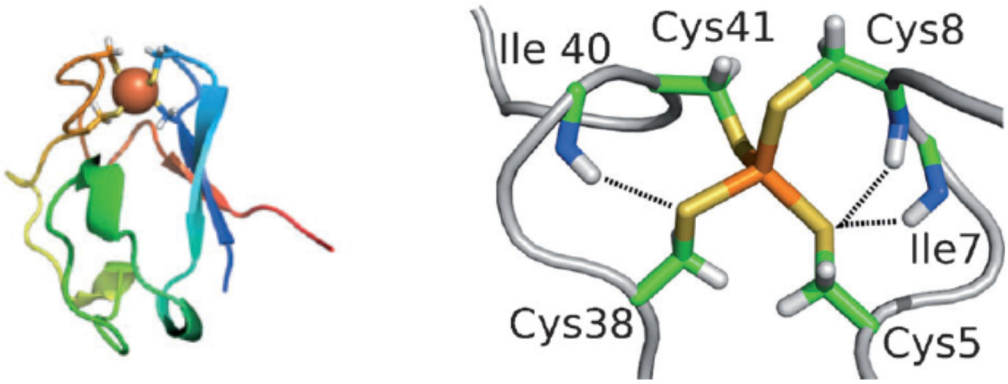

Figure 2.2: Structure of Rubredoxin[4]

An enormous amount of work has been done to mimic the various [Fe-S] clusters as well as the active sites of the enzymes synthetically. Pioneers of this work are Holm using o,o'-oxalyldithiol and Coucovanis using benzenethiol (Figure 2.3).[5-8]

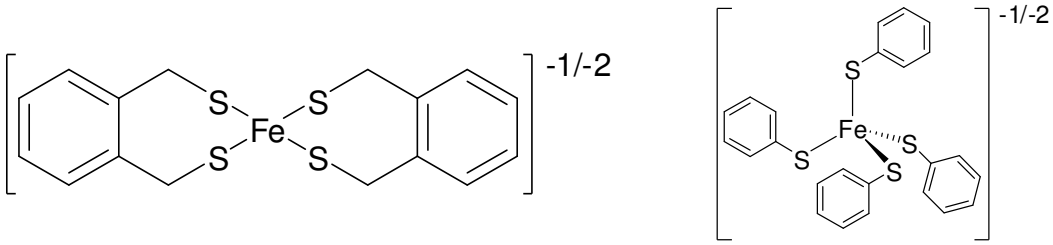

Figure 2.3: Fe-Complexes with o,o'-Oxalyldithiol & Benzenethiol

Millar was the first to realize the potential and to use sterically encumbered thiolates to form iron-thiolate compounds that were not easily accessible by other routes. The thrust to make the synthetic structures robust via the concept of using bulky thiolate ligands came into picture. Millar and Koch first reported a stable structurally characterized $[Fe^{III}(SR)_4]^-$ compound, where 2,3,5,6-tetramethyl-benzene thiolate was used.[9] The approach was simple and elegant. Reaction of four equivalents of the thiolate salt in dimethylformamide

(DMF) with $FeCl_3$ and $(Et_4N)Br$ followed by crystallization of the product from hot DMF provided the compound. Electrochemical measurements reveal that the $[Fe^{III}(SR)_4]^-$ unit was more favored. The idea here is that the electron-rich thiolates can stabilize the higher oxidation state of the metals. But, at the same time it may also be possible that the thiolates initiate the autoredox reaction (Eq. 2.1). The use of sterically demanding thiolates inhibit the autoredox process and hence, account for the stability of the $[Fe(SR)_4]^-$ unit.

$$2\ Fe^{3+} + 2\ RS^- \rightarrow 2\ Fe^{2+} + RSSR \qquad \text{(Eq. } \mathbf{2.1}\text{)}$$

In further work, Millar and Koch used the 2,4,6-triisopropylbenzene thiolate[10] and the 2-phenylbenzene thiolate[11] to synthesize and characterize two more complexes of the type $[Fe^{III}(SR)_4]^{1-}$ (Figure 2.4).

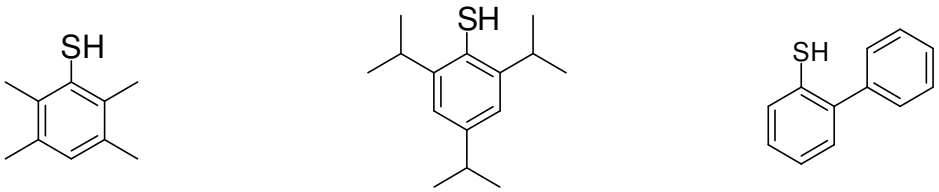

2,3,5,6-tetramethyl benzenethiol | 2,4,6-triisopropyl benzenethiol | 2-phenyl benzenethiol

Figure 2.4: Model Substituted Benzenethiol Ligands

Subsequently, Power used the significantly more bulky thiolate, 2,6-bis(2,4,6-triisopropylbenzene)benzene thiolate $[S\text{-}C_6H_3\text{-}2,6\text{-}(C_6H_2\text{-}2,4,6\text{-}i\text{-}Pr_3)_2]$, to acquire two-coordinate Fe(II) complexes, $[Fe^{II}(SR)_2]$.[12] Another low coordination Fe(II) complexes of the type $[Fe^{II}(SR)_3]^{1-}$ was acquired by Power via the use of the 2,4,6-tri(*t*-butyl)benzene thiolate ligand $[S\text{-}C_6H_2\text{-}2,4,6\text{-}(t\text{-}Bu)_3]$; under different conditions, a 4-coordinate dimeric Fe(II) iron compound was acquired, $[Fe^{II}_2(SR)_4]$ (Figure **2.5**).[13]

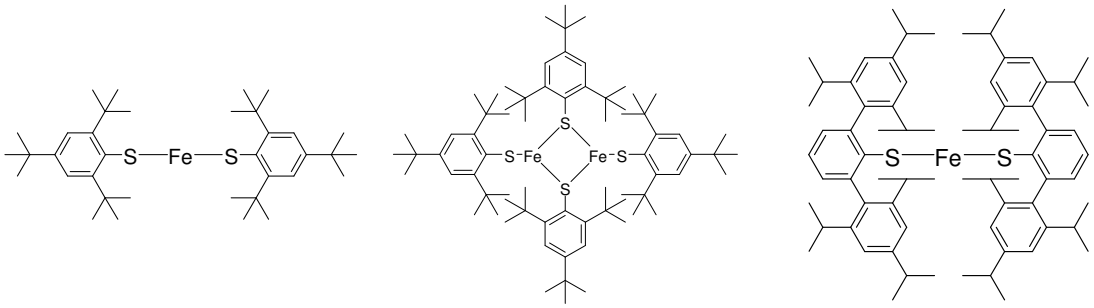

Figure 2.5: Fe^{II} Complexes of Bulky Thiolate Ligands

2.1.3 Iron-Sulfur Tetrameric Clusters

Fe-S metalloclusters are ubiquitous in anaerobic bacteria, primarily engaged in electron transport. They are collectively called ferredoxins – 2Fe, 3Fe or 4Fe (Figure 2.1). A variety of enzymes such as nitrogenase, carbon monoxide dehydrogenase (CODH), hydrogenase possess the Fe-S clusters in conjunction with their active sites.[14] In these [Fe-S] clusters, the irons are coordinated to cysteinyl sulfurs, and usually also inorganic sulfurs. The most important structural feature observed in the proteins was that the [Fe-S] clusters are embedded deep inside the cavities of the polypeptide chain of the protein. The polypeptide chain resists solvent reaching the clusters and subsequently mutilating them.[15]

In one group of the 4Fe–4S proteins are the 'high potential iron proteins' (HiPiP) and in another group are the low potential iron-sulfur proteins. These clusters have a cubane type structure and are the most important class of Fe–S proteins.[16,17] In the low potential ferredoxins, the formal oxidation states for iron are [$2Fe^{2+}$, $2Fe^{3+}$] ⇆ [$1Fe^{3+}$, $3Fe^{2+}$] and for HiPiP are [$3Fe^{3+}$, $1Fe^{2+}$] ⇆ [$2Fe^{2+}$, $2Fe^{3+}$] (Figure 2.6).[18]

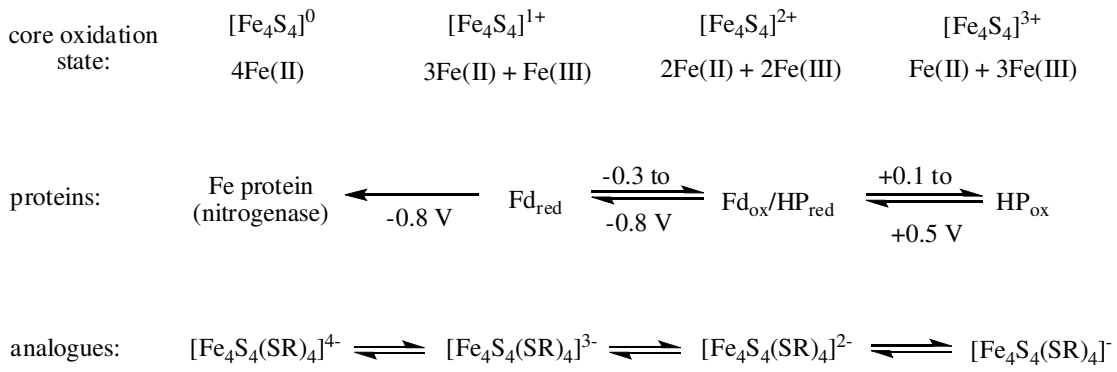

Figure 2.6: Different Types of Fe-S Clusters and their Redox Relationships

Holm and co-workers were the pioneers in the field of synthetic analogues of $[Fe_4S_4]^{2+}$ cores. Using various derivatives of benezenethiol, a large body of biomimetic models were synthesized (Figure 2.7).[19-24]

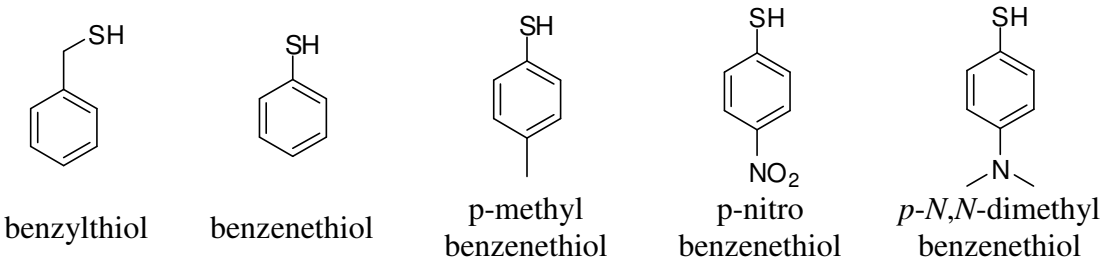

Figure 2.7: Derivatives of Benzenethiol for $[Fe_4S_4]^{n+}$ Core Models

Lawson-Daku and coworkers[25] & Nakamura and coworkers[26] have synthesized numerous $[Fe_4S_4(SR)_4]^{2-}$ complexes with numerous sterically encumbered thiolate ligands, including the thiolate derivative of $[HS\text{-}C_6H_3\text{-}2,6\text{-}(phenyl)_2]$. None of the compounds could be reversibly oxidized to the $[Fe_4S_4]^{3+}$ core level.

Aqueous stability of these complexes have often been investigated, where the synthetic models bear hydrophobic groups such as long alkyl chains.[27] Study by Nakamura and co-workers have concluded that the $[Fe_4S_4]^{+}$ cores are highly moisture sensitive in terms of redox behavior, but the $[Fe_4S_4]^{2+}$ cores are relatively stable.[28] A more systematic

study of the solvent dependency on redox behavior of $[Fe_4S_4(SPh)_4]^{2-}$ was done by Jordanov and coworkers. The basic character of the solvent is the decisive factor for the stability.[29]

The first synthetic $[Fe_4S_4(SR)_4]^{1-}$ cluster (structurally characterized) at the oxidized $[Fe_4S_4]^{3+}$ level was synthesized by Millar and co-workers using 2,4,6-triisopropylbenzenethiol.[30] Thus the steric influence of the stability of the $[Fe_4S_4]^{3+}$ core been established. The $[Fe_4S_4]^{3+}$ core was characterized by single crystal diffraction method (Figure 2.8). Tatsumi and coworkers have reported $[Fe_4S_4]^{3+}$ core with 2,6-bis(2,4,6-triisopropylbenzene)benzene thiolate.[31] The synthetic route started from an all ferric core with amide ligands. They extended this approach with series of other exotic benzenethiols with derivatized benzene rings as *ortho*-substituents (Figure 2.8).[32]

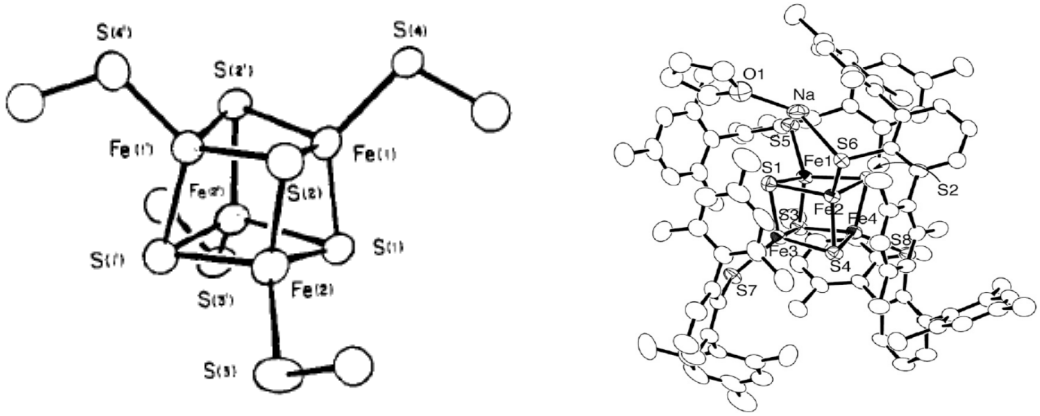

$[Fe_4S_4(2,4,6\text{-triisopropyl-benzenethiol})_4]^{-1}$

$[Fe_4S_4(2,6\text{-bis}(2,4,6\text{-triisopropyl-benzene})\text{benzenethiol})_4]^{-1}$

Figure 2.8: Some Representative $[Fe_4S_4]^{3+}$ core

2.2 Aim of the Project

In attempts to synthesize metal complexes with unique coordination geometries and properties researchers have turned to the design and preparation of new ligands systems that possess considerable steric capacity. In numerous cases, sterically encumbered ligands have been used to form new metal complexes as mimics for significant metal centers in metalloproteins. The idea is that since the metal centers in metalloproteins are surrounded by and protected by the polypeptide backbone, these metal centers are best mimicked by ligands that are sterically encumbered. This idea has turned out to be true in many cases. The field has evolved to the extreme via the tedious syntheses of exotic thiolate ligands (coupling reactions) with super-steric properties – the benzenethiolate ligands with the phenyl-groups[33,34], the mesityl groups[35] and the 2,4,6-triisopropylbenzene groups[12,36,37] (Figure 2.9) in the *ortho*-positions of the benzenethiol.

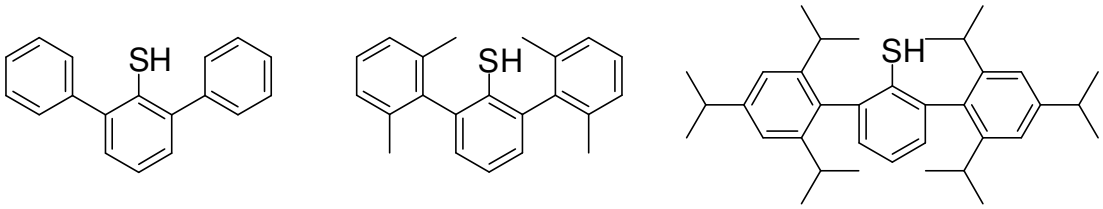

2,6-diphenyl benzenethiol | 2.6-dimesityl benzenethiol | 2,6-di-(2,4,6-triisopropyl) benzenethiol

Figure 2.9: Exotic Thiolate Ligands

One of the very first examples of this approach was by the use of 2,3,5,6-tetramethylbenzene thiolate [TetMBT] and 2,4,6-triisopropylbenzene thiolate [TIPBT] to create models – $[Fe^{III}(SR)_4]^{1-}$ for the iron center in the oxidized form of rubredoxin[9] and $[Fe_4S_4(SR)_4]^{n-}$ (n = 0, 1, 2, 3, 4) systems found in high potential iron proteins (HPiP)[30]. Therefore, it was discovered that these steric thiolates form iron-thiolate complexes (in high oxidation states) that are not readily accessible by other routes.

In an effort to extend the steric capacity of *ortho*-methyl and *ortho*-isopropyl ligands, we have sought out a new class of ligands which contain cyclohexyl substituents in the *ortho*-position. These should exhibit steric capacity analogous to that of the 2,6-diphenylbenzene derivatives, yet be more basic in their donor capacity. So in the context of this report, numerous derivatives of 1,3,5-tricyclohexylbenzene have been synthesized (Figure 2.10). Attempts to make the thiol derivative have been successful. Attempts to acquire metal complexes of this ligand were carried out but were not as successful.

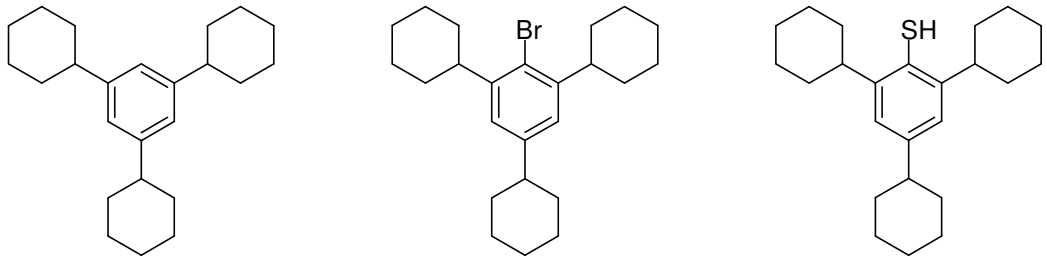

1,3,5-tricyclohexylbenzene | 2,4,6-tricyclohexyl bromobenzene | 2,4,6-tricyclohexyl benzenethiol

Figure 2.10: Derivatives of 1,3,5-tricyclohexylbenzene

2.3 Experimental

2.3.1 General Remarks

All the manipulations were carried out under nitrogen unless and otherwise noted. Solvents were distilled according to literature procedures [diethyl ether (Et_2O) and tetrahydrofuran (THF) over Na/benzophenone, dichloromethane (CH_2Cl_2) over P_2O_5, acetonitrile (CH_3CN) over CaH_2, methanol (CH_3OH) over Mg/I_2], and stored under nitrogen. . ^1H & ^{13}C NMR spectra were recorded on a Brüker 300 MHz instrument in $CDCl_3$ and standardized with residual solvent peak at 7.26 ppm and 77.23 ppm respectively. Electron absorption spectra were recorded on a Varian Cary 100 spectrophotometer in a 1 cm long quartz cell. Wherever applicable, X-ray quality crystals were grown from suitable solvents using appropriate techniques.

2.3.2 Synthesis of 1,3,5 – Tricyclohexylbenzene [$Ph(Cy)_3$]

The compound was prepared according to a literature procedure.[38] 100.0 g (0.75 mol) of $AlCl_3$ and 333 mL (293.0 g, 3.76 mol) of anhydrous benzene taken in a 3-necked flask was evenly mixed with a mechanical stirrer for 10 minutes under closed condition. 1.22 L (987.4 g, 12.02 mol) of cyclohexene was added dropwise to this mixture over a period of 3 hours maintaining the temperature between 3ºC to 18ºC. After the addition was complete, the mixture was allowed to stir for overnight. The excess of $AlCl_3$ was quenched with 62.5 mL (12 M) HCl. The products were mixtures of monocyclohexylbenzene, 1,4-dicyclohexylbenzene, 1,3,5-tricyclohexylbenzene and 1,2,4,5-tetracyclohexylbenzene. The desired compound was recrystallized from acetone. Yield 609 g (50%). ^1H NMR ($CDCl_3$) δ 6.89 (s, 3H, *Ar-H*), 2.47 (q, 3H, Ar-*CH*$_2$-), 1.2 –

1.8 (30H, cyclohexyl ring) ppm. ^{13}C NMR ($CDCl_3$) δ 148.0, 123.1, 45.0, 34.8, 27.3, 26.5 ppm. Crystals were grown by vapor diffusion method using diethyl ether/methanol.

2.3.3 Synthesis of 2,4,6 – Tricyclohexylbromobenzene [$Ph(Cy)_3Br$]

The compound was prepared according to a literature procedure.[39] In a 500 mL round bottom flask was added 32.4 g (0.01 mol) of $Ph(Cy)_3$. 250 mL trimethylphosphate was added to cover the solid which was then warmed to 80°C to obtain a homogenous mixture. 1.93 g (0.012 mol) of Br_2 in ~60 mL of trimethylphosphate was added to this solution dropwise over a period of 10 minutes. After the complete addition of Br_2, a faint orange color remained. The heat source was removed and the mixture was stirred overnight. The solid was filtered and washed with 60 mL (2 X 30 mL) of ice-cold MeOH. Yield 39.2 g (97.6%). ^1H NMR ($CDCl_3$) δ 6.94 (s, 2H, *Ar-m-H*), 3.07 (q, 2H, Ar-*o*-CH_2-), 2.46 (q, 1H, Ar-*p*-CH_2-), 1.2 – 1.8 (30H, cyclohexyl ring) ppm. ^{13}C NMR δ ($CDCl_3$) 147.0, 146.5, 124.2, 123.5, 44.7, 44.5, 34.7, 33.8, 26.6, 26.4 ppm. Crystals were grown by vapor diffusion method using diethyl ether/methanol.

2.3.4 Synthesis of 2,4,6 – Tricyclohexylbenzenesulfonylchloride [$Ph(Cy)_3SO_2Cl$]

The compound was prepared according to a literature procedure.[40] In a 5 l flask, fitted with stirrer, separatory funnel, exit tube, and thermometer, was placed 350 g (3 moles) of chlorosulfonic acid and to it was slowly added, with continuous stirring, 324 g (1 moles) of benzene, keeping the temperature between 20°C and 25°C by means of cold water. The addition required two to three hours; when this was complete, the mixture was stirred for one hour, and poured upon 5 kg of crushed ice. The aqueous layer was extracted twice in dichloromethane. The combined extracts are washed with dilute sodium carbonate, and dried over anhydrous sodium sulfate. The solvent was stripped off by rotary

evaporator. Yield 381 g (90%). ^{1}H NMR ($CDCl_3$) δ 7.17 (s, 2H, *Ar-m-H*), 3.83 (q, 2H, Ar-*o*-CH_2-), 2.5 (q, 1H, Ar-*p*-CH_2-), 1.2 – 1.6 & 1.8 – 2.0 (m, 30H, cyclohexyl rings) ppm. ^{13}C NMR ($CDCl_3$)

2.3.5 Synthesis of 2,4,6 – Tricyclohexylbenzenethiol [$Ph(Cy)_3SH$]

2.3.5.1 Synthesis of $Ph(Cy)_3SH$ from $Ph(Cy)_3Br$

The compound was prepared according to a literature procedure.[41] In a 500 mL 3-necked flask, fitted with a condenser, was taken 0.4 g (0.017 moles) of magnesium turnings and gently heated. After cooling, single crystal of sublimed iodine and 70.0 mL of freshly distilled THF was added. The mixture was stirred for 10 minutes when the iodine decolorized slightly. 4.9 g (0.012 moles) of $Ph(Cy)_3Br$ dissolved in ~60 mL of freshly distilled THF was added to the mixture which was refluxed for overnight. 0.77 g (0.024 moles) of sublimed sulfur was added to the solution, refluxed for overnight followed by the addition of 0.5 g (0.013 moles) of $LiAlH_4$ and refluxed for 6 h longer. The excess of the $LiAlH_4$ was quenched by first adding ethyl acetate, followed by methanol and finally, dilute HCl. The aqueous layer was extracted twice in diethyl ether. The combined extracts are washed with brine solution, and dried over anhydrous sodium sulfate. The solvent was stripped off by rotary evaporator. Yield 3.3 g (55.0%).

2.3.5.2 Synthesis of $Ph(Cy)_3SH$ from $Ph(Cy)_3SO_2Cl$

The compound was prepared according to a literature procedure.[42,43] In a 3-necked flask, attached to a condenser at 0°C was added 2.95 g (0.077 moles) $LiAlH_4$ in 50 mL of THF to get a suspension. 2.01 g (0.005 moles) of $Ph(Cy)_3SO_2Cl$, dissolved in ~100 mL of THF, was added to the suspension of $LiAlH_4$. After the vigorous reaction has stopped (*evolution of hydrogen gas stops in Hg-trap when N_2 line is closed*), the mixture was

refluxed for 48 h. The mixture was cooled and then the excess $LiAlH_4$ was quenched at 0°C by ethyl acetate followed by methanol and finally by dilute HCl. The aqueous layer was extracted twice in diethyl ether. The combined extracts are washed with brine solution, and dried over anhydrous sodium sulfate. The solvent was stripped off by rotary evaporator. Yield 0.8 g (43.0%).

^{1}H NMR ($CDCl_3$) δ 6.96 (s, 2H, *Ar-m-H*), 3.05 (q, 2H, Ar-*o*-CH_2-), 2.46 (q, 1H, Ar-*p*-CH_2-), 1.2 – 1.8 (30H, cyclohexyl ring) ppm. ^{13}C NMR ($CDCl_3$) δ 147.2, 146.3, 124.8, 122.6, 44.8, 42.9, 33.9, 27.3, 26.6, 26.4 ppm. Crystals suitable for single crystal diffraction measurement were grown by vapor diffusion method using diethyl ether and methanol.

2.3.6 Synthesis of $[Et_4N][Fe(SPh(Cy)_3)_4]$

The compound was prepared according to a modified literature procedure.[44] To 214 mg (0.60 mmol) of $Ph(Cy)_3SH$ was dissolved in *n*-hexane was added 0.24 mL of 2.5 (M) *n*-BuLi in hexane. After stirring for 15 minutes, the solvent was removed and CH_3CN was added. $FeCl_3$•$6H_2O$ (32.0 mg, 0.12 mmol) and Et_4NBr (51 mg, 0.24 mmol) were added successively. An intense deep red colored solution developed and it was stirred for 6 hours. The solution was filtered through a celite pad and layered with *n*-hexane. Deep red colored microcrystalline precipitate was filtered and dried under vacuum. Yield: 108.5 mg (68%)

2.3.7 Synthesis of $[Et_4N]_2[Fe(SPh(Cy)_3)_4]$

The compound was prepared according to a modified literature procedure.[44] To 214 mg (0.60 mmol) of $Ph(Cy)_3SH$ was dissolved in *n*-hexane was added 0.24 mL of 2.5 (M) *n*-BuLi in hexane. After stirring for 15 minutes, the solvent was removed and CH_3CN was added. $FeCl_2$•$4H_2O$ (24 mg, 0.12 mmol) and Et_4NBr (51 mg, 0.24 mmol) were added

successively. A pale orange colored solution developed and it was stirred for 6 hours. The solution was filtered through a celite pad and layered with *n*-hexane. Pale tan colored microcrystalline precipitate was filtered and dried under vacuum. Yield: 136.5 mg (76%)

2.3.8 Synthesis of $[Et_4N]_2[Co(SPh(Cy)_3)_4]$

The compound was prepared according to a modified literature procedure.[44] To 214 mg (0.60 mmol) of $Ph(Cy)_3SH$ was dissolved in *n*-hexane was added 0.24 mL of 2.5 (M) *n*-BuLi in hexane. After stirring for 15 minutes, the solvent was removed and CH_3CN was added. $CoCl_2 \cdot 6H_2O$ (28.5 mg, 0.12 mmol) and Et_4NBr (51 mg, 0.24 mmol) were added successively. A lime green colored solution developed and it was stirred for 6 hours. The solution was filtered through a celite pad and layered with *n*-hexane. Bright green colored microcrystalline precipitate was filtered and dried under vacuum. Yield: 140.4 mg (78%)

2.3.9 Synthesis of $[Et_4N]_2[Ni(SPh(Cy)_3)_4]$

The compound was prepared according to a modified literature procedure.[44] To 214 mg (0.60 mmol) of $Ph(Cy)_3SH$ was dissolved in *n*-hexane was added 0.24 mL of 2.5 (M) *n*-BuLi in hexane. After stirring for 15 minutes, the solvent was removed and CH_3CN was added. $NiCl_2 \cdot 6H_2O$ (28.5 mg, 0.12 mmol) and Et_4NBr (51 mg, 0.24 mmol) were added successively. A deep red colored solution developed and it was stirred for 6 hours. The solution was filtered through a celite pad and layered with *n*-hexane. Red colored microcrystalline precipitate was filtered and dried under vacuum. Yield: 108.5 mg (68%)

2.3.10 Synthesis of $[n\text{-}Bu_4N]_2[Fe_4S_4Cl_4]$

The compound was prepared according to a modified literature procedure.[45] In a 500 mL side-arm flask 1.81 g (78.7 mmol) of metallic sodium was dissolved in ~50 mL ethanol. After the complete dissolution of the metal, the solution was degassed and 8.0 mL

(78.0 mmol) of thiophenol was added. After 10 minutes of stirring, the ethanol was removed under reduced pressure. 10.33 g (51.9 mmol) of $FeCl_2.4H_2O$, 8.1 g (27.3 mmole) [*n*-Bu_4N]Cl and 3.34 g (104 mmol) of elemental sulfur was added followed by 150 mL acetonitrile. The mixture was stirred for 1 hr, after which the solution was refluxed for 2 h and then cooled overnight while stirring. The solution was filtered through celite and washed with acetonitrile. The volume of the filtrate was reduced to half of the original volume. 50 mL of diethyl ether was slowly added to the solution and left to stir for overnight. The black precipitate was filtered and dried under vacuum and characterized by UV-Vis spectroscopy in dichloromethane. Yield 11.1 g (87.1%).

2.3.11 Synthesis of [*n*-$Bu_4N]_2[Fe_4S_4(Ph(Cy)_3S)_4]$

The compound was prepared according to a modified literature procedure.[30] To 2.47 g (6.9 mmol) of $Ph(Cy)_3SH$ was dissolved in *n*-hexane was added 3.0 mL of 2.5 (M) *n*-BuLi in hexane. After stirring for 15 minutes, the solvent was removed. Yield 2.48 g (99%). To the lithiated thiol was added 1.65 g (1.7 mmol) of [*n*-$Bu_4N]_2[Fe_4S_4Cl_4]$ followed by 50 mL of acetonitrile. A deep brownish orange color developed. The solution was stirred for 3 hrs and then the solvent was removed under vacuum. 40 mL of ethanol was added and the product started to crystallize. Then ~20 mL of 2-propanol was added and stirred for half an hour. The solution was left to sit for overnight. The product was filtered and dried under vacuum. Yield 1.60 g (41.7%).

2.4 Results & Discussion

2.4.1 Synthesis & Characterization of the Ligands

$Ph(Cy)_3$ was synthesized under no-air condition to arrest moisture destroying the catalyst $AlCl_3$ starting from commercially available materials. The two precursor compounds to $Ph(Cy)_3SH$ were $Ph(Cy)_3Br$ and $Ph(Cy)_3SO_2Cl$ (Scheme 2.1). Both were dried thoroughly to make free of water and methanol.

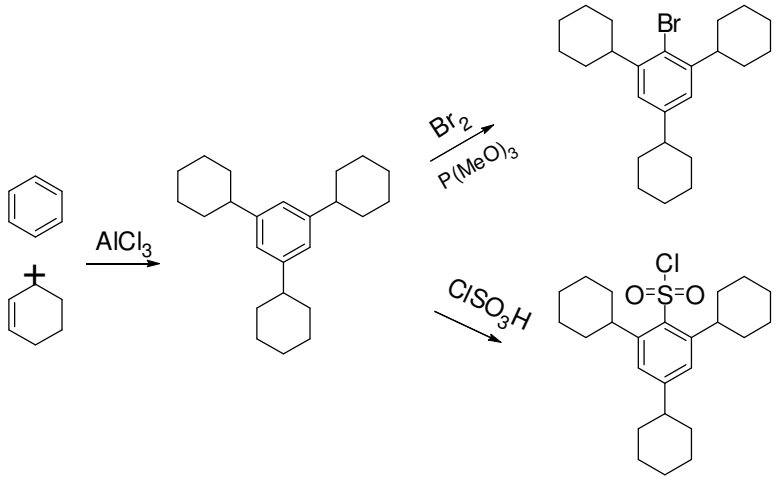

Scheme 2.1: Synthesis of $Ph(Cy)_3$, $Ph(Cy)_3Br$ & $Ph(Cy)_3SO_2Cl$

Although the crystal structure of the $Ph(Cy)_3Br$ has been recently reported[46], we also solved it independently (Figure 2.11). The compound crystallizes in a monoclinic structure with $P2_1/c$ space group. The *ortho*-cyclohexyl rings are perpendicular to the planar benzene ring. The three cyclohexyl rings are mutually orthogonal in space. The two *ortho*-substituted rings are related by a plane of symmetry. This fact is also confirmed in ^1H NMR where the *ortho*- benzylic protons give a different chemical shift compared to the *para*-benzylic proton. The C-Br bond length is 1.9 Å and the distance between Br-atom and *ortho* hydrogens on cyclohexyl groups is 2.7 Å. The distance between the *ortho*-

benzylic hydrogens and bromine atom shows that there is no hydrogen bonding present in the molecule.

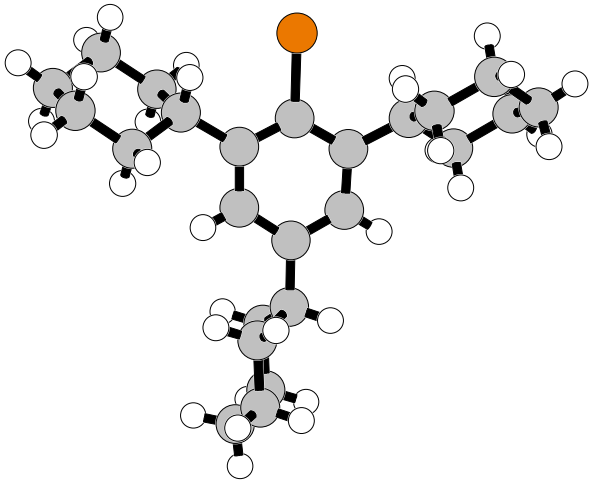

Figure 2.11: Crystal Structure of $Ph(Cy)_3Br$

The two synthetic routes followed for 2,4,6-tricyclohexylbenzenethiol (Scheme 2.2). The first method includes the use of Grignard reagent[41] reacting with sulfur. In the second method, $Ph(Cy)_3SO_2Cl$ was reduced by $LiAlH_4$.[42,43] Among the two methods applied for the synthesis of $Ph(Cy)_3SH$, the first route gave the best results. The reduction of sulfonyl chloride yielded the thiol as well the partially a reduced product as seen in ^1H NMR.

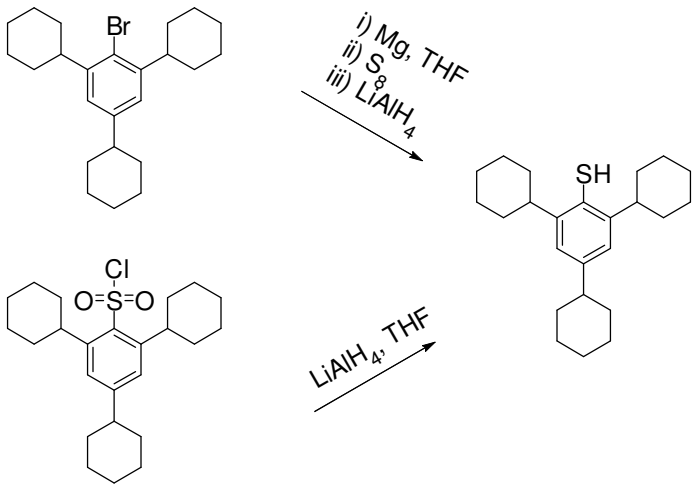

Scheme 2.2: Synthesis of $Ph(Cy)_3SH$

The compound $Ph(Cy)_3SH$ crystallizes in a monoclinic structure in the $P2_1/c$ space group. The features observed in the crystal structure does not differ much from that of the $Ph(Cy)_3Br$. The C-S bond length is 1.8 Å while the S-H bond length is 1.55 Å. The distance between the S-atom and the *ortho* hydrogens on cyclohexyl groups is 2.6 Å on average. This indicates that there is no hydrogen bonding in the molecule, as expected. The thiol H-atom is di[illegible]ostituents. Instead, it is pointed to the spa

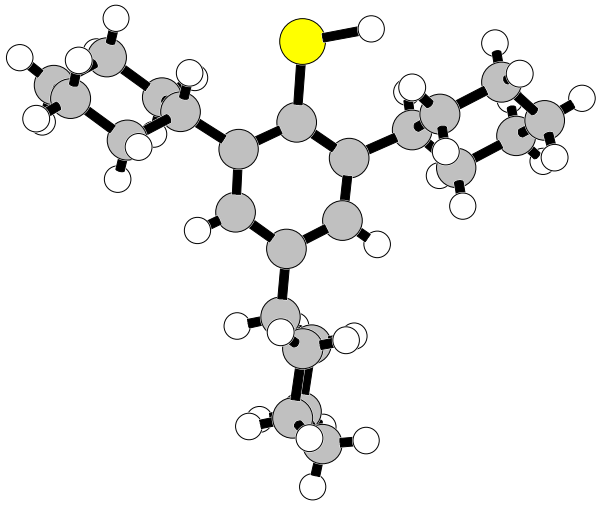

Figure 2.12: Crystal Structure of $Ph(Cy)_3SH$

Table 2.1: Selected Crystallographic Data for $Ph(Cy)_3Br$ & $Ph(Cy)_3SH$

		$Ph(Cy)_3Br$	$Ph(Cy)_3SH$
Bond Distance (Å)	C(1) – Br(1)	1.921(7)	N/A
	C(1) – S(1)	N/A	1.788(2)
	S(1) – H(1)	N/A	1.542(1)
Bond Angle (°)	Br(1) – C(1) – C(2)	118.14(6)	N/A
	S(1) – C(1) – C(2)	N/A	119.95(4)
	H(1) – S(1) – C(1)	N/A	104.39(2)

Table 2.2: Crystallographic Parameters for $Ph(Cy)_3X$ reagents (X = Br, SH)

	$Ph(Cy)_3Br$	$Ph(Cy)_3SH$
Empirical Formula	$C_{24}H_{35}Br$	$C_{24}H_{36}SH$
Formula Weight	403.4	356.6
Crystal System	monoclinic	monoclinic
Space Group	$P2_1/c$	$P2_1/c$
a (Å)	15.64(9)	15.61(8)
b (Å)	11.94(0)	11.95(1)
c (Å)	11.44(9)	11.44(9)
α (°)	90.0	90.0
β (°)	99.95(3)	100.14(1)
γ (°)	90.0	90.0
Z	4	4
Cell Volume ($Å^3$)	2106.7	2103.8
Crystal Color	white	white
Crystal Dimensions (mm)	0.5 x 0.4 x 0.2	0.5 x 0.3 x 0.2
Crystal Morphology	plate	plate
Calc. Density (g cm^{-3})	1.27(2)	1.12(6)
F_{000}	856	784
μ (mm^{-1})	1.95(5)	0.15(8)
R_{obs}	0.037(6)	0.021(5)
Temperature (K)	293(2)	293(2)
θ range (°)	1.3 – 28.3	1.3 – 28.3
Radiation (Mo Kα)	0.71073	0.71073

As expected, the UV-Vis spectra (Figure 2.13) of the ligands do not show any characteristic bands in the visible region. The band at 230 nm corresponds to π → π* transition. With S-based ligands the bands are shifted and accompanied by a shoulder.

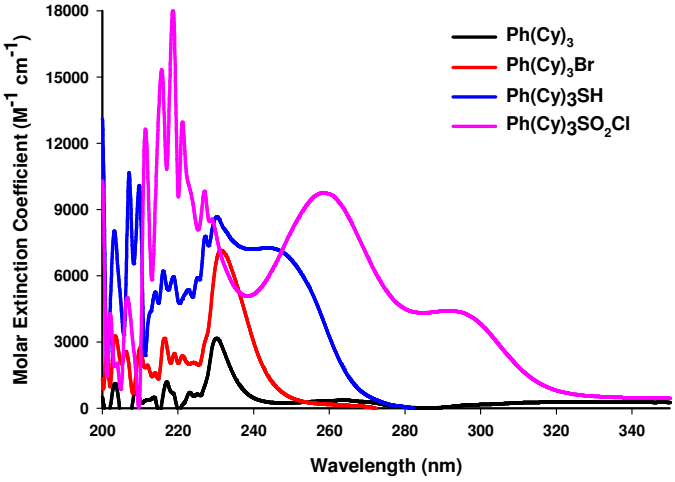

Figure 2.13: Electron Absorption Spectra of $Ph(Cy)_3X$ (X = H, Br, SH, SO_2Cl)

2.4.2 Comparison: $Ph(Cy)_3X$ Reagents with $Ph(Ph)_3X$ Reagents

Comparing the synthetic schemes for triphenyl analogues, ease of synthesis is obvious (Figure 2.14). Thus, the $Ph(Cy)_3X$ reagents are more readily accessible than the $Ph(Ph)_3X$ reagents. The large-scale synthesis of the $Ph(Ph)_3X$ reagents is not practically much viable owing to the number of steps involved.

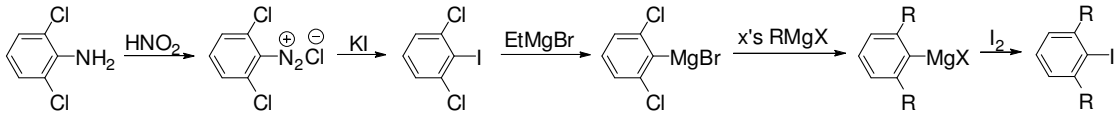

Figure 2.14: Synthesis of $Ph(Ph)_3X$ Analogues

The triphenylbromobenzene does not react with magnesium to form Grignard reagents.[47] So, the synthesis of the bulky thiol $Ph(Ph)_3SH$ requires a different method that includes Newman-Kurtman rearrangement of O-aryl dialkylthiocarbamate derivatives to O-aryl-S-aryl thiocarbonates (Figure 2.15).[48,49] The inherent problem is that the maximum yield will always be 50%. But the $Ph(Cy)_3SH$ can be produced in 60% yield. Also, due to the involvement of high heating to facilitate the rearrangement reactions, there are chances of decomposition of the products. In contrast, the $Ph(Cy)_3SH$ reagent can be obtained by a cleaner synthetic pathway.

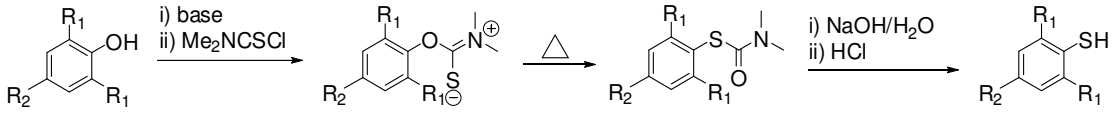

Figure 2.15: Synthesis of Substituted Aryl Thiols

2.4.3 Monomeric Metal Thiolate Chemistry

2.4.3.1 Synthesis of Monomeric Metal Thiolate Compounds

Monomeric metal thiolate complexes of the type $[M(SAr)_4]^{n-}$ (n = 1, 2) can be directly synthesized in a polar, aprotic medium by combining stoichiometric amount of

metal chloride salts and lithiated thiol ligands (Scheme 2.3).[9,10,44,50-52] The optimum choice of solvent is acetonitrile combining its polarity, aprotic nature and relatively high boiling point. Also, the lithium salts produced as by-products are insoluble in acetonitrile aiding easy separation and recrystallization of the desired products.

$$5\ Ph(Cy)_3SH + 5\ n\text{-}BuLi \rightarrow 5\ Ph(Cy)_3SLi + 5\ \textit{n}\text{-}BuH$$

$$4\ Ph(Cy)_3SLi + MCl_2{\bullet}6H_2O + 2\ Et_4NBr \rightarrow [Et_4N]_2[M^{II}(SPh(Cy)_3)_4] + 2\ LiCl + 2\ LiBr$$

$$4\ Ph(Cy)_3SLi + FeCl_3{\bullet}6H_2O + Et_4NBr \rightarrow [Et_4N][Fe^{III}(SPh(Cy)_3)_4] + 3\ LiCl + LiBr$$

Scheme 2.3: Synthesis of Metal-Thiolate Monomers

2.4.3.2 Electron Absorption Spectroscopy of Monomeric Metal Thiolate Compounds

The electronic absorption spectrum (Figure 2.16) of the isolated products – $[M(SAr)_4]^{2-}$ (M = Fe, Co, Ni) Monomers – show that in the visible region of the spectrum, these compounds do not give very intense bands. In the UV region, all the compounds show an intense peak at 233 nm with an accompanying shoulder at 260 nm. This feature can be attributed to the $\pi \rightarrow \pi^*$ transition associated with benzene ring of the thiolate ligand.

The $[Fe^{III}(SPh(Cy)_3)_4]^-$ complex in CH_3CN shows an intense band at 450 nm that is characteristic of these complexes arising from S → Fe charge transfer (Figure 2.17). In the UV-range, the spectra is similar to that of the $[M(SAr)_4]^{2-}$ complexes. Electronic optical properties in solution for the similar model compounds show that these compounds fall in the same region of wavelength and molar extinction coefficient values (Table 2.3). The electronic absorption bands of the model compounds show near to where the native, wild type enzyme shows (*Clostridium pasteurianum* – 380 & 490 nm; *Desulfovibrio gigas* 370 & 507 nm).

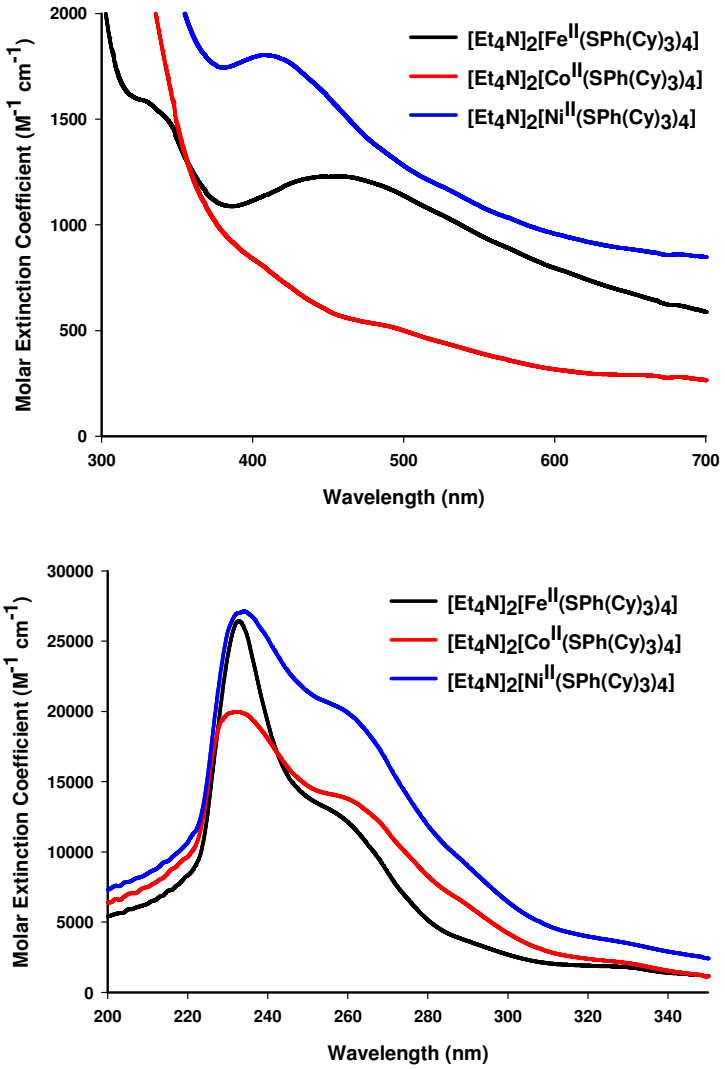

Figure 2.16: Electronic Absorption Spectra of $[M(SAr)_4]^{2-}$ (M = Fe, Co, Ni)

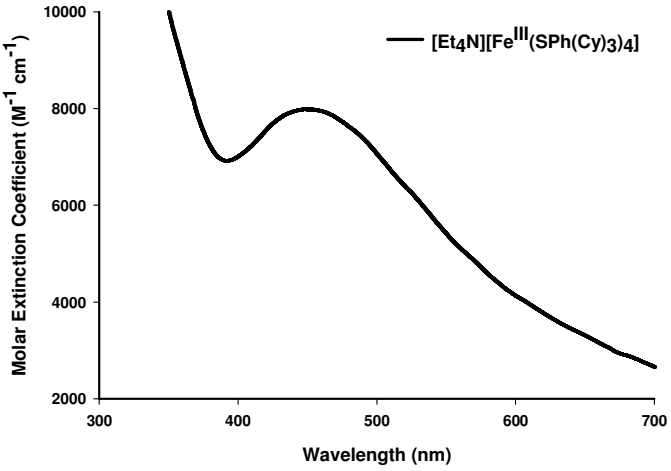

Figure 2.17: Electronic Absorption Spectra of $[Fe^{III}(SAr)_4]^-$ Monomer

Table 2.3: Electronic Absorption Features of Selected $[Fe(SAr)_4]^-$ Monomer

Compound	λ_{max} (nm) ($\varepsilon_{M;}$ M^{-1} cm^{-1})	λ_{max} (nm) ($\varepsilon_{M;}$ M^{-1} cm^{-1})
$[Fe^{III}(SPh)_4]^{2-}$	342 (18,000); sh 387 (12,4000)	556 (10,000)
$[Fe^{III}(SPh(Me)_4)_4]^{2-}$	295 (14,300); 344 (6880)	450 (7230)
$[Fe^{III}(SPh(i\text{-}Pr)_3)_4]^{2-}$	sh 288 (11,300); 347 (8870)	470 (12,500)
$[Fe^{III}(SPh(Cy)_3)_4]^{2-}$	229 (1000); sh 260 (267)	452 (7975)

2.4.3.3 Electrochemical Properties of Monomeric Metal Thiolate Compounds

Redox properties of these monomeric complexes could not be presented at this time. The compounds seem to decolorize at the slight contact with air.

2.4.4 Iron-Sulfur Tetrameric Clusters

2.4.4.1 Synthesis & ^{1}H NMR of Iron-Sulfur Tetrameric Clusters

The $[Fe_4S_4(SPh(Cy)_3)_4]^{2-}$ tetramer was synthesized by an exchange reaction of the lithiated thiolate with the chloro tetramer (Scheme 2.4).[30] The by-product of exchange reaction is lithium chloride, which is insoluble in acetonitrile and removed by simple filtration. The $[Fe_4S_4(SPh(Cy)_3)_4]^{2-}$ tetramer precipitated out as a black powder.

$$12\ Na + 12\ EtOH \rightarrow 12\ NaOEt + 6H_2$$

$$12\ PhSH + 12\ NaOEt \rightarrow 12\ PhSNa + 12\ EtOH$$

$$8\ FeCl_2{\bullet}4H_2O + 12\ PhSNa + S_8 + 4\ [n\text{-}Bu_4N]Cl \rightarrow 2[n\text{-}Bu_4N]_2[Fe_4S_4Cl_4] + 6Ph_2S_2 + 12\ NaCl$$

$$8\ Ph(Cy)_3SH + 8\ n\text{-}BuLi \rightarrow 8\ Ph(Cy)_3SLi + 8\ n\text{-}BuH$$

$$2[n\text{-}Bu_4N]_2[Fe_4S_4Cl_4] + 8\ Ph(Cy)_3SLi \rightarrow 2[n\text{-}Bu_4N]_2[Fe_4S_4(SPh(Cy)_3)_4] + 8\ LiCl$$

Scheme 2.4: Synthesis of $[Fe_4S_4(SPh(Cy)_3)_4]^{2-}$ Tetramer

The ^{1}H NMR of $[Fe_4S_4(SPh(Cy)_3)_4]^{2-}$ shows no –S*H* peak at 3.00 ppm. The aromatic peaks shifted from 6.94 ppm to 7.9 ppm in the metal complex (Figure 2.18). This clearly indicates Fe-S bonding which, in turn, is responsible for the downfield shift of the aromatic protons.

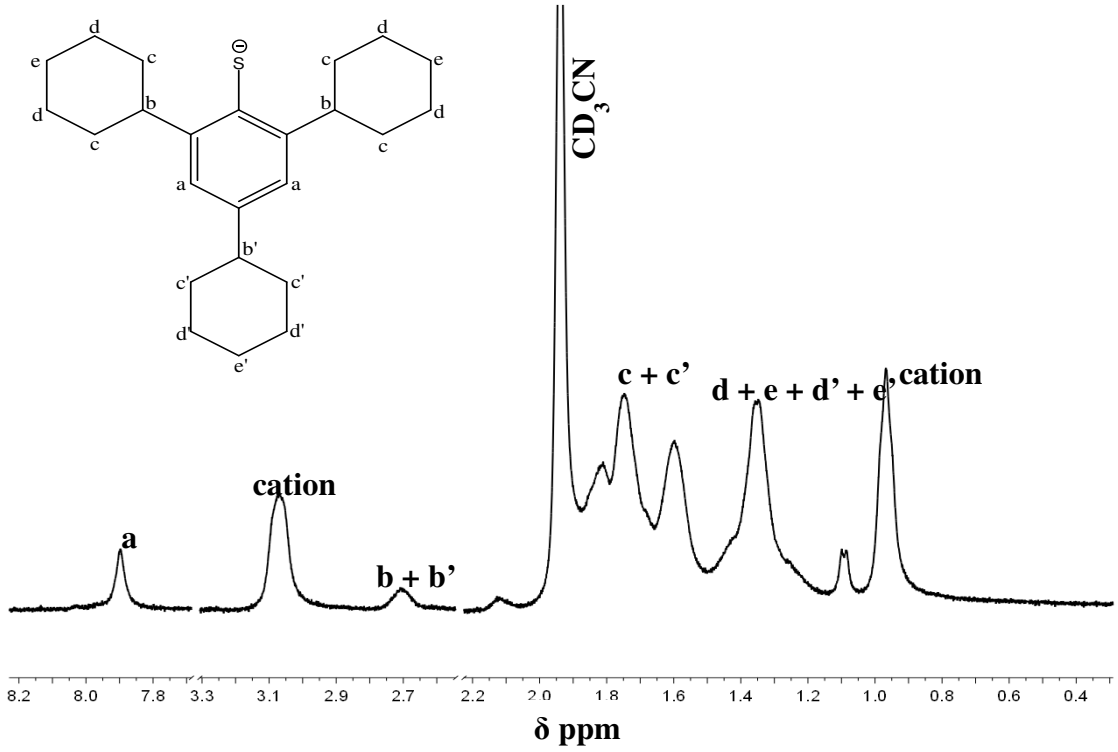

Figure 2.18: ^{1}H NMR of $[Fe_4S_4(SPh(Cy)_3)_4]^{2-}$ Tetramer

2.4.4.2 Electron Absorption Spectroscopy of Iron-Sulfur Tetrameric Clusters

As a part of the physical characterization of the metal complexes, the electronic absorption spectrum of both chloro- and thiolato-tetramer have been recorded in dichloromethane and acetonitrile respectively (Figure 2.19). The thiolato tetramer has intense peaks in the 400 – 700 nm region. This is the range where biologically important proteins such as ferredoxin and high potential proteins appear.[53] The *Bacillus stearothermophilus* ferredoxin and *Bacillus thermoproteolyticus* ferredxoin show absorption maxima at 390 nm. For $[Fe_4S_4Cl_4]^{2-}$ in CH_2Cl_2, two peaks (690 nm, 513 nm) and a shoulder (275 nm),[45] whereas, for $[Fe_4S_4(S\text{-}Ph(Cy)_3)_4]^{2-}$ in CH_3CN, two peaks (414 nm, 339 nm) and two shoulders (246 nm, 207 nm) was observed.

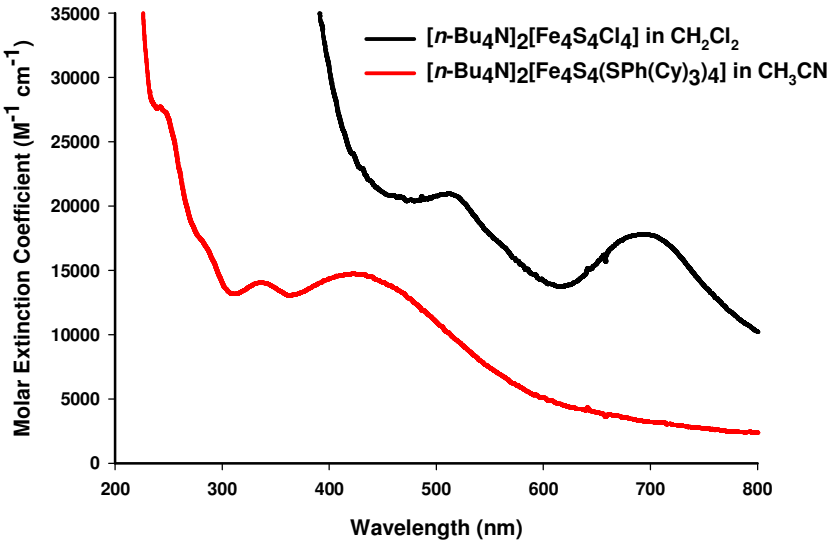

Figure 2.19: Electronic Absorption Spectra of Chloro- and Thiolato-Tetramers

The appearance of peaks in this region indicates the viability of the compound as synthetic model for Fe-S cluster (Table 2.4).[20-24,30] The absorption maxima in this region is attributed to S → Fe charge transfer bands.[26]

Table 2.4: Electronic Absorption Features of Selected $[Fe_4S_4(SAr)_4]^{2-}$ Moieties

Compound	λ_{max} (nm) (ε_M; M^{-1} cm^{-1})	λ_{max} (nm) (ε_M; M^{-1} cm^{-1})
$[Fe_4S_4(SPh)_4]^{2-}$	260 (45,000)	457 (17,700)
$[Fe_4S_4(SCH_2Ph)_4]^{2-}$	sh 280 (27,000)	420 (18,000)
$[Fe_4S_4(SPh(Me)_4)_4]^{2-}$	sh 245 (42,300); 342 (18,200)	414 (22,200)
$[Fe_4S_4(SPh(iPr)_3)_4]^{2-}$	sh 245 (52,800); 335 (19,400)	410 (24,500)
$[Fe_4S_4(SPh(Cy)_3)_4]^{2-}$	sh 246 (12,500); 339 (14,060)	414 (14,680)

2.4.4.3 Electrochemical Properties of Iron-Sulfur Tetrameric Clusters

Redox properties of the $[Fe_4S_4(SPh(Cy)_3)_4]^{2-}$ tetramer was studied in CH_2Cl_2 solvent medium (Figure 2.20). The 2-/3- core oxidation change is observed around -1.3 V, in agreement with other similar models. The peak at ~-2.0 V can be attributed to the formation of $[Fe_4S_4]^{+}$ core. Unfortunately, it is not reversible. The reversible peak at $E_{½}$ -0.38 V is due to 1-/2- core oxidation states.

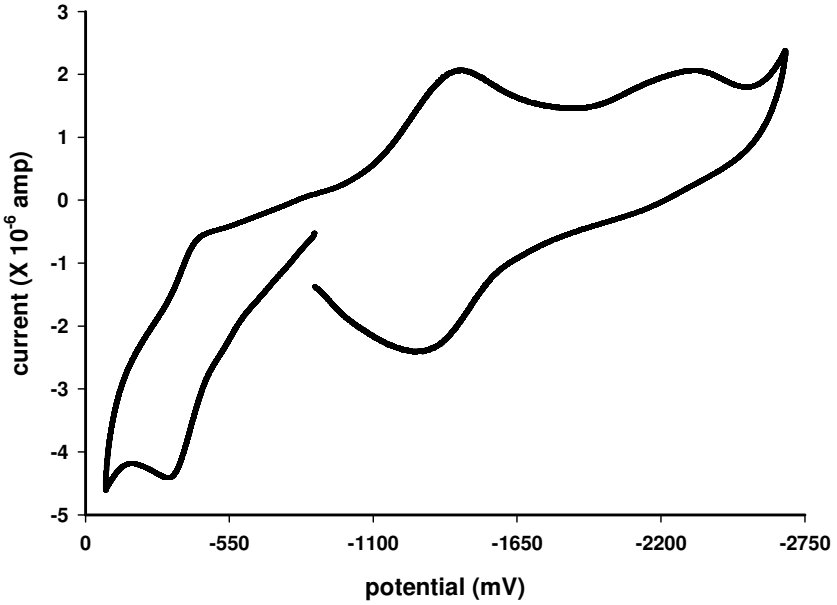

Figure 2.20: CV of $[Fe_4S_4(SPh(Cy)_3)_4]^{2-}$ in CH_2Cl_2

Comparing the redox behavior of the similar model compounds with the 2,4,6-tricyclohexylbenzenethiol analogue (Table 2.5), it can be seen that the E½ value for 2-/3- core conversion is in the same range. The more the electron donating property of the susbtituents on the benzenethiol, more negative the potential. This is because due to increased electron density, the core is easier to oxidize (Figure 2.21).

Table 2.5: Redox Properties of Selected $[Fe_4S_4(SAr)_4]^{2-}$ Moieties (vs. SCE)

Compound	E½ (V)	solvent
$[Fe_4S_4(SPh)_4]^{2-}$	-1.00	CH_2Cl_2
$[Fe_4S_4(SCH_2Ph)_4]^{2-}$	-1.22	PhCN
$[Fe_4S_4(SPh(Me)_4)_4]^{2-}$	-1.10	CH_2Cl_2
$[Fe_4S_4(SPh(i\text{Pr})_3)_4]^{2-}$	-1.20	CH_2Cl_2
$[Fe_4S_4(SPh(Cy)_3)_4]^{2-}$	-1.36	CH_2Cl_2

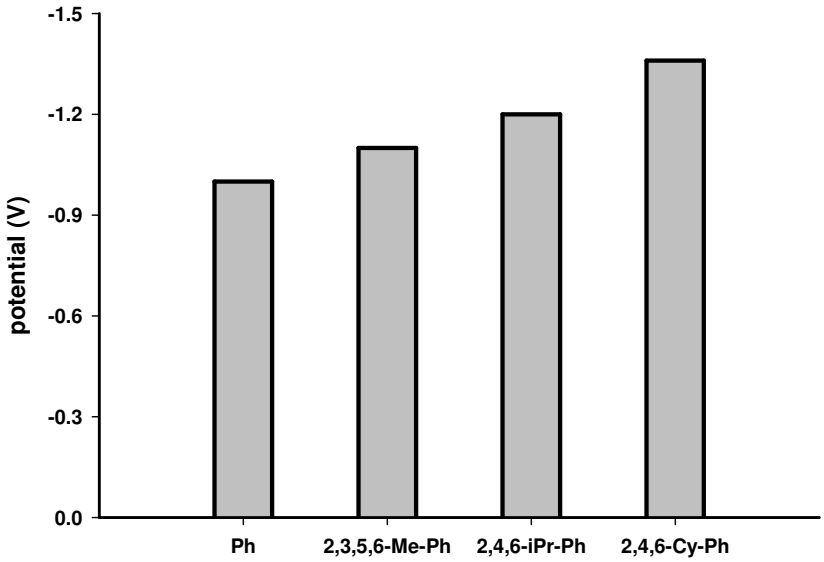

Figure 2.21: Correlation of $E_{½}$ to +I Effect of Substituents

The $[Fe_4S_4]^{2+}$ core can essentially show a variety of redox behavior. Starting from $[Fe_4S_4]^{0}$ i.e., an all ferrous analogue to $[Fe_4S_4]^{4+}$ i.e., an all ferric analogue are possible. The extreme redox states are difficult to achieve owing to their high reactivity towards solvent and/or dioxygen.[27] The most stable states of the core are $[Fe_4S_4]^{+}$ ($3Fe^{2+}$, Fe^{3+}), $[Fe_4S_4]^{2+}$ ($2Fe^{2+}$, $2Fe^{3+}$) and $[Fe_4S_4]^{3+}$ (Fe^{2+}, $3Fe^{3+}$). Although, $[Fe_4S_4]^{3+}$ core stability is highly dependent on solvent polarity and steric bulk of the thiolate ligand being used to construct the clusters.[28,29]

2.5 Conclusions & Future Work

In the conclusion, it can be said that a series of sterically hindered symmetric trisubstituted phenyl ligands, such as the 2,4,6-tricyclohexylbenzene reagents [$Ph(Cy)_3X$ where X = -H, -Br, -SH] have been synthesized for the first time. Except for the $Ph(Cy)_3Br$ compound, none of the other derivatives are reported in the literature. In all cases the pure product can be isolated with a >50% yield. Comparing the ease of synthesis with symmetric triphenyl analogues, tricyclohexyl compounds show this series to be a very practical approach for synthesis of sterically hindered ligands. The crystal structures of the native ligands proved more insight for the steric bulk associated with the ligand. All the new compounds have been characterized by ^1H & ^{13}C NMR spectroscopy in $CDCl_3$, IR spectroscopy by KBR pellet method and UV-VIS spectroscopy in $CHCl_3$. The NMR and crystal structure clearly shows that the two *ortho* cyclohexyl groups are symmetry related but with the *para* substituted cyclohexyl ring being unique. Metal complexes, such as, $[Fe_4S_4(SPh(Cy)_3)_4]^{2-}$, $[M(SPh(Cy)_3)_4]^{n-}$ (n = 1, 2) (M = Fe, Co, Ni) type to mimic biologically relevant compounds has been synthesized using $Ph(Cy)_3SH$. The compound has been characterized by UV-VIS and ^1H NMR spectroscopy.

Future work includes but is not limited to (a) structural characterization of the $[Fe_4S_4(SPh(Cy)_3)_4]^{n-}$ (n = 1, 2) tetramer complex; (b) electrochemical characterization of $[Fe_4S_4(SPh(Cy)_3)_4]^{n-}$ (n = 1, 2) tetramer complex; (c) structural characterization of metal complexes of the type $[M(SPh(Cy)_3)_4]^{n-}$ (n = 1, 2) (M = Fe, Co, Ni).

2.6 References

(1) Kiley, P. J.; Beinert, H. *Curr. Opin. Microbiol.* **2003**, *6*, 181.

(2) Lippard, S. J. *Acc. Chem. Res.* **1973**, *6*, 282.

(3) Watenpaugh, K. D.; Sieker, L. C.; Herriot, J. R.; Jensen, L. H. *Acta. Cryst. B.* **1973**, *B29*, 943.

(4) Sieker, L. C.; Stenkamp, R. E.; Jensen, L. H.; Prickril, B.; LeGall, J. *FEBS Lett.* **1986**, *208*, 73.

(5) Lane, R. W.; Ibers, J. A.; Frankel, R. B.; Papaefthymiou, G. C.; Holm, R. H. *J. Am. Chem. Soc.* **1977**, *99*, 84.

(6) Lane, R. W.; Ibers, J. A.; Frankel, R. B.; Holm, R. H. *Proc. Natl. Acad. Sci.* **1975**, *72*, 2868.

(7) Holah, D. G.; Coucouvanis, D. *J. Am. Chem. Soc.* **1975**, *97*, 6917.

(8) Swenson, D.; Baenzinger, N. C.; Coucouvanis, D. *J. Am. Chem. Soc.* **1978**, *100*, 1932.

(9) Millar, M.; Lee, J. F.; Koch, S. A.; Fikar, R. *Inorg. Chem.* **1982**, *21*, 4106.

(10) Millar, M.; Koch, S. A.; Fikar, R. *Inorg. Chim. Acta.* **1984**, *88*, L15.

(11) Silver, A.; Koch, S. A.; Millar, M. *Inorg. Chim. Acta.* **1993**, *205*, 9.

(12) Nguyen, T.; Panda, A.; Olmstead, M. M.; Richards, A. F.; Stender, M.; Brynda, M.; Power, P. P. *J. Am. Chem. Soc.* **2005**, *127*, 8545.

(13) MacDonnell, F. M.; Ruhlandt-Senge, K.; Ellison, J. J.; Holm, R. H.; Power, P. P. *Inorg. Chem.* **1995**, *34*, 1815.

(14) Rees, D. C.; Howard, J. B. *Science* **2003**, *300*, 929.

(15) McRee, D. E.; Richardson, D. C.; Richardson, J. S.; Siegel, L. M. *J. Biol. Chem.* **1986**, *261*, 10277.

(16) Moulis, J.-C.; Sieker, L. C.; Wilson, K. S.; Dauter, Z. *Prot. Sci.* **1996**, *5*, 1765.

(17) Strop, P.; Takahara, P. M.; Chiu, H.-J.; Angove, H. C.; Burgess, B. K.; Rees, D. C. *Biochem.* **2001**, *40*, 651.

(18) Rao, P. V.; Holm, R. H. *Chem. Rev.* **2004**, *104*, 527.

(19) Herskovitz, T.; Averill, B. A.; Holm, R. H.; Ibers, J. A.; Phillips, W. D.; Weiher, J. F. *Proc. Natl. Acad. Sci.* **1972**, *69*, 2437.

(20) Averill, B. A.; Herskovitz, T.; Holm, R. H.; Ibers, J. A. *J. Am. Chem. Soc.* **1973**, *95*, 3523.

(21) Bobrik, M. A.; Que Jr., L.; Holm, R. H. *J. Am. Chem. Soc.* **1974**, *96*, 285.

(22) Holm, R. H.; Phillips, W. D.; Averill, B. A.; Mayerle, J. J.; Herskovitz, T. *J. Am. Chem. Soc.* **1974**, *96*, 2109.

(23) DePamphilis, B. V.; Averill, B. A.; Herskovitz, T.; Que Jr., L.; Holm, R. H. *J. Am. Chem. Soc.* **1974**, *96*, 4159.

(24) Que Jr., L.; Bobrik, M. A.; Ibers, J. A.; Holm, R. H. *J. Am. Chem. Soc.* **1974**, *96*, 4168.

(25) Lawson Daku, L. M.; Pecaut, J.; Lenormand-Foucaut, A.; Vieux-Melchoir, B.; Ivenson, P.; Jordanov, J. *Inorg. Chem.* **2003**, *42*, 6824.

(26) Ueyama, N.; Yamada, Y.; Okamura, T.; Kimura, S.; Nakamura, A. *Inorg. Chem.* **1996**, *35*, 6473.

(27) Tanaka, K.; Tanaka, T.; Kawafune, I. *Inorg. Chem.* **1984**, *23*, 518.

(28) Ohno, R.; Ueyama, N.; Nakamura, A. *Chem. Lett.* **1989**, 399.

(29) Blonk, H. L.; Kievit, O.; Roth, E. K. H.; Jordanov, J.; van der Linden, J. G. M.; Steggerda, J. J. *Inorg. Chem.* **1991**, *30*, 3231.

(30) O'Sullivan, T.; Millar, M. M. *J. Am. Chem. Soc.* **1985**, *107*, 4096.

(31) Ohki, Y.; Tanifuji, K.; Yamada, N.; Imada, M.; Tajima, T.; Tatsumi, K. *Proc. Natl. Acad. Sci.* **2011**, *108*, 12635.

(32) Tanifuji, K.; Yamada, N.; Tajima, T.; Sasamori, T.; Tokitoh, N.; Matsuo, T.; Tamao, K.; Ohki, Y.; Tatsumi, K. *Inorg. Chem.* **2014**, *53*, 4000.

(33) Olmstead, M. M.; Power, P. P. *J. Organomet. Chem.* **1991**, *408*, 1.

(34) Ruhlandt-Senge, K.; Power, P. P. *Bull. Soc. Chim. Fr.* **1992**, *129*, 594.

(35) Ellison, J. J.; Power, P. P. *J. Organomet. Chem.* **1996**, *1996*, 263.

(36) Sigel, G. A.; Power, P. P. *Inorg. Chem.* **1987**, *26*, 2819.

(37) Schiemenz, B.; Power, P. P. *Organomet.* **1996**, *15*, 958.

(38) Corson, B. B.; Ipatieff, V. N. *J. Am. Chem. Soc.* **1937**, *59*, 645.

(39) Pearson, D. E.; Frazer, M. G.; Frazer, V. S.; Washburn, L. C. *Synthesis* **1976**, *138*, 621.

(40) Reid, J. R.; Dufresne, R. F.; Richard, F.; Chapman, J. J. *Org. Synth. Coll.* **1997**, *74*, 217.

(41) Roger, M.; Barros, N.; Arliguie, T.; Thuery, P.; Maron, L.; Ephritikhine, M. *J. Am. Chem. Soc.* **2006**, *128*, 8790.

(42) Blower, P. J.; Dilworth, J. R.; Hutchinson, J.; Nicholson, T.; Zubieta, J. A. *J. Chem. Soc. Dalton Trans.* **1985**, 2639.

(43) Blower, P. J.; Dilworth, J. R.; Hutchinson, J.; Zubieta, J. A. *J. Chem. Soc. Dalton Trans.* **1985**, 1533.

(44) Koch, S. A.; Fikar, R.; Millar, M.; O'Sullivan, T. *Inorg. Chem.* **1984**, *23*, 122.

(45) Wong, G. B.; Bobrik, M. A.; Holm, R. H. *Inorg. Chem.* **1978**, *17*, 578.

(46) Mague, J. T.; Linhardt, L.; Fink, M. J. *Acta. Cryst. E.* **2008**, *E64*, o335.

(47) Kohler, E. P.; Blanchard Jr, L. W. *J. Am. Chem. Soc.* **1935**, *54*, 367.

(48) Bishop, P. T.; Dilworth, J. R.; Zubieta, J. A. *J. Chem. Soc. Dalton Trans.* **1985**, 257.

(49) Newman, M. S.; Karnes, H. A. *J. Org. Chem.* **1966**, *31*, 3980.

(50) Koch, S. A.; Maelia, L. E.; Millar, M. *J. Am. Chem. Soc.* **1983**, *105*, 5944.

(51) Hagen, K. S.; Holm, R. H. *Inorg. Chem.* **1984**, *23*, 418.

(52) Rosenfield, S. G.; Armstrong, W. H.; Mascharak, P. K. *Inorg. Chem.* **1986**, *25*, 3014.

(53) Ragsdale, S. W.; Ljungdahl, L. G. *J. Bacteriol.* **1984**, *157*, 1.

Chapter 3:

Structural Modelling of i) α-Diimine ii) Pyridine Bisanil Complexes using 2,4,6-Tricyclohexyl-aninline

3.1 Introduction

3.1.1 General Introduction

In our effort to extend the 1,3,5-tricyclohexylbenzene moiety beyond the metal thiolate chemistry, we have explored the N-atom bearing ligand to search for compounds relevant to olefin polymerization catalysts.

3.1.2 Bulky α-Diimine Metal Complexes

In the middle of the 1990s, Brookhart and co-workers have reported a novel type of olefin polymerization catalysts.[1] These catalysts were based on Ni(II) and Pd(II) complexes with halides and α–diimines. The polyethenes produced using these catalyst showed products from being highly linear to moderately branched. One of the factors governing the tendency to form either linear or branched polymers is the catalyst structure. If the bulkiness of the catalyst been reduced, more linear polymeric product with low molecular weight been formed.[2] The late transition metals (Fe, Co, Ni) have garnered more attention than the early transition metals in this catalytic field because they are less oxophilic and more tolerant towards functionalized olefins. So, a large variety of functionalized polymers can also be synthesized using these types of catalysts.

Brookhart and co-workers have reported α–diimines with the variations in both the aniline part as well as the diketone moiety (Figure 3.1). The various R-groups those are

being explored as *ortho* substituents on the aniline are methyl, ethyl, isopropyl, tertiary butyl, and phenyl. For the diketones, R-groups have been hydrogen, methyl, methoxy and fused phenyl ring systems as well.

Rieger and co-workers have reported α–diimine ligands with aniline moieties having *ortho* diphenyl substituents.[3] Owing to the presence of these groups on the *ortho* phenyl substituents, the axial approach of the incoming monomer was greatly hindered. This, in turn, facilitated the optimal coordination of the monomer to the Ni-center for the polymerization to proceed in the chain migration direction and not towards chain growth. The effect of the 4-Bu^t group has been described to be the dominant one (Figure 3.1).[4]

Gibson and co-workers have reported Cu-diimine catalysts (Figure 3.1) for olefin polymerization.[5] The *ortho* phenyl substituents yielded better result compared to the isopropyl substituents. This, once again, has proved the requirement of the bulky substituents at the *ortho* positions. Another reason for such an observation in activity could be the transition state being better stabilized by some kind of π–interaction of the phenyl rings with the metal center.

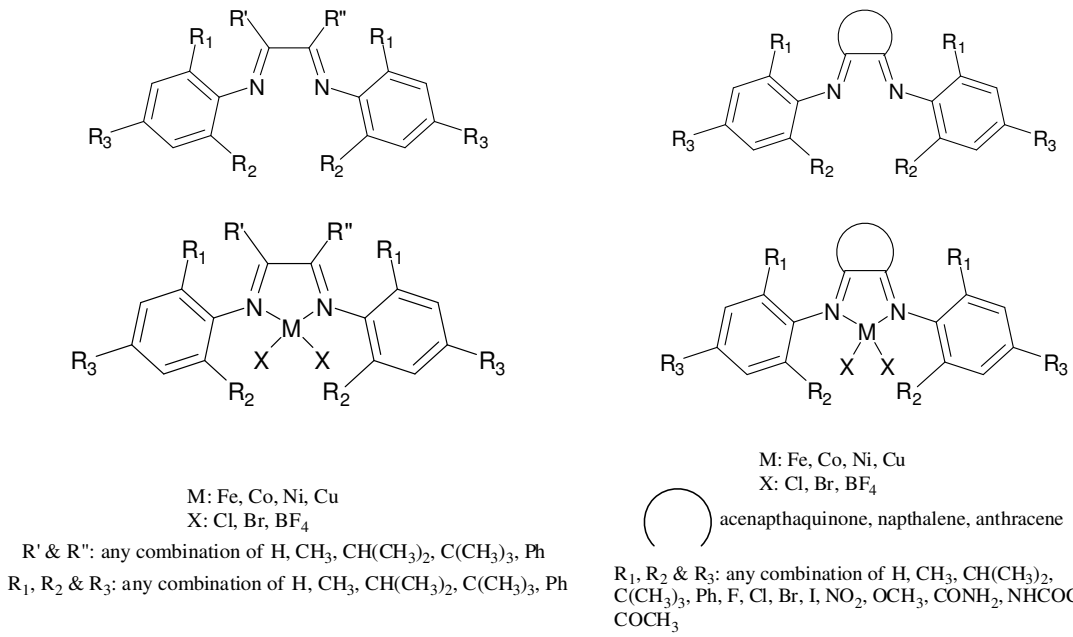

Figure 3.1: Representative α-diimine Ligands & Metal Complexes

3.1.3 Steric Pyridine Bisanil Metal Complexes

In the late 1990s, Brookhart and co-workers have reported a novel type of olefin polymerization catalyst with late transition metal (Fe, Co, Ni) complexes with a variety of pyridine bisanil ligands (Figure 3.2).[6] Subsequently, a thorough study by Gibson and coworkers delineated the ligand structure importance.[7] These compounds have garnered more attention than the early transition metals in this catalytic field because they are less oxophilic, and more tolerant towards functionalized olefins. So, a large variety of functionalized polymers can also be synthesized using these types of catalyst.[8]

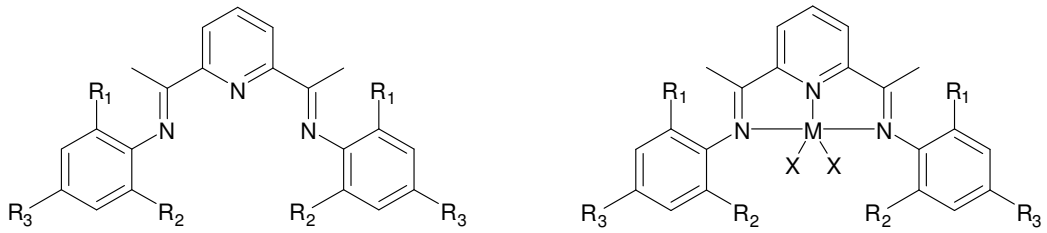

Figure 3.2: Representative Pyridine Bisanil Ligand & Metal Complexes

These catalysts require less harsh conditions as compared to the SHOP (Shell Higher Olefin Process) or aluminum alkyl processes, and are stable over a widetemperature range. The polymers produced from the olefins are highly dependent on both the metals and the ligand structure. It has been conclusively proved that the steric bulk at the *ortho*-position of the aniline derivatives in the ligand plays a crucial role.[6,7,9,10] The chain propagation is favored with electron-withdrawing groups, but the rate of chain transfer is favored over the same for propagate on if the *ortho*-positions have electron-donating groups. At the *para*-position, it is solely the steric factor to determine the catalyst activity. With both the *ortho*-positions occupied by bulky alkyl groups, the catalysts selectively produce high molecular weight polymers from ethane. The metal center also has a profound influence on the catalytic activity. In has been reported that, in general, the Fe(II) catalysts are more effective as compared to the Co(II) analogues. With the α-diimines, the nickel complexes showed the most promising result. Subsequently, a large portion of the pyridine bisanil ligand metal complex research was also focused on Ni(II) complexes.

3.2 Aim of the Project

In an effort to extend the steric capacity of *ortho*-methyl and *ortho*-isopropyl ligands we have sought out a new class of ligands which contain cyclohexyl substituents in the *ortho*-position (Figure 3.3). These should exhibit steric capacity analogous to that of the 2,6-diphenylbenzene derivatives, yet be more basic in their donor capacity. Our target compound was the 1-nitro-2,4,6-tricylohexylbenzene compound which was then reduced to 2,4,6-tricyclohexyl-aniline, a starting material for α-diimine ligands and pyridine bisanil ligand for metal ion complex formation.

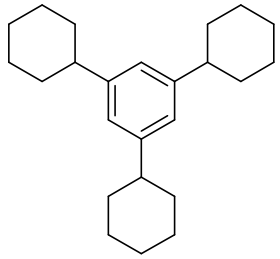

1,3,5-tricyclohexylbenzene

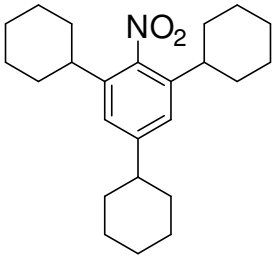

2,4,6-tricyclohexyl nitrobenzene

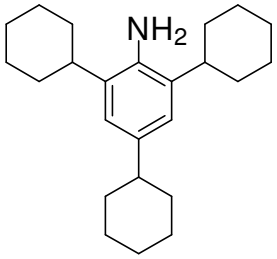

2,4,6-tricyclohexyl aniline

Figure 3.3: 2,4,6-Tricylohexylbenzene Moieties

3.3 Experimental

3.3.1 General Comments

Solvents were distilled according to literature procedures [methanol over Mg/I_2, tetrahydrofuran (THF) and diethyl ether (Et_2O) over Na/benzophenone, dichloromethane (DCM) over P_2O_5, acetonitrile (MeCN) over CaH_2], and stored under nitrogen before use. All the manipulations involving metal complexes were carried out under nitrogen in standard schlenk procedure unless and otherwise noted. The ^1H & ^{13}C NMR spectra were recorded on a Brüker 300 MHz instrument in $CDCl_3$ and standardized with residual solvent peak at 7.26 ppm and 77.23 ppm respectively. IR spectra were collected on a Thermo Fischer Scientific Nicolet iS10 by KBr pellet method. Electron absorption spectra were recorded on a Varian Cary 100 spectrophotometer in a 1 cm long quartz cell.. Wherever applicable, X-ray quality crystals were grown from suitable solvents using appropriate techniques.

3.3.2 Synthesis of 1,3,5 – Tricyclohexylbenzene [$Ph(Cy)_3$]

The compound was prepared according to a literature procedure.[11] 100.0 g (0.75 mol) of $AlCl_3$ and 333 mL (293.0 g, 3.76 mol) of anhydrous benzene taken in a 3-necked flask was evenly mixed with a mechanical stirrer for 10 minutes under closed condition. 1.22 L (987.4 g, 12.02 mol) of cyclohexene was added dropwise to this mixture over a period of 3 hours maintaining the temperature between 3°C to 18°C. After the addition was complete, the mixture was allowed to stir for overnight. The excess of $AlCl_3$ was quenched with 62.5 mL (12 M) HCl. The products were mixtures of monocyclohexylbenzene, 1,4-dicyclohexylbenzene, 1,3,5-tricyclohexylbenzene and 1,2,4,5-tetracyclohexylbenzene. The desired compound was recrystallized from acetone.

Yield 609 g (50%). ^{1}H NMR ($CDCl_3$) δ 6.89 (s, 3H, *Ar-H*), 2.47 (q, 3H, Ar-*CH_2*-), 1.2 – 1.8 (30H, cyclohexyl ring) ppm. ^{13}C NMR ($CDCl_3$) δ 148.0, 123.1, 45.0, 34.8, 27.3, 26.5 ppm. Crystals were grown by vapor diffusion method using diethyl ether/methanol.

3.3.3 Synthesis of 2,4,6 – Tricyclohexylnitrobenzene [$Ph(Cy)_3NO_2$]

The compound was prepared according to a modified literature procedure.[12-14] In a 100 mL round bottom flask was added 10.0 g (0.03 moles) of $Ph(Cy)_3$ in 40.0 mL of acetic anhydride just to cover the solid at 0 ºC. To a solution of 10.0 mL of acetic anhydride and 10.0 mL of acetic acid in an ice-bath 2.8 g fuming HNO_3 was slowly added. The acid mixture was added dropwise to the solution of $Ph(Cy)_3$ over a period of 20 minutes. The ice-bath was removed after complete addition of acid. The mixture was stirred overnight at room temperature with a moisture trap. The solution in flask was slowly poured in ice-cold water with stirring and the yellow solid obtained was filtered. The compound was air-dried. Yield 11.0 g (99.0%). ^{1}H NMR ($CDCl_3$) δ 7.02 (s, 2H, *Ar-m-H*), 2.51 (q, 1H, Ar-*p-CH_2*-), 2.39 (q, 2H, Ar-*o-CH_2*-), 1.2 – 1.8 (m, 30H, cyclohexyl ring) ppm. ^{13}C NMR ($CDCl_3$) δ 150.0, 149.0, 138.0, 123.3, 45.0, 39.9, 34.4, 27.0, 26.8, 26.2 ppm. Crystals were grown by vapor diffusion method using diethyl ether/methanol.

3.3.4 Synthesis of 2,4,6 – Tricyclohexylaniline [$Ph(Cy)_3NH_2$]

The compound was prepared according to a modified literature procedure.[14,15] In a 100 mL 3-necked flask, fitted with a condenser, was added 5.0 g (0.014 moles) of $Ph(Cy)_3NO_2$ in 100 mL of acetic and refluxed. HCl gas was passed through the solution under reflux. 3.55 g (0.054 moles) Zn dust was added in small portions over a period of 3 h. The solution was refluxed overnight. The excess of acetic acid was quenched by a KOH solution and the amine was extracted with ether. The organic layer was dried over Na_2SO_4

and the solvent was stripped off using a rotary evaporator. Yield 3.6 g (76.0%). ^{1}H NMR ($CDCl_3$) δ 6.86 (s, 2H, *Ar-m-H*), 3.4 – 3.7 (b, 2H, -N*H*$_2$), 2.4 – 2.6 (q, 3H, Ar-*o*/*p*-C*H*$_2$-), 1.2 – 2.0 (m, 30H, cyclohexyl ring) ppm. ^{13}C NMR ($CDCl_3$) δ 138.4, 138.2, 131.9, 121.9, 44.6, 39.3, 33.3, 27.5, 27.3, 26.7, 26.5 ppm. Crystals were grown by vapor diffusion method using diethyl ether/methanol.

3.3.5 Synthesis of [Glyoxal bis(2,4,6-tricyclohexylbenzene)diimine]

The compound was prepared according to a modified literature procedure.[1] In a 100 mL round-bottom flask was added 1.0 g (0.003 moles) of $Ph(Cy)_3NH_2$ in ~50 mL MeOH. 0.22 g of glyoxal (40wt% aq. solution) was added to it followed by 10 drops of HCO_2H. The mixture was stirred for overnight and then the yellow product was filtered. Yield 0.58 g (55.0%). ^{1}H NMR ($CDCl_3$, 25 ^{o}C) 8.1 (s, 2H, vinylic-*H*), 6.98 (s, 4H, *Ar-m-H*), 2.2 – 2.6 (q, 6H, Ar-*o*/*p*-CH_2-), 1.2 – 2.0 (m, 60H, cyclohexyl ring) ppm. ^{13}C NMR ($CDCl_3$, 25 ^{o}C) δ 163.4, 146.2, 144.6, 135.9, 122.4, 44.8, 39.2, 34.2, 27.4, 26.5 ppm. Crystals suitable for single crystal diffraction measurement were grown by vapor diffusion method using diethyl ether and methanol.

3.3.6 Synthesis of [Acenaphthenequinone bis(2,4,6-tricyclohexylbenzene)diimine]

The compound was prepared according to a modified literature procedure.[16] In a 100 mL round-bottom flask, fitted with a condenser, was added 0.54 g (3 mmoles) of acenaphthenequinone and 26 mL acetonitrile solvent. The mixture was refluxed for 30 min and then 5.4 mL of glacial acetic acid was added. The mixture was further refluxed until the entire solid was dissolved. 2.1 g (6.2 mmoles) of solid $Ph(Cy)_3NH_2$ was added to the solution and then refluxed for 24 h. The mixture was treated with excess NaOH to quench the acetic acid. The organic compound was extracted in methylene chloride and dried over anhydrous Na_2SO_4. The solvent was stripped off in rotary evaporator leaving an orange-brown solid.

The yellow-orange product obtained after cooling the solution or stripping off the solvent was filtered and dried in air. Yield 56.0%. ^{1}H NMR ($CDCl_3$, 25 ^{o}C) δ 6.4 – 7.8 (m, 10H, *Ar-H*), 2.6 (q, 6H, Ar-*o*/*p*-CH_2-), 1.0 – 2.0 (m, 68H, cyclohexyl rings) ppm. Crystals suitable for single crystal diffraction measurement were grown by vapor diffusion method using diethyl ether and methanol.

3.3.7 Synthesis of [Pyridine bis(2,4,6-tricyclohexylbenzene)diimine]

The compound was prepared according to a modified literature procedure.[7] In a 100 mL round-bottom flask, fitted with a condenser, was added 0.35 g (2.2 mmoles) of 2,6-diacetylpyridine and 1.5 g (4.4 mmoles) of solid $Ph(Cy)_3NH_2$ in 26 mL methanol solvent. The mixture was refluxed for 24 h with formic acid as a catalyst. The yellow product obtained after cooling the solution was filtered and dried in air. Yield 64.0%. ^{1}H NMR ($CDCl_3$, 25 ^{o}C) δ 8.45 (2H, d, Py-H_m), 7.92 (1H, t, Py-H_p), 7.12 (4H, m, Ph-H), 2.50 (4H, q, Ph-*o*-H), 2.42 (2H, q, Ph-*p*-H), 1.60 – 2.20 (60H, m, cyclohexyl ring) ppm. Crystals suitable for single crystal diffraction measurement were grown by vapor diffusion method using diethyl ether and methanol.

3.3.8 Metal-Diimine Complexes

These compounds were prepared according to a modified literature procedure.[17] Equimolar amounts of the hydrated metal chlorides ($MCl_2.6H_2O$; M = Co, Ni) and diimine ligands were dissolved in THF and stirred for overnight under inert atmosphere. The THF was removed *in vacuo* and CH_2Cl_2 was added to dissolve the residue. Microcrystalline precipitates were obtained by layering with Et_2O.

3.3.9 Metal-Pyridine Bisimine Complexes

These compounds were prepared according to a modified literature procedure.[18] Equimolar amounts of the hydrated metal chlorides ($MCl_2.6H_2O$; M = Co, Ni) and pyridine bisimine ligand were dissolved in THF and stirred for overnight under inert atmosphere. The THF was removed *in vacuo* and CH_2Cl_2 was added to dissolve the residue. Microcrystalline precipitates were obtained by layering with Et_2O.

3.3.10 X-ray Crystal Structure Determination

Cell parameters and data collection summaries for the complexes are given throughout the chapters. X–ray data of these complexes were collected on an Oxford single crystal X–ray diffractometer operating at 50 kV and 40 mA using Mo Kα (λ = 0.71073 Å) radiation. The X–ray diffractometer was operated using CrysAlisPro, version 171.33.66. All samples were collected at 100 K. The structure refinement was done with SHELXL–97 (Sheldrick).[19] All of the crystal structures were solved by direct methods using WinGX, version 1.80.05. Anisotropic refinement for all non–hydrogen atoms was done by a full–matrix least squares method.

3.4 Results & Discussion

3.4.1 Synthesis of the Ligands & the Metal Complexes

$Ph(Cy)_3$ was synthesized under no-air condition to arrest moisture destroying the catalyst $AlCl_3$ starting from commercially available materials. Nitration of $Ph(Cy)_3$ with fuming nitric acid in glacial acetic acid/acetic anhydride mixture affords $Ph(Cy)_3NO_2$ (Scheme 3.1).[12-14] If fuming HNO_3 was not used, the conversion was not that effective as the yield was only 65% and chromatographic separation was required. Various reagents that can be used for the reduction of $Ph(Cy)_3NO_2$ are Zn/HCl,[14,15] ultra-sound technique in combination with hydrazine/Raney-Ni,[20] sodium telluride,[21] sodium hydrogen telluride[22]. For maximum yield the Zn/HCl method was followed. But, aqueous HCl cannot be added as the nitro compound being hydrophobic, precipitates out of the solution even under reflux condition. Hence, HCl gas was passed through the solution.

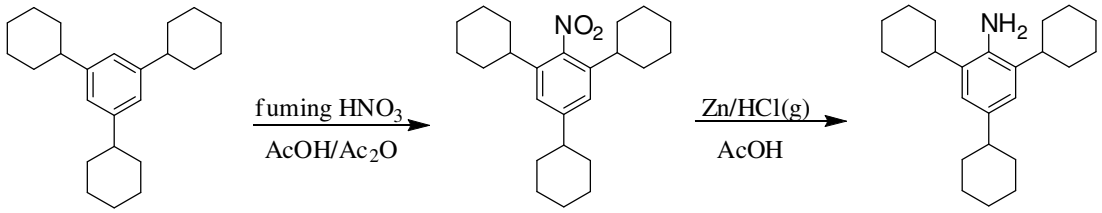

Scheme 3.1: Synthesis of Nitro & Amino Derivative of 1,3,5-tricyclohexylbenzene

The α-diimine compound with glyoxal (Scheme 3.2) was synthesized at room temperature. Literature reports have suggested that elevated temperature gives less than 10% yield.[23] For the synthesis of the acenapthaquinone based α-diimine ligand (Scheme 3.2), considering the steric nature of the amine used, the reflux time was set to 24 h. Increasing the time of reflux from 24 h to 48 h did not change the yield. Considering the steric nature associated with the amine [$Ph(Cy)_3NH_2$], the yield being ~60% is justified.

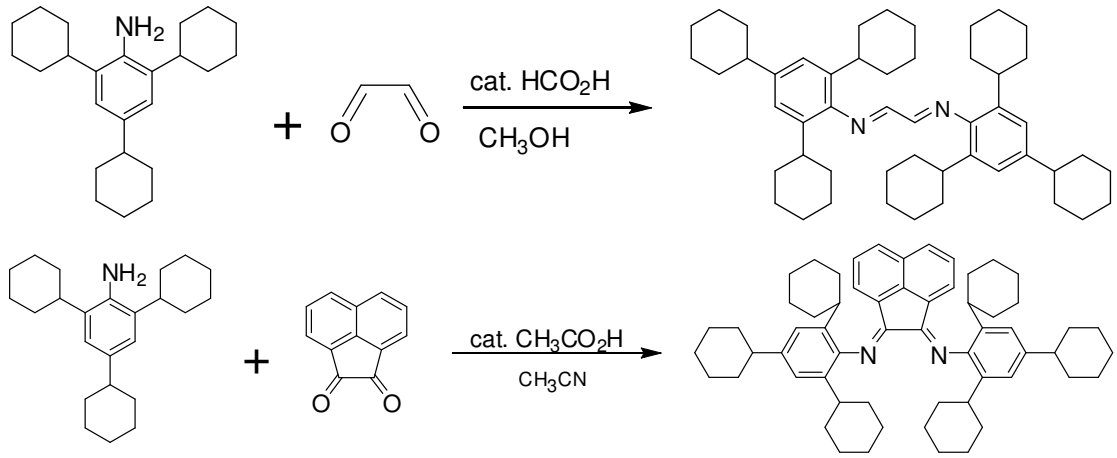

Scheme 3.2: Synthetic Scheme for α-Diimine Ligands
(Upper: glyoxal based ligands; Lower: acenapthaquinone based ligands)

Reaction of the amine with 2,6-diacetylpyridine in 2:1 equivalence ratio produced the triimine ligand - NNN-Cy (Scheme 3.3). The optimum reflux time is 24h. Lesser time gives low yields of the product but higher time does not increase the yield.

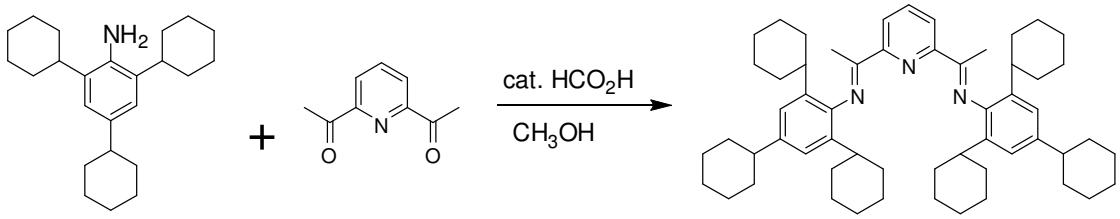

Scheme 3.3: Synthetic Scheme for Pyridine Bisanil Ligands

All the metal complexes can be synthesized in moderate yields by reaction of hydrated chloride salts of the metals and the ligand in 1:1 ratio in THF (Scheme 3.4 & 3.5). The complexes can be recrystallized from DCM/Et_2O solvent pair to give pure compounds.

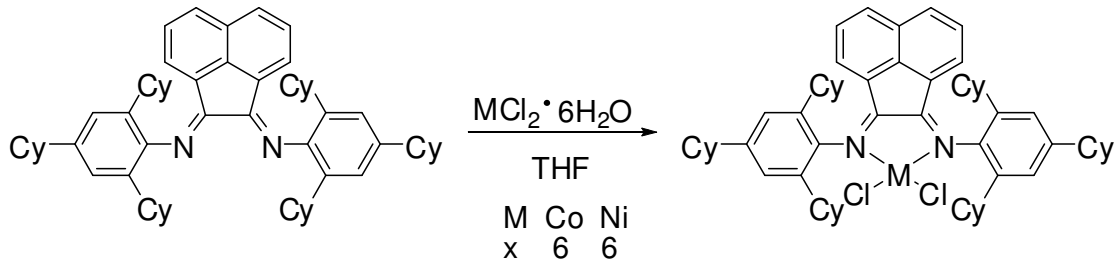

Scheme 3.4: Synthetic Scheme for α-Diimine Metal Complex

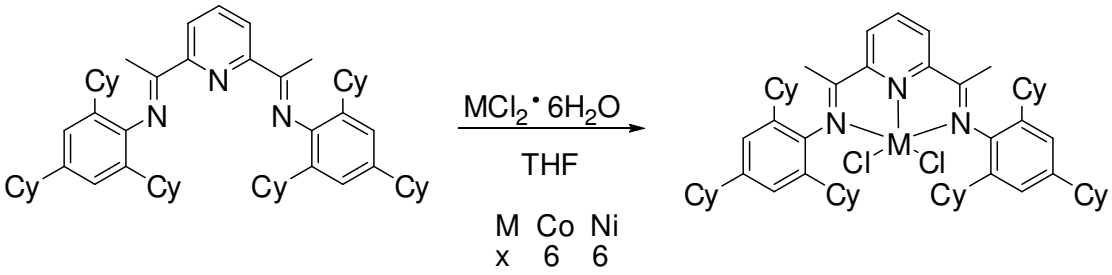

Scheme 3.5: Synthetic Scheme for Pyridine Bisanil Metal Complex

3.4.2 Comparison: $Ph(Cy)_3X$ Reagents with $Ph(Ph)_3X$ Reagents

For the synthesis of triphenylaniline (Figure 3.4)[24], The use of $Pd(PPh_3)_4$ reagent makes it very costly. But the $Ph(Cy)_3NH_2$ was synthesized using commercially available and cheap starting materials. The scheme shows a coupling reaction between phenylboronic acid and halogenated derivative of aniline. The purification step for these reactions requires chromatographic separation for the desired compound. Compared with Scheme 3.1, the $Ph(Cy)_3NH_2$ can be readily isolated in high yields by extraction with ether. The triphenylaniline must be synthesized under nitrogen atmosphere whereas, $Ph(Cy)_3NH_2$ can be synthesized in air, thereby increasing the ease of synthesis.

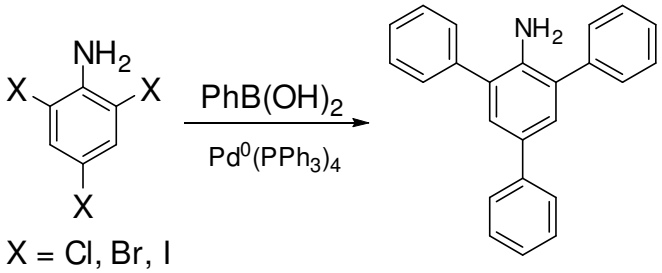

Figure 3.4: Synthesis of Triphenylaniline

3.4.3 Spectral Characterization of the Ligands & the Metal Complexes

The IR spectrum of the hydrocarbon shows the characteristic C-H bond stretching around 3000 cm^{-1} and this is also observed in both the nitro and the amino compounds (Figure 3.5). For the nitro compound, strong N-O stretching is found between 1500 and 1600 cm^{-1}; for the amino compound, C-N stretching appears around 1260 cm^{-1} and strong N-H scissoring bands appear around 1600 cm^{-1}.

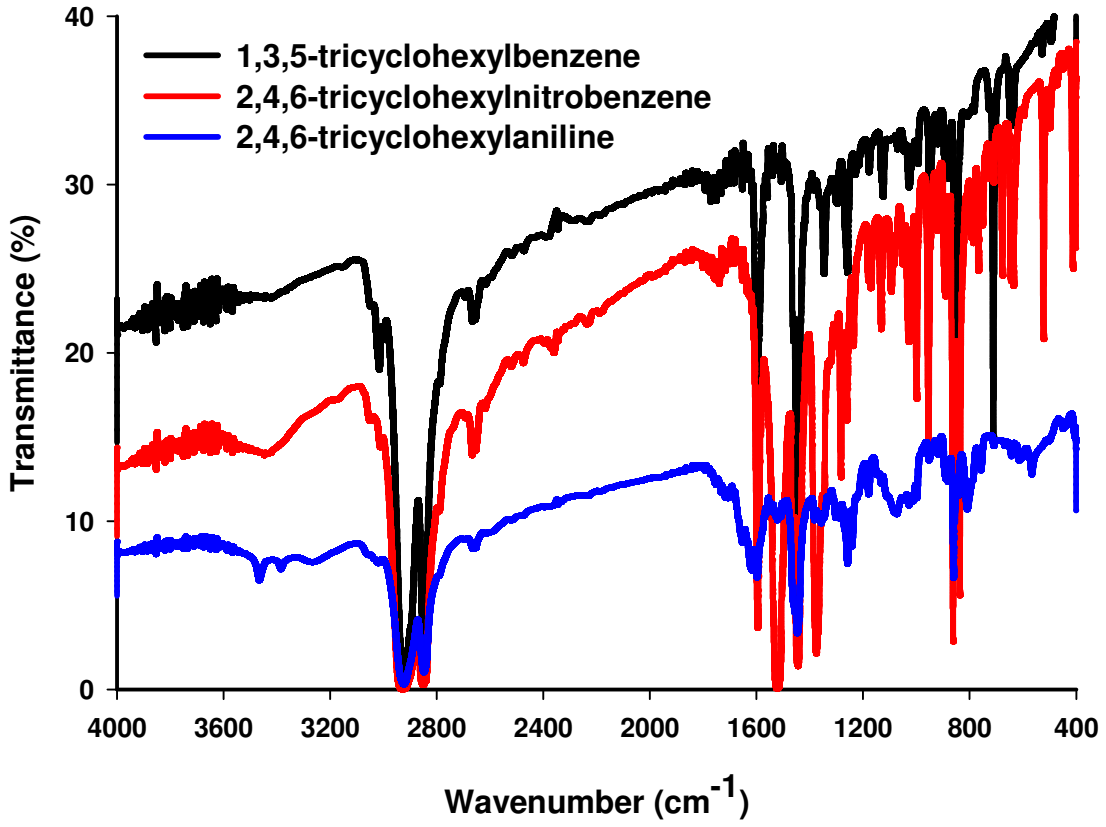

Figure 3.5: IR Spectra (KBr) of Tricyclohexylbenzene Derivatives

The presence of C=N bonds in the α-diimine and pyridine bisanil compounds provides an interesting point for IR study of these compounds. For the α-diimine compounds, the study is not very extensive but typically these bands appear between 1600 cm^{-1} to 1700 cm^{-1} (Table 3.1).[25] The ligand band intensity is much stronger as compared to

the metal complexes (Figure 3.6). The coordination of the N-atoms to the metal ions causes this decrease in intensity. Also, the peak position suffers red shift.

Table 3.1: IR ($\nu_{C=N}$) Frequencies for Selected Metal α-Diimine Complexes

Compound	IR Frequency (cm^{-1})
Co^{II}(NN-Me)Cl_2	1652
Co^{II}(NN-*i*Pr)Cl_2	1646
Ni^{II}(NN-*i*Pr)Cl_2	1656
Co^{II}(NN-Cy)Cl_2	1638
Ni^{II}(NN-Cy)Cl_2	1637

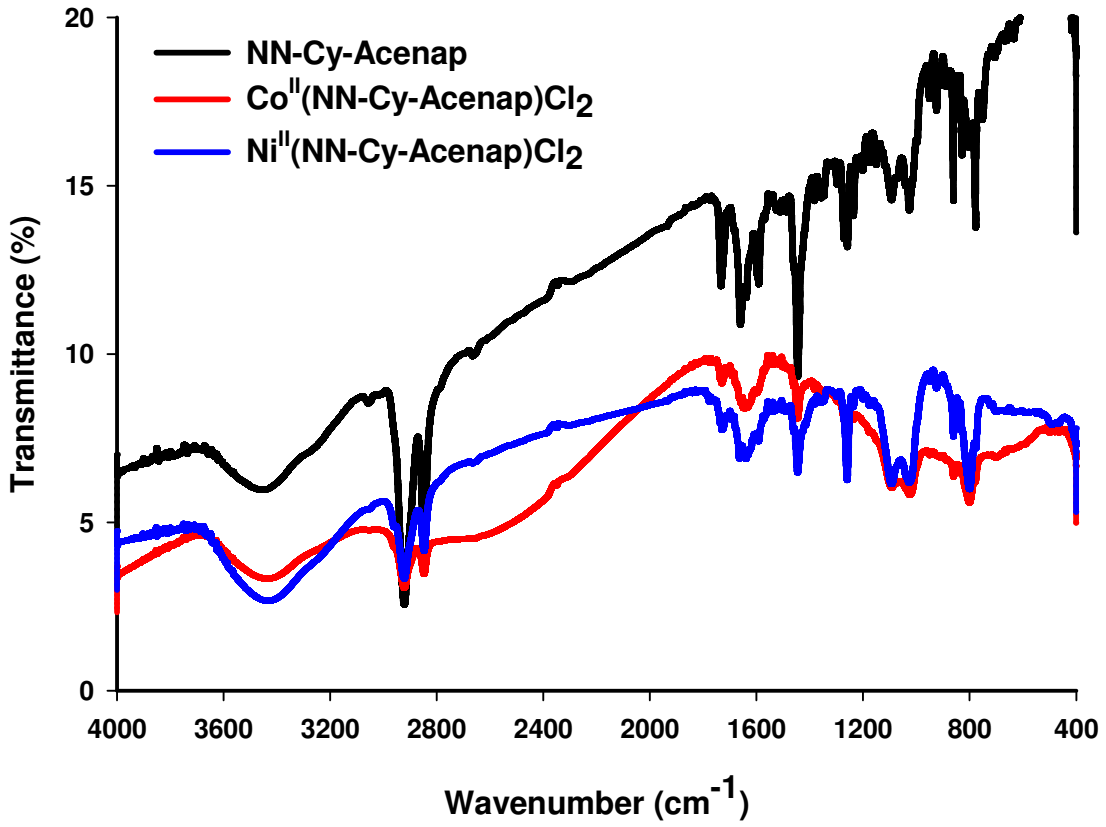

Figure 3.6: IR Spectra (KBr) of α-Diimine Compounds

For the pyridine bisnail compounds, the red shift in the C=N bond frequency in free ligand and ligand coordinated to the metal is observed as well (Table 3.2). In almost all the

cases, the Ni^{II} complexes show a greater blue shift of the $\nu_{C=N}$ band as compared to the Co^{II} complexes (Figure 3.7).[9,10]

Table 3.2: IR ($\nu_{C=N}$) Frequencies for Selected Metal Pyridine Bisanil Complexes

Comp.	IR Freq. (cm^{-1})	Comp.	IR Freq. (cm^{-1})	Comp.	IR Freq. (cm^{-1})	Comp.	IR Freq. (cm^{-1})	Comp.	IR Freq. (cm^{-1})
NNN-H	1635	NNN-Me	1641	NNN-^{i}Pr	1643	NNN-^{t}Bu	1636	NNN-Cy	1635
Co^{II}(NNN-H)Cl_2	1628	Co^{II}(NNN-Me)Cl_2	X	Co^{II}(NNN-^{i}Pr)Cl_2	X	Co^{II}(NNN-^{t}Bu)Cl_2	1630	Co^{II}(NNN-Cy)Cl_2	1631
Ni^{II}(NNN-H)Cl_2	1623	Ni^{II}(NNN-Me)Cl_2	1625	Ni^{II}(NNN-^{i}Pr)Cl_2	1624	Ni^{II}(NNN-^{t}Bu)Cl_2	1628	Ni^{II}(NNN-Cy)Cl_2	1630

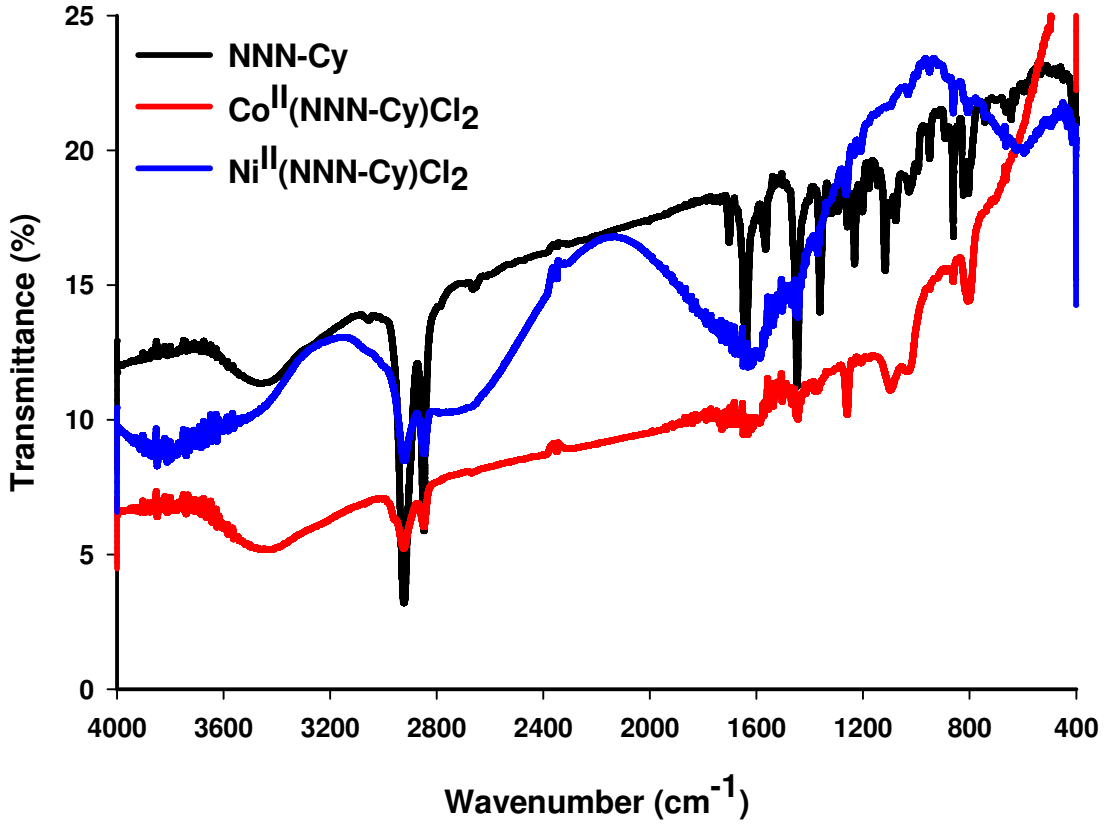

Figure 3.7: IR Spectra (KBr) of Pyridine Bisanil Compounds

For Me and ^{i}Pr compounds, the blue shift is relatively higher. If this is any indication of the binding capability of the ligands to the metal, the ^{i}Pr ligand binds the strongest. This may have an influence on the catalytic activity of the metal complexes. Interestingly, the ligand with the bulky ^{t}Bu group has the IR data comparable to the Cy one. But at the same time, the compound derived from aniline falls in the same range as well (Figure 3.8).

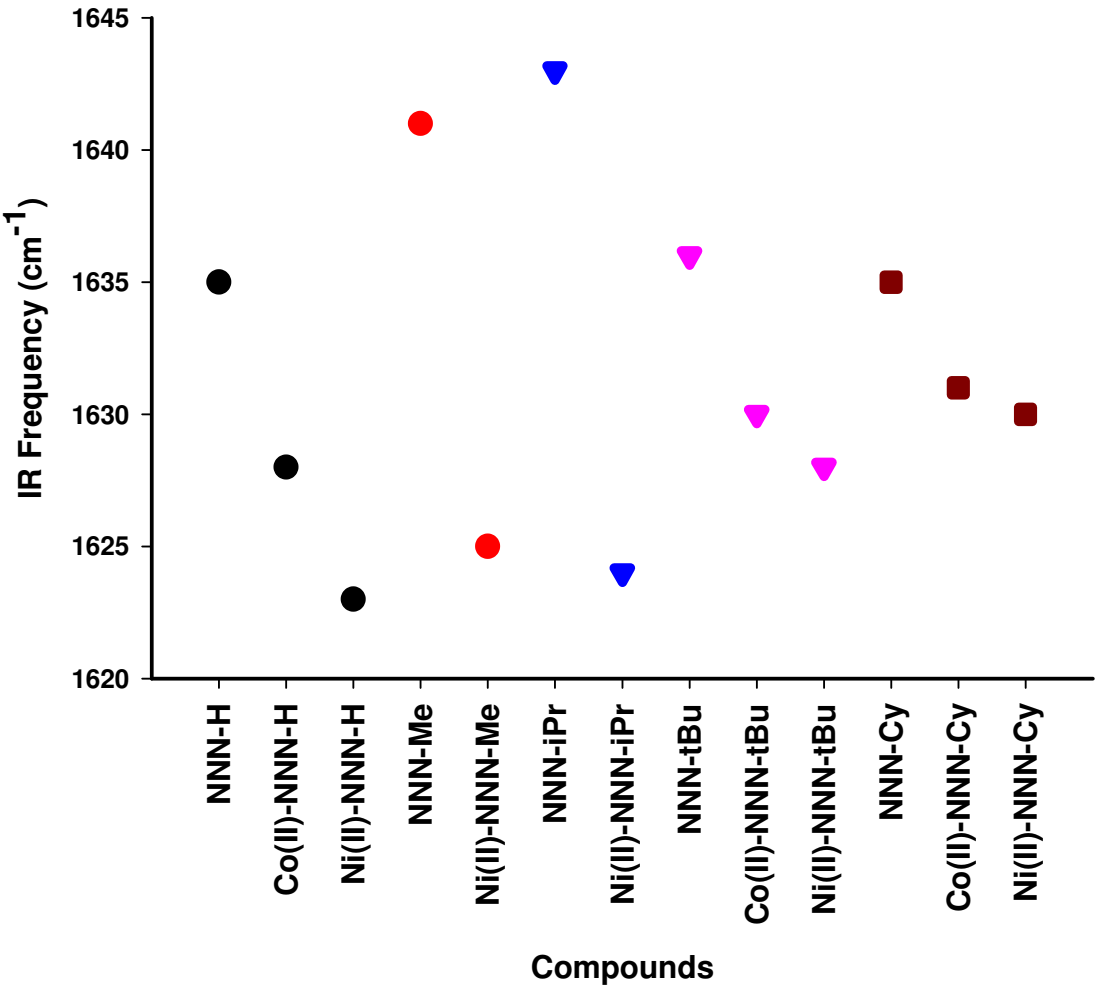

Figure 3.8: Comparison of IR Frequencies for Ligands & Metal Complexes

Electronic absorption spectra of the tricyclohexyl compounds show strong $\pi \rightarrow \pi^*$ transition around 230 nm (Figure 3.9). The electron withdrawing group ($-NO_2$) and the electron donating group ($-NH_2$) make the band to blue shift and red shift respectively.

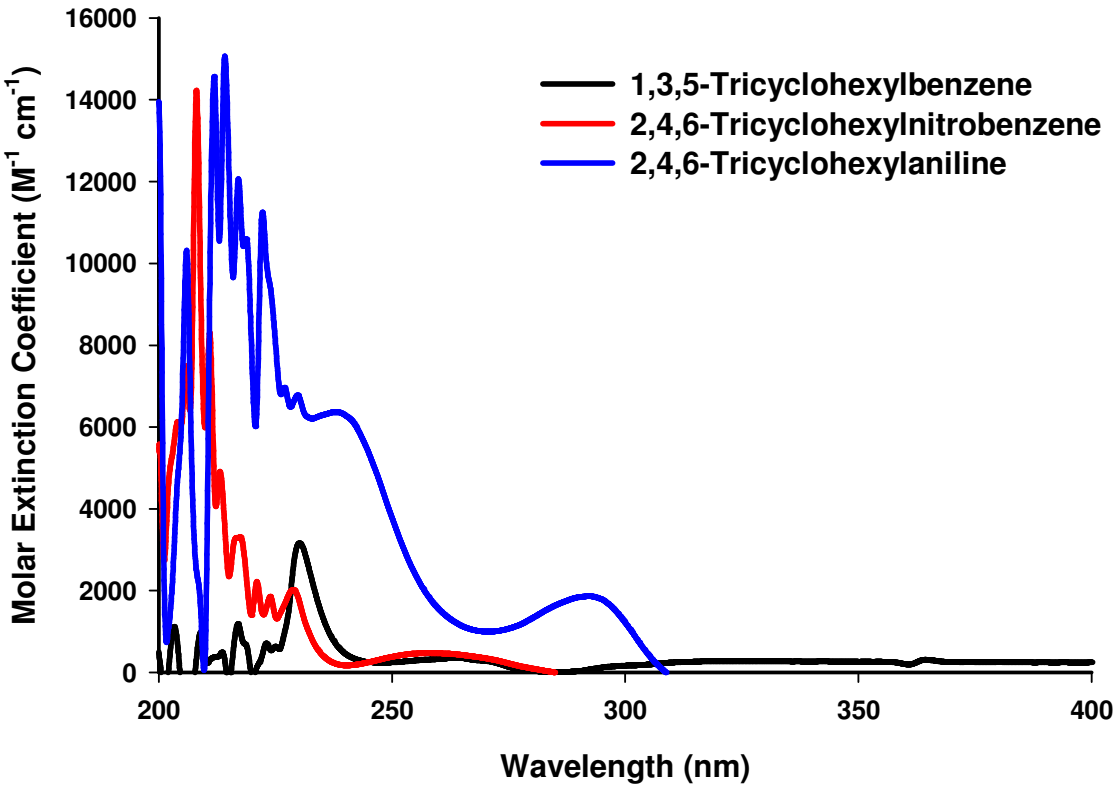

Figure 3.9: Electronic Absorption Spectra of Tricyclohexylbenzene Derivatives

Electronic absorption spectrum of the α-diimines show band positions around 450 nm (Figure 3.10). Comparing to the ^{i}Pr analogue of the Ni^{II} compound, the shift is almost 100 nm. At this point, there is not enough data to correlate this observation with steric bulk of the ligands.

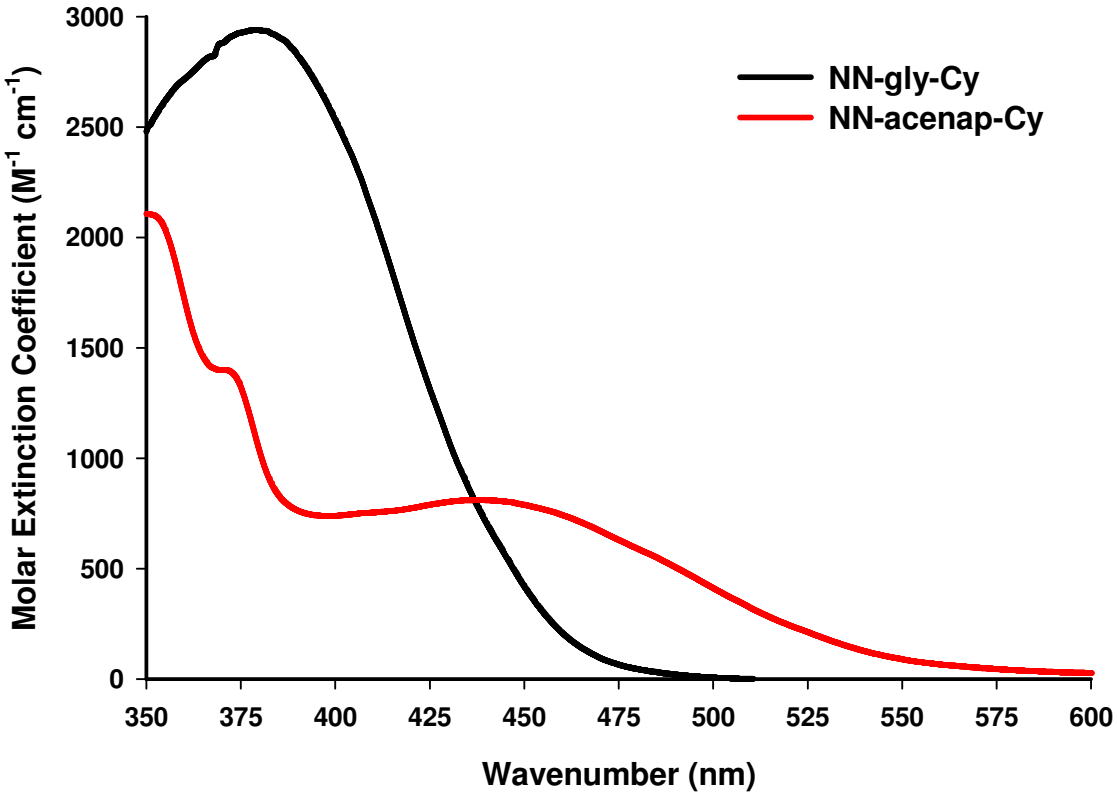

Figure 3.10: Electronic Absorption Spectra of α-Diimine Compounds (Visible Region)

Electronic absorption spectrum of the pyrdine bisanil metal complexes show band positions near 550 and 700 nm (Figure 3.11). The ^{i}Pr analogue of the Co^{II} & Ni^{II} compunds show band positions in the similar range. As is the case with the α-diimine compounds, there is not enough data to correlate this observation with steric bulk of the ligands. In the UV region, the $\pi \rightarrow \pi^*$ transition is dominant.

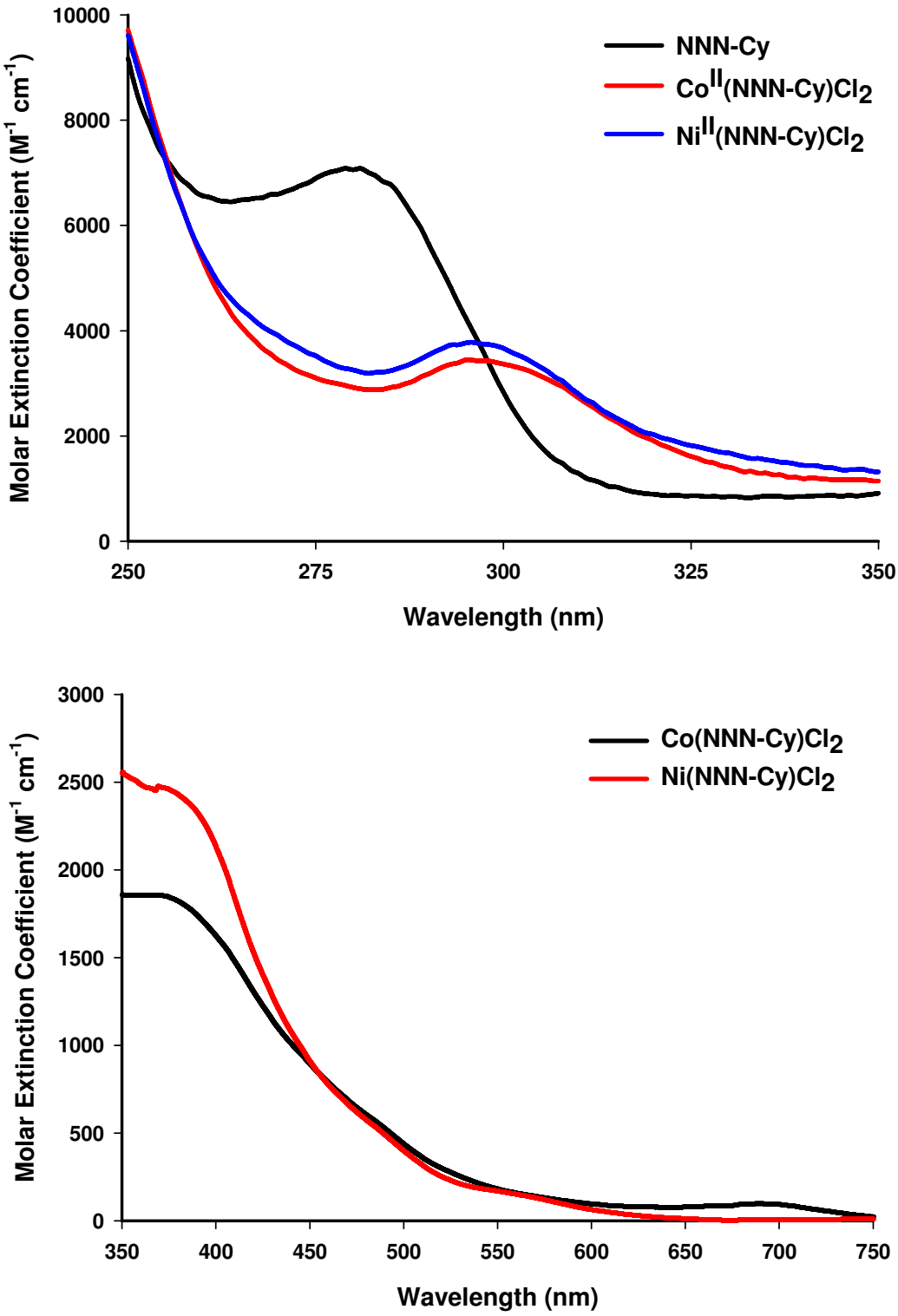

Figure 3.11: Electronic Absorption Spectra of Pyridine Bisanil Compounds (Upper: UV Region; Lower; Visible Region)

3.4.4 Structural (XRD) Characterization of the Ligands & the Metal Complexes

The compound $Ph(Cy)_3NO_2$ crystallizes in a triclinic structure with the P_1 space group (Figure 3.12). The *ortho*-cyclohexyl rings are perpendicular to the planar benzene ring, as observed with other similar 2,6-disubstituted derivatives of nitrobenzene.[26-28] The three cyclohexyl rings are mutually orthogonal in space. The two *ortho*-substituted rings are related by a plane of symmetry. This fact is also confirmed in ^1H NMR where the *ortho*-benzylic protons give a different chemical shift compared to the *para*-benzylic proton. The crystal structure shows that the $-NO_2$ group is perpendicular to the plane of the benzene ring. This proves that the *ortho*-substituents are bulky enough to rotate the $-NO_2$ group out of the plane of the benzene ring. The average distance between O-atoms of the $-NO_2$ and *ortho* hydrogens on cyclohexyl groups is 2.8 Å, which indicates no hydrogen bonding is present in the molecule. The average N=O bond distance is 1.19 Å while the N-O average bond distance is 1.21 Å. The average C-N bond distance is 1.47(9) Å.

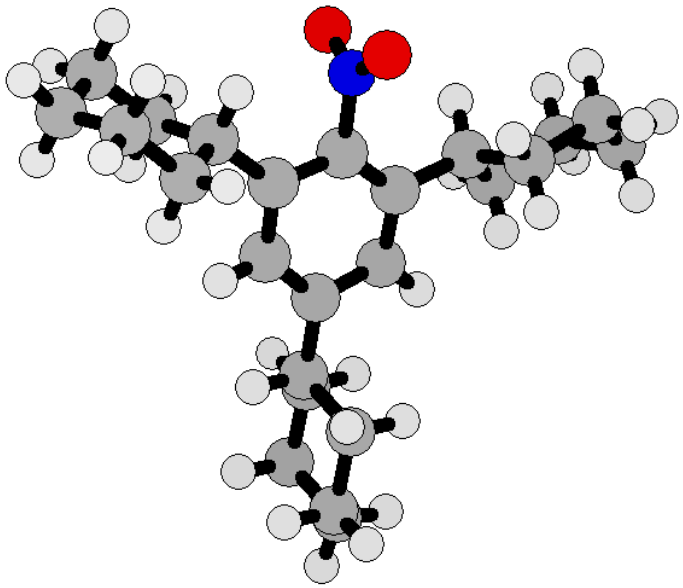

Figure 3.12: Crystal Structure of $Ph(Cy)_3NO_2$
[H-atoms omitted for clarity]

Table 3.3: Selected Crystallographic Data for $Ph(Cy)_3NO_2$

Bond Lengths (Å)	Bond Angles (°)
C(1) – N(1): 1.484(6)	N(1) – C(1) – C(2): 116.56(6)
N(1) – O(1): 1.220(3)	N(1) – C(1) – C(6): 117.86(4)
N(1) – O(2): 1.189(5)	O(1) – N(1) – O(2): 123.43(2)

The compound $Ph(Cy)_3NH_2$ crystallizes in an orthorhombic structure with the *P*bcn space group (Figure 3.13). The hydrogens of the amino group are oriented in space in such a way so as to minimize the steric repulsion with two *ortho*-benzylic protons. There is no H-bonding observed between the individual molecules.[28,29] Regarding the orientation the three cyclohexyl rings, the features are the same as that of the $Ph(Cy)_3NO_2$ compound.

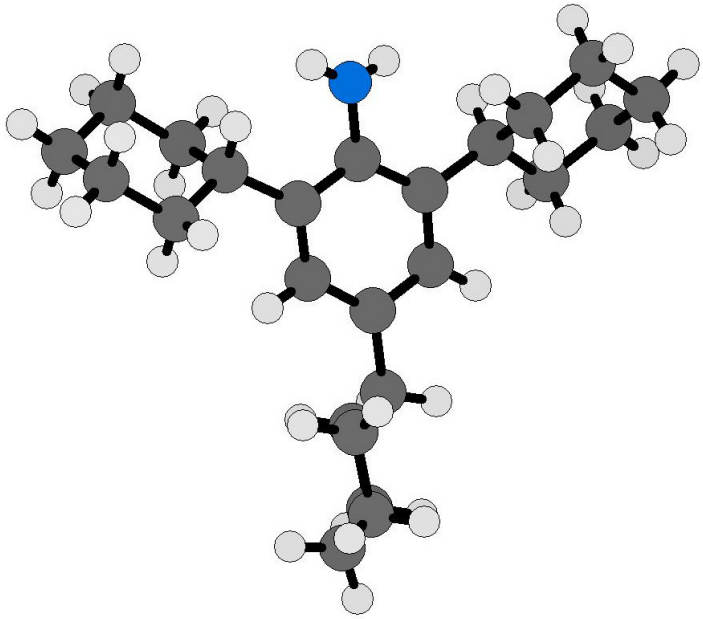

Figure 3.13: Crystal Structure of $Ph(Cy)_3NH_2$
[H-atoms omitted for clarity]

Table 3.4: Selected Crystallographic Data for $Ph(Cy)_3NH_2$

Bond Lengths (Å)	Bond Angles (°)
C(1) – N(1): 1.425(4)	N(1) – C(1) – C(2): 119.87(5)
N(1) – H(1): 1.001(8)	N(1) – C(1) – C(6): 119.64(1)
N(1) – H(2): 1.005(5)	H(1) – N(1) – H(2): 104.43(7)

The compound NN-Cy-gly crystallizes in a monoclinic structure with the $P2_1/c$ space group. The structure (Figure 3.14) of the diimine shows that the compound is composed of two symmetric units with a *s*-trans conformation around the sp^2C-sp^2C single bond of the glyoxal. The C=N bond length is 1.25 Å while the sp^2C-sp^2C single bond distance is 1.47 Å. The C=N bonds are oriented in space in between the two *ortho*-substituents in a way to experience minimum steric repulsion from both. For each half of the molecule, the two *orth*-cyclohexyl groups are orthogonal to the plane of the benzene ring while, the *para*-substituent is parallel to the plane.

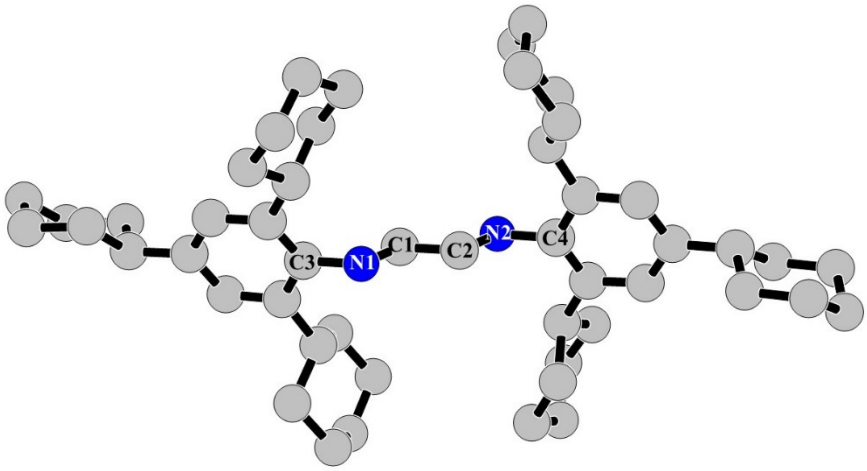

Figure 3.14: Crystal Structure of NN-Cy-gly
[H-atoms omitted for clarity]

Table 3.5: Selected Crystallographic Data for NN-Cy-gly

Bond Lengths (Å)	Bond Angles (°)
C(3) – N(1): 1.433(5)	C(3) – N(1) – C(1): 120.05(4)
N(1) – C(1): 1.245(3)	N(1) – C(1) – C(2): 121.43(3)
C(1) – C(2): 1.462(1)	C(1) – C(2) – N(2):121.18(5)
C(2) – N(2): 1.245(9)	C(2) – N(2) – C(4): 120.23(2)
N(2) – C(4): 1.435(2)	

The compound NN-Cy-acenap crystallizes in a triclinic structure with the P_1 space group (Figure 3.15). The acenapthaquinone based α-diimine ligands are locked in *s*-cis-

conformation around the sp^2 C-sp^2 C single bond. The geometric considerations observed in each unit for the α–diimine from glyoxal are present here as well. The C=N bond length is 1.25 Å. The angle between the *ipso* C-atom, *ortho*-C-atom and C-atom on the cyclohexyl ring connected to benzene ring is 124°. The dihedral angle between N-atom, *ipso*-C-atom, *ortho*-C-atom and C-atom on the cyclohexyl ring connected to benzene ring is 1.2°. There is one molecule of acetic acid in the crystal. The acidic hydrogen atom of the acetic acid does not show any preference to any one of the N-atoms.

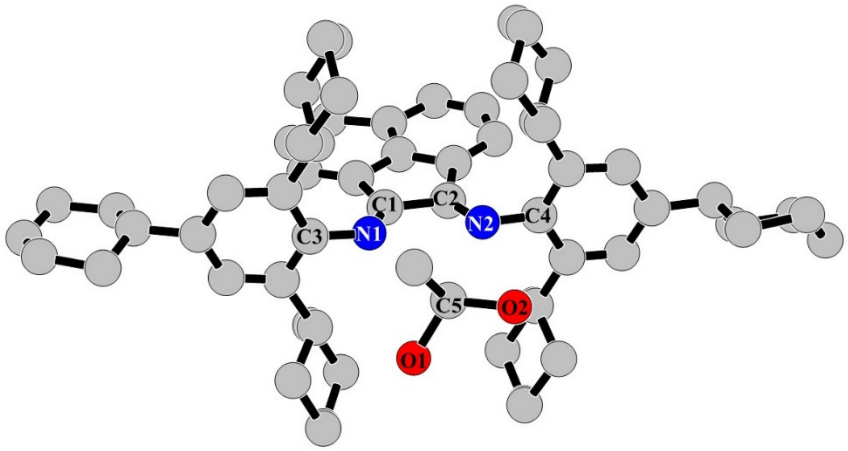

Figure 3.15: Crystal Structure of NN-Cy-acenap
[H-atoms omitted for clarity]

Table 3.6: Selected Crystallographic Data for NN-Cy-acenap

Bond Lengths (Å)		Bond Angles (°)
C(3) – N(1): 1.451(5)	C(5) – O(1): 1.615(3)	C(3) – N(1) – C(1): 113.60(6)
N(1) – C(1): 1.213(6)	C(5) – O(2): 1.627(1)	N(1) – C(1) – C(2): 120.76(9)
C(1) – C(2): 1.601(1)	N(1) – O(1): 3.545(1)	C(1) – C(2) – N(2): 117.61(2)
C(2) – N(2): 1.294(6)	N(2) – O(2): 3.761(5)	C(2) – N(2) – C(4): 116.88(5)
N(2) – C(4): 1.438(4)		O(1) – C(5) – O(2): 115.83(4)

The compound Ni(NNN-Cy)Cl_2 crystallizes in a monoclinic crystal system with $P2_1/c$ space group. The crystal structure (Figure 3.16) shows that the Ni^{II} center has a distorted trigonal bipyramidal geometry. The Ni-Cl bonds are unequal in length, so are the Ni-N_{imine} bonds. The Ni-$N_{pyridine}$ bond is shorter as compared to the Ni-N_{imine} bonds. As

observed in the parent amine crystal structure, the cyclohexyl rings are mutually orthogonal in space and are orthogonal to the benzene ring.

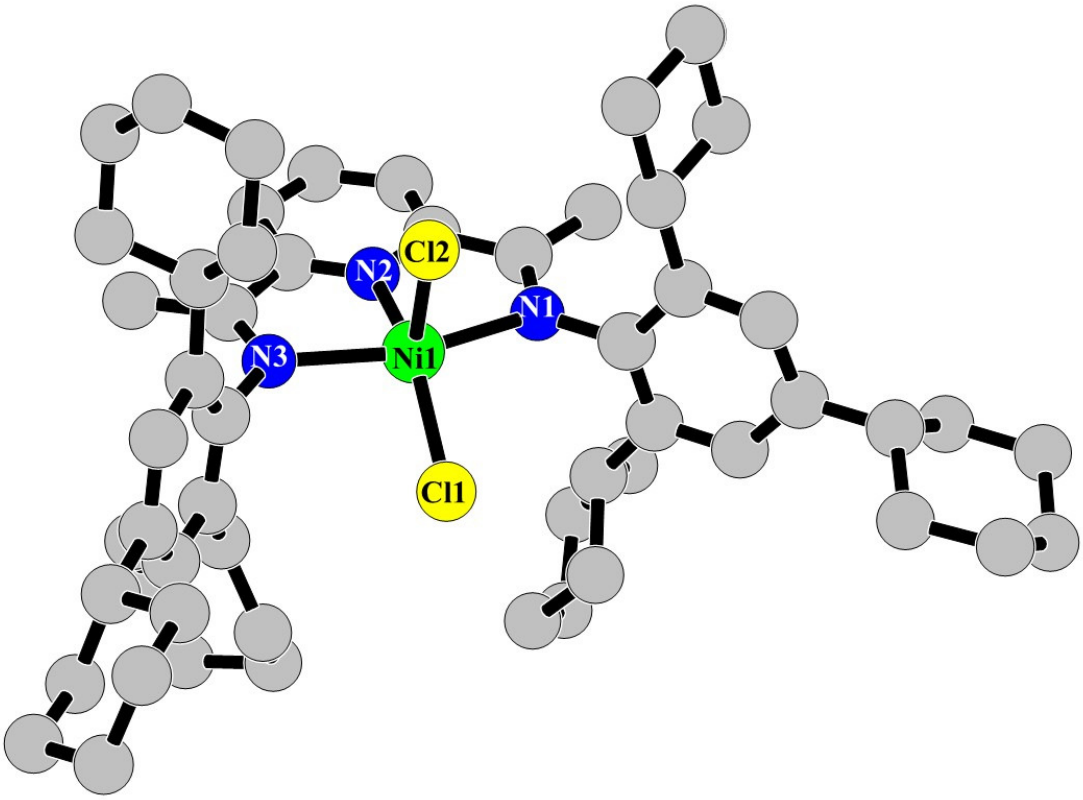

Figure 3.16: Crystal Structure of Ni(NNN-Cy)Cl_2
[H-atoms omitted for clarity]

Table 3.7: Selected Crystallographic Data for Ni(NNN-Cy)Cl_2

Bond Lengths (Å)	Bond Angles (°)	
Ni(1) – Cl(1): 2.227(5)	Cl(1) – Ni(1) – Cl(2): 114.83(6)	N(1) – Ni(1) – Cl(2): 93.94(6)
Ni(1) – Cl(2): 2.270(6)	N(1) – Ni(1) – N(2): 76.99(3)	N(2) – Ni(1) – Cl(1): 145.21(5)
Ni(1) – N(1): 2.214(7)	N(2) – Ni(1) – N(3): 77.24(2)	N(2) – Ni(1) – Cl(2): 99.96(3)
Ni(1) – N(2): 1.972(2)	N(3) – Ni(1) – N(1): 153.70(5)	N(3) – Ni(1) – Cl(1): 98.27(2)
Ni(1) – N(3): 2.183(1)	N(1) – Ni(1) – Cl(1): 99.83(6)	N(3) – Ni(1) – Cl(2): 95.59(5)

Table 3.8: Crystallographic Parameters for $Ph(Cy)_3X$ (X = NO_2, NH_2) α–diimines, $Ni(NNN\text{-}Cy)Cl_2$

	$Ph(Cy)_3NO_2$	$Ph(Cy)_3NH_2$	NN-Cy-gly	NN-Cy-acenap	$Ni(NNN\text{-}Cy)Cl_2$
Empirical Formula	$C_{24}H_{35}NO_2$	$C_{24}H_{37}N$	$C_{50}H_{72}N_2$	$C_{62}H_{81}N_2O_2$	$C_{57}H_{79}N_3NiCl_2$
Formula Weight	369.34	339.55	701.1	886.29	935.86
Crystal System	triclinic	orthorhombic	monoclinic	triclinic	monoclinic
Space Group	*P*-1	*P*bcn	$P2_1/c$	P_1	$P2_1/c$
a (Å)	11.52(2)	11.43(9)	13.48(3)	12.57(1)	13.1920(2)
b (Å)	12.21(4)	11.70(0)	16.87(2)	15.33(2)	27.2180(6)
c (Å)	31.19(7)	31.01(9)	20.40(9)	15.94(4)	16.3310(7)
α (°)	89.95(5)	90	90	88.46(2)	90
β (°)	79.82(3)	90	107.62(5)	74.07(8)	94.739(4)
γ (°)	89.89(2)	90	90	70.49(5)	90
Z	8	8	4	2	4
Cell Volume ($Å^3$)	4321.2(5)	4153.6(3)	4424.9(2)	2778.4(6)	5843.80(4)
Crystal Color	white	pale brown	yellow	orange	red
Crystal Dimensions (mm)	1.0 x 0.8 x 0.5	1.0 x 0.3 x 0.1	1.5 x 1.0 x 0.5	1.5 x 0.8 x 0.4	0.5 x 0.4 x 0.2
Crystal Morphology	plate	prism	prism	plate	prism
Calc. Density (g cm^{-3})	1.13(5)	1.08(6)	1.05(2)	1.05(9)	1.06(3)
F_{000}	1828	1504	1544	966	2335.7
μ (mm^{-1})	0.08(0)	0.06(1)	0.06(0)	0.06(2)	0.645
R_{obs}	0.094(4)	0.037(5)	0.065(6)	0.127(5)	0.068(0)
Temperature (K)	293(2)	293(2)	293(2)	293(2)	100(2)
θ range (°)	0.66 – 28.3	1.3 – 28.3	1.6 – 28.3	1.3 – 23.3	2.9 – 30.7
Radiation (Mo Kα)	0.71073	0.71073	0.71073	0.71073	0.71073

Comparing to the ^{i}Pr analogue[10], there are few similarities and differences with respect to the structural aspect. The basic geometry around the Ni^{II} center is distorted trigonal bipyramidal. Among the two structures, he Ni-Cl bonds are comparable, but the Ni-$N_{pyridine}$ bond is ~0.02 Å smaller for the Cy analogue (Table 3.9).

Table 3.9: Comparison of Selected Crystallographic Data of Ni^{II}(NNN-^{i}Pr)Cl_2 & Ni^{II}(NNN-Cy)Cl_2 Complexes

Ni^{II}(NNN-^{i}Pr)Cl_2	Parameters	Ni^{II}(NNN-Cy)Cl_2
P-1	Space Group	$P2_1/c$
2.156 Å	Ni-N_{imine}	2.214 Å
2.161 Å		2.183 Å
1.996 Å	Ni-$N_{pyridine}$	1.972 Å
2.289 Å	Ni-Cl	2.227 Å
2.233 Å		2.270 Å
distorted trigonal bipyramidal	Ni Geometry	distorted trigonal bipyramidal

3.5 Conclusions

In the conclusion, it can be said that a series of sterically hindered symmetric trisubstituted phenyl ligands, such as the 2,4,6-tricyclohexylbenzene reagents [$Ph(Cy)_3X$ where X = -H, $-NO_2$, $-NH_2$] have been synthesized for the first time. In all cases the pure product can be isolated with a >50% yield. Comparing the ease of synthesis with symmetric triphenyl analogues, tricyclohexyl compounds show this series to be a very practical approach for synthesis of sterically hindered ligands. The crystal structures of the native ligands proved more insight for the steric bulk associated with the ligand. All the new compounds have been characterized by ^{1}H & ^{13}C NMR spectroscopy in $CDCl_3$, IR spectroscopy by KBR pellet method and UV-VIS spectroscopy in $CHCl_3$. The NMR and crystal structure clearly shows that the two *ortho* cyclohexyl groups are symmetry related but with the *para* substituted cyclohexyl ring being unique.

A new class of sterically hindered α-diimine ligands has been synthesized. It has been observed (as anticipated) that if the α–C-atoms of the α-diketone are not locked in a *cis* conformation, the α-diimine forms a *s-trans* configuration around the C-C bond of the diketone.

Another class of compounds, such as pyridine bisanil ligands, have also been synthesized. The Ni^{II} complex provides a comparative study with the ^{i}Pr analogue.

Future work includes but is not limited to better structural elucidation of the native α-diimine ligands, synthesis, structural and spectroscopic characterization of metal-diimine complexes with the new class of sterically hindered a-diimines and pyridine bisanil ligands.

3.6 References

(1) Johnson, L. K.; Killian, C. M.; Brookhart, M. *J. Am. Chem. Soc.* **1995**, *117*, 6414.

(2) Ittel, S. D.; Johnson, L. K.; Brookhart, M. *Chem. Rev.* **2000**, *100*, 1169.

(3) Schmid, M.; Eberhardt, R.; Klinga, M.; Leskela, M.; Rieger, B. *Organomet.* **2001**, *20*, 2321.

(4) Schmid, M.; Eberhardt, R.; Kukral, J.; Rieger, B. *Z. Naturforsch.* **2002**, *57b*, 1141.

(5) Gibson, V. C.; Tomov, A.; Wass, D. F.; White, A. P. J.; Williams, D. J. *J. Chem. Soc. Dalton Trans.* **2002**, 2261.

(6) Small, B. L.; Brookhart, M.; Bennett, A. M. A. *J. Am. Chem. Soc.* **1998**, *120*, 4049.

(7) Britsovek, G. J. P.; Bruce, M.; Gibson, V. C.; Kimberley, B. S.; Maddox, P. J.; Mastroianni, S.; McTavish, S. J.; Redshaw, C.; Solan, G. A.; Stromberg, S.; White, A. P. J.; Williams, D. J. *J. Am. Chem. Soc.* **1999**, *121*, 8728.

(8) Gibson, V. C.; Redshaw, C.; Solan, G. A. *Chem. Rev.* **2007**, *107*, 1745.

(9) Chen, J.; Huang, Y.; Li, Z.; Zhang, Z.; Wei, C.; Lan, T.; Zhang, W. *J. Mol. Cat. A: Chem.* **2006**, *259*, 133.

(10) Huang, J.; Chen, J.; Chi, L.; Wei, C.; Zhang, Z.; Li, Z.; Li, A.; Zhang, L. *J. Appl. Polym. Sci.* **2009**, *112*, 1486.

(11) Corson, B. B.; Ipatieff, V. N. *J. Am. Chem. Soc.* **1937**, *59*, 645.

(12) Powell, G.; Johnson, F. R. *Org. Synth. Coll.* **1943**, *2*, 449.

(13) Bartlett, P. D.; Roha, M.; Stiles, R. M. *J. Am. Chem. Soc.* **1954**, *76*, 2349.

(14) Clark, G. R.; Nielson, A. J.; Richard, C. E. F. *J. Chem. Soc. Dalton Trans.* **1996**, 4265.

(15) Grubert, L.; Jacobi, D.; Buck, K.; Abraham, W.; Mugge, C.; Krause, E. *Eur. J. Org. Chem.* **2001**, 3921.

(16) El-Ayaan, U.; Abdel-Aziz, A. A. *Eur. J. Med. Chem.* **2005**, *40*, 1214.

(17) Helldorfer, M.; Backhaus, J.; Milius, W.; Alt, H. G. *J. Mol. Cat. A: Chem.* **2003**, *193*, 59.

(18) Long, Z.; Wu, B.; Yang, P.; Li, G.; Liu, Y.; Yang, X.-J. *J. Organomet. Chem.* **2009**, *694*, 3793.

(19) Farrugia, L. J. *J. Appl. Cryst.* **2012**, *45*, 849.

(20) Heropoulos, G. A.; Georgakopoulos, S.; Steele, B. R. *Tet. Lett.* **2005**, *46*, 2469.

(21) Suzuki, H.; Manabe, H.; Inouye, M. *Chem. Lett.* **1985**, 1671.

(22) Osuka, A.; Shimizu, H.; Suzuki, H. *Chem. Lett.* **1983**, 1373.

(23) Yang, K.; Lachiotte, R. J.; Eisenberg, R. *Organomet.* **1997**, *16*, 5234.

(24) Kohler, E. P.; Blanchard Jr, L. W. *J. Am. Chem. Soc.* **1935**, *54*, 367.

(25) Rosa, V.; Carabiniero, S. A.; Aviles, T.; Gomes, P. T.; Welter, R.; Campos, J. M.; Ribiero, M. R. *J. Organomet. Chem.* **2008**, *693*, 769.

(26) Trotter, J. *Acta. Cryst.* **1959**, *12*, 605.

(27) De Ridder, D. J. A.; Schenk, H. *Acta. Cryst. C.* **1993**, *C49*, 1970.

(28) Pohl, E.; Herbst-Irmer, R.; Kohler, K.; Roesky, H. W.; Sheldrick, G. M. *Acta. Cryst. C.* **1993**, *C49*, 2141.

(29) Ugono, O.; Cowin, S.; Beatty, A. M. *Acta. Cryst. E.* **2010**, *E66*, 01777.

Chapter 4:

Late Transition Metal Chemistry with Norbornane 1,2 –Dithiol – A Conformationally Fixed/Locked Alkane Dithiol

4.1 Introduction

4.1.1 General Introduction

Late transition metal atoms (particularly Fe, Co & Ni) surrounded by four thiolate ligands (RS^-: from the cysteine residues of the protein backbone) in different geometrical arrangements is a well-known structural motif for the active sites of various biologically relevant and important metalloenzymes such as nitrile hydratase, carbon monoxide dehydrogenase, hydrogenase, nitrogenase. RS^- are typically soft ligands and are rich in electrons with high affinity for a large number of metal cations. The thiolate ligands coordinated completely or partially to the metal centers often play important roles in the structure and function of the metalloenzymes. The coordinated metal ions, the side chain along with the bridging and terminal ligands define the first coordination sphere of the metal ions geometry of which depend on the oxidation state (OS) of the metal (Table 4.1).[1]

Table 4.1: Metal Ions in Biological Systems with their Geometry and CN

metals	OS	d^n	CN	effective geometry
Fe	+2	d^6	4	tetrahedral, square planar
			5	square pyramidal, trigonal bipyramidal
			6	octahedral
	+3	d^5	4	tetrahedral
			5	square pyramidal
	+4	d^4	4	tetrahedral
Co	+2	d^7	4	tetrahedral
			5	square pyramidal, trigonal bipyramidal
			6	octahedral
	+3	d^6	6	octahedral
Ni	+2	d^8	4	tetrahedral, square planar
			5	square pyramidal, trigonal bipyramidal
			6	octahedral
	+3	d^7	4	square planar
			5	square pyramidal
			6	octahedral
	+4	d^6	6	octahedral

Most of the enzymes of interest to mankind are involved in catalysis and/or gas-processing (CH_4, CO, H_2, NH_3) under anaerobic conditions (Table 4.2). The catalysis is often metallocentered, and the active site is embedded deeply inside the protein backbone. The common feature observed among the enzymes is the complexity of the active site. The protein matrix often determines the specificity of the reaction, modulation of the redox potential, and gas diffusion to and from the active site through hydrophobic/hydrophilic tunnels. In [NiFe] hydrogeanse, [FeFe] hydrogenase and CODH, the aforesaid tunnels are primarily hydrophobic whereas for nitrogeanse the same is hydrophilic.[2]

A major thrust in research has always been directed towards the understanding of the mechanism of the catalytic/biosynthetic processes performed by the metalloenzymes. To completely elucidate the process, detail knowledge of the structures of both the first and

the second coordination spheres of the metal center is of paramount importance. To correlate the structure-function-property trio, systematic alteration to the active site structure is required. At this point, the synthetic models become extremely helpful. By using the native biological system to study the properties, complications may arise owing to the limitations imposed by the system itself or the techniques employed. Small molecule analogues, those can reproduce the spectroscopic data of the native system, often provide valuable information about the catalytic/biosynthetic pathways.[3,4]

Table 4.2: Gas-Processing Enzymes with Metal-Thiolate Centers

Enzyme	Catalyzing Reaction	Structure
N2ase	$N_2 + 8H^+ + 8e^- + 16ATP \rightleftharpoons 2NH_3 + H_2 + 16ADP + 16\ P_i$	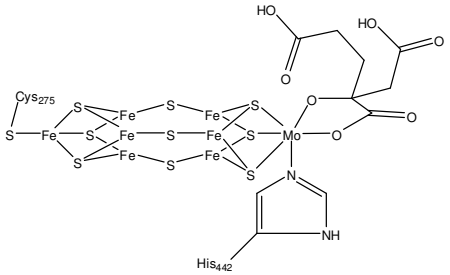 FeMo-Cofactor
H2ase	$H_2 \rightleftharpoons H^+ + H^-$	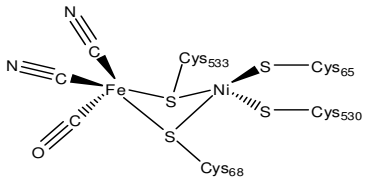 [Ni-Fe]
	$H^- \rightleftharpoons H^+ + 2e^-$	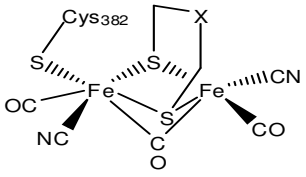 [Fe-Fe] X = $-CH_2-$, -NH-, -O-
	$CO_2 + 4\ H_2 \rightleftharpoons CH_4 + 2\ H_2O$	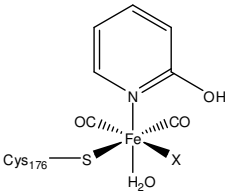 [Fe]only
CODH	$CO_2 + 2e^- + 2H^+ \rightleftharpoons CO + H_2O$	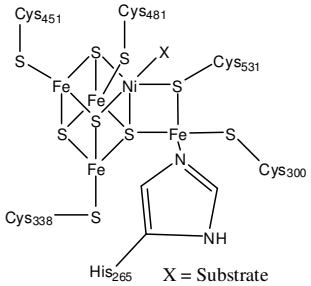 X = Substrate C-Cluster
NHase	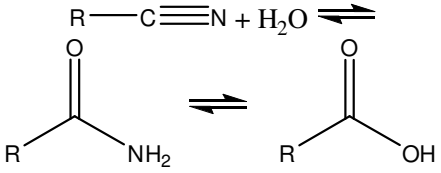	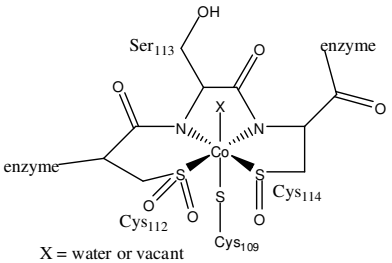 X = water or vacant

4.1.2 Nitrogenase Enzyme (N2ase)

Nitrogenase is the catalyst for biosynthesis of ammonia from atmospheric dinitrogen (Table 4.2). The enzyme consists of two distinct metal bearing parts: (a) iron protein (Fe protein or P-cluster), which is S-bridged two [4Fe-4S] clusters with the sole purpose of being one-electron donor. (b) iron-molybdenum cofactor (FeMo-co), which is the site for the reduction of dinitrogen to ammonia. Apart from the function mentioned above, this enzyme also catalyzes reaction of a variety of small molecules such as azides, N_2O, RCN, RNC and alkynes. To understand the catalytic pathway, it is essential to have a knowledge of the small molecule interaction with the enzyme.[6]

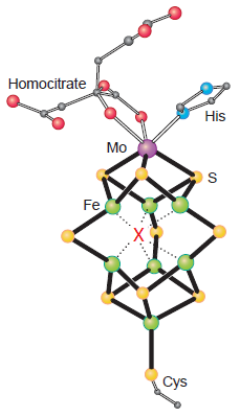

Figure 4.1: Active Site of Nitrogenase Enzyme[5]

The active site or the FeMo-co extracted from *Azatobacter vinelandii* is composed of [4Fe-3S] and [3Fe-3S-Mo] clusters linked together by three μ_2-S-atoms. The bridging S-atoms are of inorganic origin. The [4Fe-3S] cluster shows unusually distorted trigonal coordination environment around Fe-atoms. One of the Fe-atoms has cysteinyl-S-atom (Cys_{275}) satisfying the fourth coordination site. The Mo-atom has three S-atoms coordinating, one homocitrate motif and the sixth position is imidazole N-atom of His_{442} residue. The homocitrate binding is essential as substitution by other carboxylic acids leads to the loss of the enzyme activity.[5,7]

Another important feature of this enzyme is extensive H-bonding network around the active site. The Cys_{275} S-atom is H-bonded to Ser_{268} residue of the protein backbone. With the inorganic S-atoms of the clusters, Gly_{344}, Gly_{345}, Arg_{87}, Arg_{347} and His_{186} form

potential H-bond and/or partake in stabilization of intermediates during catalysis. The residues Gln_{182}, Glu_{368}, Glu_{467}, Gln_{480} and His_{482}, interact or H-bond with the homocitrate directly or through water molecules.[8]

A milder industrial scale production of ammonia is indeed an incentive to study the modeling of the active site of nitrogenase enzyme as ammonia is one of the most abundant chemicals produced industrially across the world employing Haber's process for the manufacture of fertilizers.

4.1.3 Hydrogenase Enzyme (H2ase)

For detail discussion on hydrogenases, please refer to Chapter **1**.

4.1.4 Carbon Monoxide Dehydrognase Enzyme (CODH)

Anaerobic carboxidotrophic bacteria (eg. *Rhodpseudomas gelatinosa*, *Carboxydothermus hydrogenoformas*) can oxidize CO to CO_2, while reducing H_2O to H_2 (Table 4.2). The reaction takes place metabolically in bacteria in the presence of the enzyme CODH, presumably at the Ni-atom.[9]

The Ni-containing CODH often function in a complex with acetyl-CoA synthase (ACS). X-ray crystallographic structure of the active site (C-cluster) reveals that it has one Ni-atom, four Fe-atoms and five S-atoms: thus, making it an asymmetrical, heteronuclear [Ni-4Fe-5S] cluster. Two of S-atoms come from the cysteine residues (Cys_{295}, Cys_{333}) of the middle domain and rest three

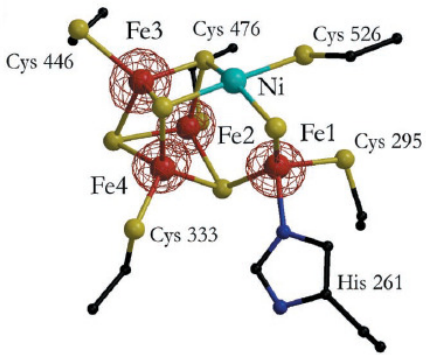

Figure 4.2: Active Site of Carbon Monoxide Dehydrogenase (CODH) Enzyme[10]

(Cys_{446}, Cys_{476}, Cys_{526}) are from the C-terminal domain. All the Fe-atoms have tetrahedral arrangement of S-atoms around them. Among the four Fe-atoms, one of them is outside the cuboidal cluster. It is linked to the Ni-atom by a bridging cysteinyl-S (Cys_{531}). The Fe-atom has its coordination sphere satisfied by one of the inorganic S-atoms from the cluster, a cysteinyl-S (Cys_{300}) and an imine N-atom (His_{261}) from the protein backbone.[10]

Previously, it was speculated based on spectroscopic evidences that the Ni-atom is an outsider and is ligated to the [4Fe-4S] cluster. But the structural studies show that Ni-atom is a very integral part of the C-cluster. The Ni-atom is surrounded by four S-atoms: three inorganic S-atoms – two μ_3-S and one μ_2-S, and the fourth one is from the residue Cys_{526}. The geometry around the Ni-atom is 'slightly tetrahedrally distorted square-planar'. This clearly indicates that the Ni-atom is in +2 oxidation state, which is corroborated by EPR studies.

Use of the enzymatic catalysis may provide a very environmentally friendly way to accomplish the task of elimination of carbon oxides that are potential greenhouse gases from the atmosphere. Hence, the design of bioinspired synthetic models is of great importance with respect to industrial use and environmental factor.

4.1.5 Nitrile Hydratase Enzyme (NHase)

NHase enzymes convert nitriles to amides, and ultimately to an acid, cleanly and rapidly under mild conditions (Table 4.2). Among the Fe and Co analogues, the latter is favored in industrial processes owing to its greater oxidative stability as compared to the former. The Co-analogues preferentially reacts with the aromatic nitriles, while the Fe-analogues catalyze the transformation of the aliphatic nitriles. This difference in reactivity

is attributed to the different conserved residues (tryptophan – Trp_{72} – in Fe-NHase; tyrosine – Tyr_{76} – in Co-NHase) in the α-subunit. These residues are believed to be involved in substrate recognition and bonding leading to the observed preference.[11]

The active site (*Pseudonocardia thermophilia*) of Co-NHase has Co-atom at the center with three cysteinyl-S-atoms (Cys_{108}, Cys_{112}, Cys_{114}) from the α-subunit. The other three sites are coordinatively satisfied by Ser_{113} (from α-subunit), Arg_{52} and Arg_{157} (both from β-subunit). The two S-atoms (Cys_{112} & Cys_{114}), the amide N-atom (Ser_{113}, Cys_{114}) are coplanar with the Co-atom at the center. A water molecule binds at the Co-center to the top-face of the plane, whereas the last cysteinyl-S-atom (Cys_{108}) binds at the bottom-face. The Cys_{112} and Cys_{114} S-atoms are post-translationally oxidized to sulfinic ($-SO_2H$) and sulfenic ($-SOH$) acids respectively. The O-atoms of the sulfinic acid group are involved in H-bonding with Arg_{52} residue, while Arg_{157} is H-bonded with the same from the sulfenic acid group.[13,14]

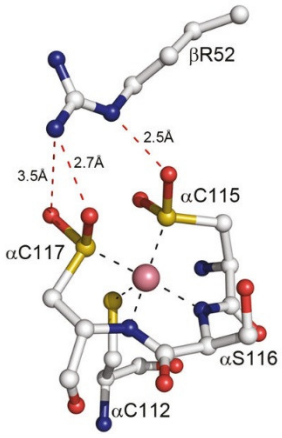

Figure 4.3: Active Site of Nitrile Hydratase Enzyme[12]

Nitriles are potentially toxic but the amides are less toxic as compared to the former. Converting and releasing a nitrile as an amide or an acid is more congenial to the environment. Design of a catalyst akin to Co-NHase that can perform under industrial scale definitely serves as the motivation to investigate structural models of NHases.

4.1.6 Modeling Active Sites with Metal-Dithiolenes Complexes

The metal (Fe, Co, Ni) complexes with the various modified dithiolenes (originating from both maleonitriledithiolene and benzenedithiol) have long been investigated structurally, spectroscopically (UV-Vis, IR, EPR, XAS), electrochemically

and/or a combination of these techniques. To investigate the vialbility of these complexes as models, reaction with small molecules (CO, NO, Ph_3P, phen) were also done spectro- or electro-kinetically.[15-21]

Dithiolene compounds (Figure 4.4) have garnered major attention to model the square-planar or slightly distorted square-planar metal complexes. With metals such as Fe and Ni, complexes where the metals possess various different oxidation states (II, III & IV) have been synthesized and characterized. The major breakthrough was observed in the electrochemical properties of maleonitriledithiolene and toluenedithiol. But this class of ligand is considered as non-innocent type because they are themselves redox active. The dithiolate ligands supposedly play very important roles in the redox processes. Hence, ligand design requires much consideration.

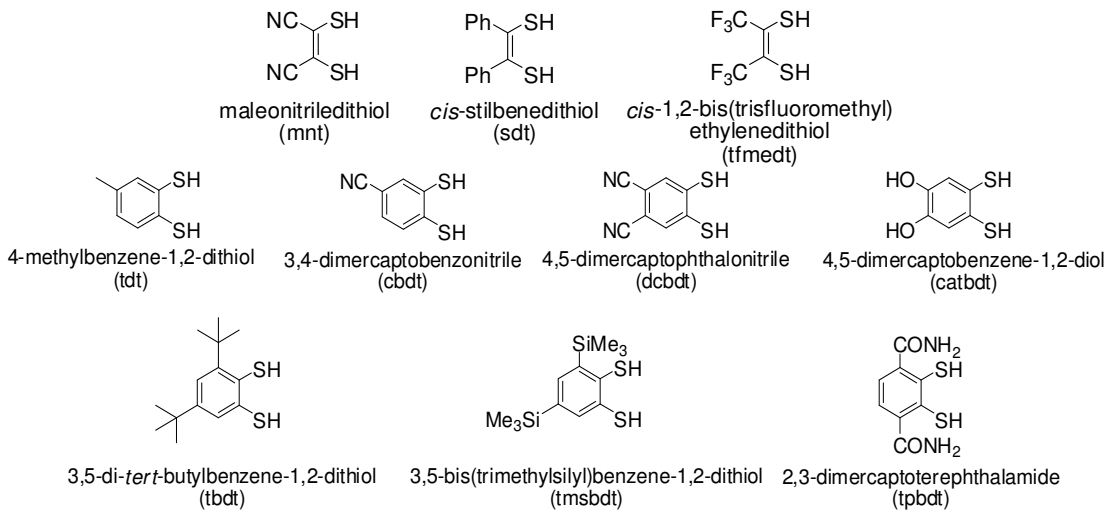

Figure 4.4: Dithiolene Ligands

4.1.7 Modeling Active Sites with Metal-Dithiol Complexes

The cysteine residues are more closely resembled using aliphatic thiols as compared to the benzenethiols or thiolenes. The aliphatic dithiols were considered to be excellent candidates as they are regarded as redox innocent ligands. Also, the aliphatic hydrocarbon

backbone provide the structural robustness and/or variety that may not be achieved otherwise. The cysteine molecule itself was ruled out for mimicking purpose due to its propensity to oligomerize. Some examples of simplest dithiols available are ethanedithiol,[22] 1,2-propanedithiol, 2,3-butanedithiol,[23] 1,2-cyclohexanedithiol[24] or derivatives of thereof. Complexes of these dithiols with the entire first row transition metals were synthesized and characterized either structurally or spectroscopically or electrochemically or a combination of any of the aforesaid.[23,25-27]

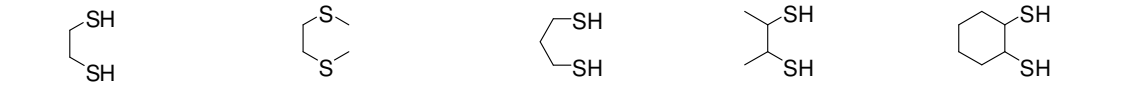

ethane-1,2-dithiol 1,2-bis(methylthio)ethane propane-1,3-dithiol butane-2,3-dithiol cyclohexane-1,2-dithiol

Figure 4.5: Dithiol Ligands

4.2 Aim of the Project

Millar and Koch groups chose a very simple, yet efficient dithiol from norbornene – a strained, aliphatic, bicyclic alkene. The sulfurization and reduction to dithiol of the alkene was known. By reacting the dithiol with LiOH produces the dithiolate, which can be reacted with metal (Fe, Co, Ni) chlorides to form two of the dithiolates coordinated to the metal center. A crystal structure of the dithiolate with Ni-metal was reported previously. In this report, we wish to describe the extension of the study with Fe- & Co-metals and also revisit the Ni-isomer.[28]

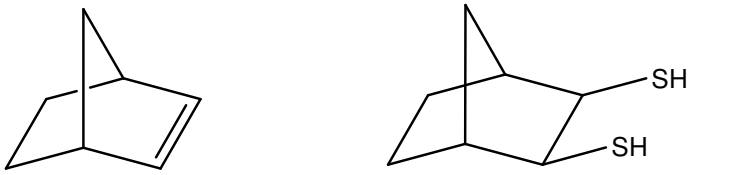

bicyclo[2.2.1]hept-2-ene bicyclo[2.2.1]heptane-2,3-dithiol

Figure 4.6: Norbornene & Norbornane Dithiol ($ndtH_2$)

4.3 Experimental

4.3.1 General Remarks

Air-sensitive manipulations were carried out under nitrogen atmosphere. Solvents were dried and purified by standard methods (THF/Na-Benzophenone, CH_2Cl_2/P_2O_5, Hexanes/Na-Benzophenone, CH_3CN/CaH_2) and were stored under nitrogen. Dimethylformamide (DMF) was used as received. The ^1H & ^{13}C NMR spectra were recorded on a Bruker 300 MHz instrument in $CDCl_3$ (unless and otherwise stated) and standardized with residual solvent peak at 7.26 ppm and 77.23 ppm respectively. Norbornene or bicyclo[2.2.1]hept-2-ene was obtained from Sigma-Aldrich and used as received. Electron absorption spectra were recorded on a Varian Cary 100 spectrophotometer in a 1 cm long quartz cell. Cyclic voltammograms (CV) were recorded on a BAS 100B/W (Version 2.3.1) electrochemical analyzer in DMF with [*n*-Bu_4N][BF_4] as supporting electrolyte (100 fold excess) with saturated calomel electrode (SCE) as the reference electrode, platinum disc as working electrode and platinum wire as auxiliary electrode.

4.3.2 Synthesis of Exo, cis-1,2,3-trithiacyclo[5.2.1.0]decane

The compound was prepared according to a modified literature procedure.[29,30] In a 500 ml 3-necked flask was added powdered sulfur (12.00 g, 0.047 moles) and reagent grade DMF (~80 ml). The flask was flushed and kept under a steady stream of dry nitrogen while passing ammonia gas through the mixture at 50°C. When the slurry turned purple, previously weighed norbornene (209 g, 2.22 moles) was added in one shot. The flask was degassed and steady flow of nitrogen was established. The mixture was heated at 110°C for 2h when it turned brown. The hot solution was poured onto crushed ice and extracted

thrice with bulk ether. The ether layers were combined and washed successively with water and brine solution. The organic layer was dried over anhydrous Na_2SO_4 and the solvent was removed under reduced pressure to yield a yellow oil of sufficient purity to proceed to the next step. Yield 194.0 g, 82.0 %. ^{1}H NMR($CDCl_3$) δ 1.05 (1H, dm), 1.75 (2H, dm), 1.92 (1H, dm), 2.45 (2H, m), 3.64 (2H, d)

4.3.2 Synthesis of Exo, cis-1,2-bicyclo[2.2.1]decanedithiol

The compound was prepared according to a modified literature procedure.[31,32] In a 500 mL 3-necked flask, fitted with a water condenser, under steady flow of nitrogen was added powdered $LiAlH_4$ (42.0 g, 1.20 moles) in THF. With temperature being lowered to 0^{o}C using an ice bath, the the trithiolan (97.0 g, 0.51 moles) solution in THF was added dropwise to the hydride slurry and refluxed overnight. Excess hydride was carefully quenched with ethyl acetate, methanol, and finally by dilute HCl to adjust the pH at 2. The aqueous phase was extracted thrice with bulk ether. The ether layers were combined and washed with water and brine solution. The organic layer was dried over anhydrous Na_2SO_4 and the solvent was removed under reduced pressure to yield a grey, oily product. Distillation of the oil at 113^{o}C under vacuum yielded a colorless oil. Yield 71.0 g, 87 %. ^{1}H NMR($CDCl_3$) δ 1.18 (1H, dt), 1.29 (2H, dm), 1.60 (2H, dm), 1.85 (2H, d), 1.95 (2H, dm), 2.25 (2H, m), 3.24 (2H, d), 3.24 (2H, d).

4.3.3 Synthesis of Metal Complexes

The compounds were prepared according to a modified literature procedure.[28] In a 100 mL flask, in an ice-bath, was taken 4eq. of Li-metal and added degassed water. After the violent reaction subsided was added 2eq. of dithiol in one shot. The entire system was degassed and put under nitrogen. After a clear solution was obtained, 1eq. of solid hydrated

metal chloride was added (for Pt; K_2PtCl_4 was used). The clear solution immediately turned colored (Fe: red; Co: lime green; Ni: green) with brown precipitates forming. The mixture was stirred for overnight and filtered through celite bed into a methanolic solution of 2 eq. of PPh_4Br salt. After stirring for 2h, the solvent was evaporated under reduced pressure until the first crop of the compound precipitated out. The solid was filtered out and upon standing at room temperature for three days x-ray quality crystals were obtained from the filtrate.

bis(tetraphenylphosphonium)di(norbornanedithiolate)ferrate(II) – $[Ph_4P]_2[Fe^{II}(ndt)_2]$: Yield 3.67 g, 70 %. δ ^{1}H NMR (CD_3OD) 24.8 (4H, br s), 7.5 – 8.2 (40H, PPh_4^+, br m), -3.8 (4H, br s), -5.8 (4H, br s)

bis(tetraphenylphosphonium)di(norbornanedithiolate)cobaltate(II) – $[Ph_4P]_2[Co^{II}(ndt)_2]$: Yield 1.38 g, 66%.

bis(tetraphenylphosphonium)di(norbornanedithiolate)nickelate(II) – $[Ph_4P]_2[Ni^{II}(ndt)_2]$: Yield 3.32 g, 66 %. δ ^{1}H NMR (CD_3OD) 0.80 (2H, dm), 0.88 (4H, dm), 1.24 (4H, dm), 1.87 (4H, br s), 2.70 (2H, dm), 2.86 (4H, d), 7.7 – 8.1 (40H, m, PPh_4^+)

bis(tetraphenylphosphonium)di(norbornanedithiolate)platinate(II) – $[Ph_4P]_2[Pt^{II}(ndt)_2]$: Yield 1.06 g 67%.

4.4 Results and Discussion

4.4.1 Synthesis of the Ligand and the Metal-Complexes

The trithiolan preparation was prepared according to a modified literature procedure as developed by Dr. Fox in the laboratory of Prof. Koch at Stony Brook University (Scheme 4.1).[29-33] It is widely accepted that the mechanism of this reaction involves generation of sulfur based radical species by the DMF/NH_3 combination. The radical species thus generated react with the desired alkene present to form the trithiolans. The reduction of the trithiolans to dithiols was accomplished using a strong reducing agent such as $LiAlH_4$ in THF under refluxing condition (Scheme 4.1). Reports say that norbornane trithiolan could not be reduced using $LiAlH_4$ in THF, but in this laboratory that method worked perfectly.[34]

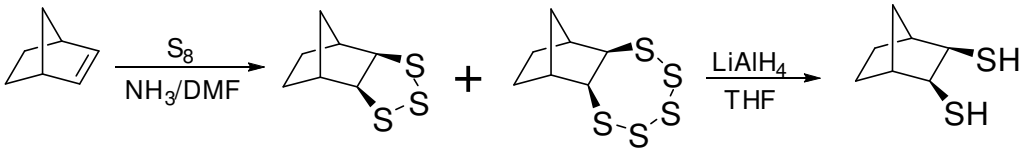

Scheme 4.1: Synthesis of the Norbornane Dithiol (H_2ndt) Ligand

Synthesis of the metal complexes was straightforward (Scheme 4.2). The dithiol was lithiated and subsequently, reacted with the divalent metal ions in aqueous medium.[23,24,26-28,35-39] The elimination of the use of toxic organic solvents and instead using water is indeed a positive step towards mimicking biological systems. These compounds are extremely air-sensitive. The water must be thoroughly flushed with dry nitrogen prior to reaction. With tetraphenylphosphonium cations, the compounds can be structurally characterized.

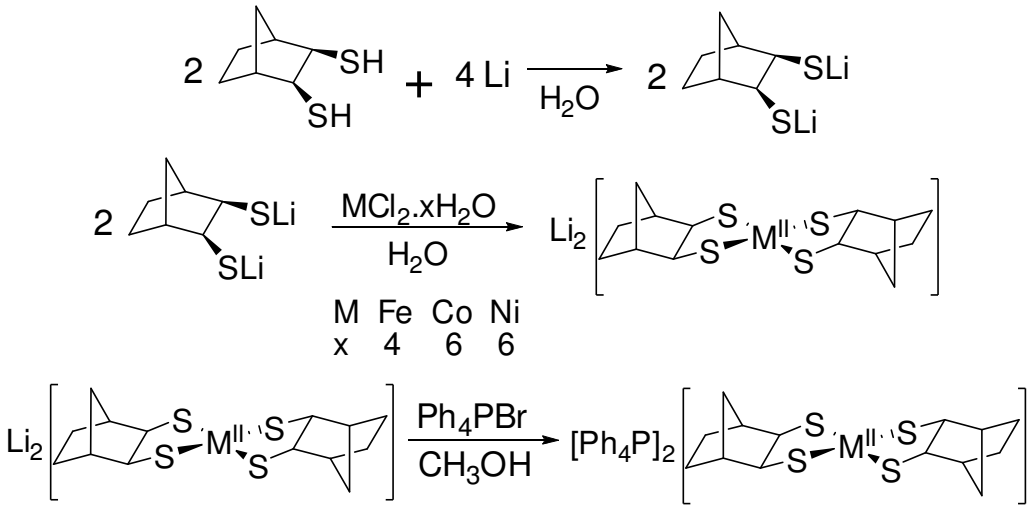

Scheme 4.2: Synthesis of the Metal-Complexes

For Fe and Co metals, the molar ratios of the the metal to ligand determines the structural variations observed. For Ni polymeric compounds of the type $[Ni(SR)_2]_\infty$ are formed. The cluster formation increases in the presence of H^+ ions in solutions or dry/wet protic solvents.[23,25-27] The clusters or the polynuclear complexes have edge-sharing units. Comparing the metal thiolates of Ni-atom, the aromatic based thiolates form a distorted tetrahedral geometry, while the other thiolates generate a square-planar coordination sphere.[40,41]

The polynuclear complexes are primarily formed when the metal ligand ratios are 1:1 or 1:2 in alkaline protic solvents. The equilibrium of the reaction for conversion of the monomer to clusters lies completely to the right (Figure 4.7**).** The reaction follows a first-order kinetics with mechanism as shown (Figure 4.7). The important feature to note is that the 'pyramidal geometry of the bridging sulfur atom and rotation about the newly formed Ni-S bond would diminish steric interference between the attacking fragment and the $[Ni(edt)_2]^{2-}$ group." Monomeric $[Ni(edt)_2]^{2-}$ was formed when the metal to ligand ratio was

1:10. The compound was found to be stable in solid state but polymerized rapidly in protic solvents and slowly in aprotic solvents.

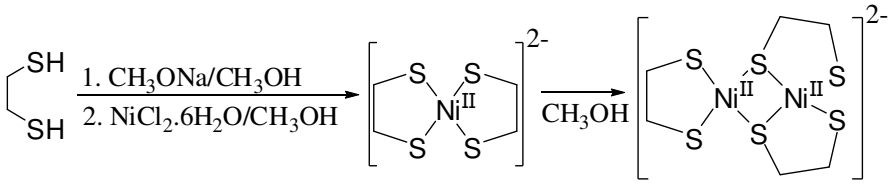

Figure 4.7: Mechanism of Formation of $[Ni_2(edt)_3]^{2-}$

For the $ndtH_2$ ligand, the cis conformation of the edt is locked in place by the norbornyl skeleton, which provides the steric bulk required to arrest the polymerization.

4.4.2 ^{1}H NMR Study of the Ligand and the Metal-Complexes

The assignment of the ^{1}H signals of the ligand is reported elsewhere (Figure 4.8).[42] For $ndtH_2$, the δ values of the different protons did not show much shift on varying the solvent (Table 4.3).

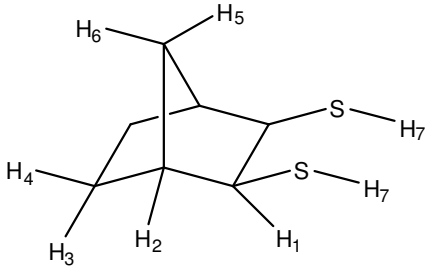

Figure 4.8: Numbering Scheme for $ndtH_2$ Ligand

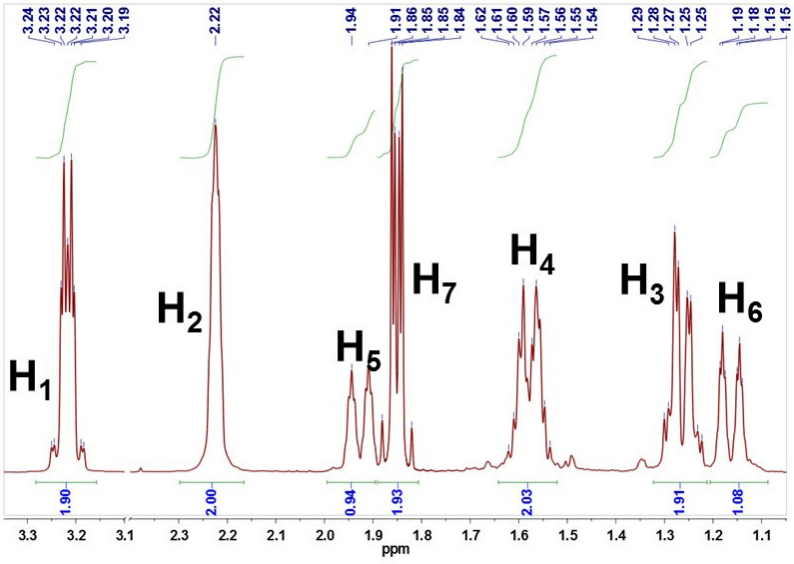

Figure 4.9: ^{1}H NMR of $ndtH_2$ in $CDCl_3$

Table 4.3: δ Values for ndtH_2 Ligand in Different Solvents[33]

Solvent	δ (ppm) (multiplicity)					
	H1	H2	H3	H4	H5	H6
$CDCl_3$	3.22 (m)	2.22 (m)	1.27 (m)	1.59 (m)	1.94 (dt)	1.18 (dt)
CH_3OH-d_4	3.25 (m)	2.19 (m)	1.30 (m)	1.58 (m)	1.95 (dt)	1.17 (dt)
DMSO-d_6	3.25 (m)	2.14 (m)	1.25 (m)	1.51 (m)	1.86 (dt)	1.10 (dt)

Of the metal complexes, $[Ni(ndt)_2]^{2-}$ gives a diamagnetic ^{1}H NMR spectrum (Figure 4.10). The presence of only as much signals of the free ligand *sans* H7 signal indicates that the two ndt moieties are related by a symmetry operation. This supports the fact that Ni^{2+} have a square planar geometry around it as expected with d^8 configuration. By ^{1}H NMR alone, it can't be said whether the ndt ligands are *anti* or *syn* to each other as in both the cases they are related by a symmetry operation; center of inversion in case of the former and mirror plane for the latter. ^{1}H NMR of $[Ni(ndt)_2]^{2-}$ in CH_3OH-d_4 shows six signals with peak ratio 4:2:4:4:4:2 (downfield → upfield).

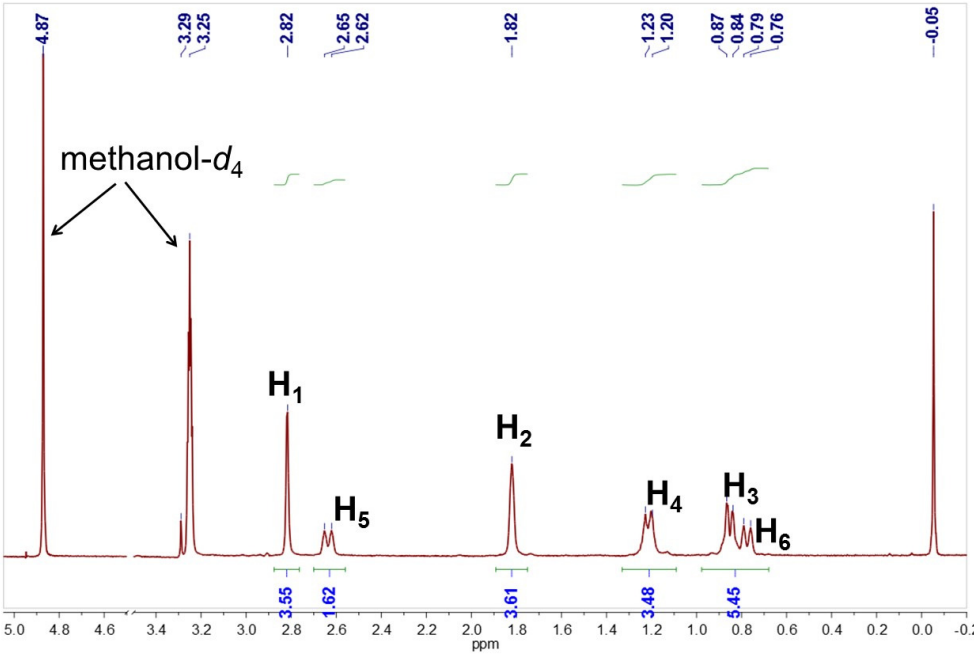

Figure 4.10: ^{1}H NMR of $[Ph_4P]_2[Ni(ndt)_2]$ in CD_3OD

4.4.3 Structural Characterization of the Metal-Complexes

The Fe^{II}-(S)4 unit of $[Ph_4P]_2[Fe^{II}(ndt)_2]\bullet(CH_3OH)_2(H_2O)_4$ (Figure 4.11) is rigorously square planar (Table 4.4). A center of inversion at the metal center requires the two ndt ligands to be in *anti* configuration. The molecule contains water and methanol as solvent of crystallization. These are bound to the S-center of ndt ligand by hydrogen bonding. A disorder in the solvent molecule arrangement has been observed. It is found that alternative unit cells have six water molecules and 4 water molecules alongside two methanol molecules.

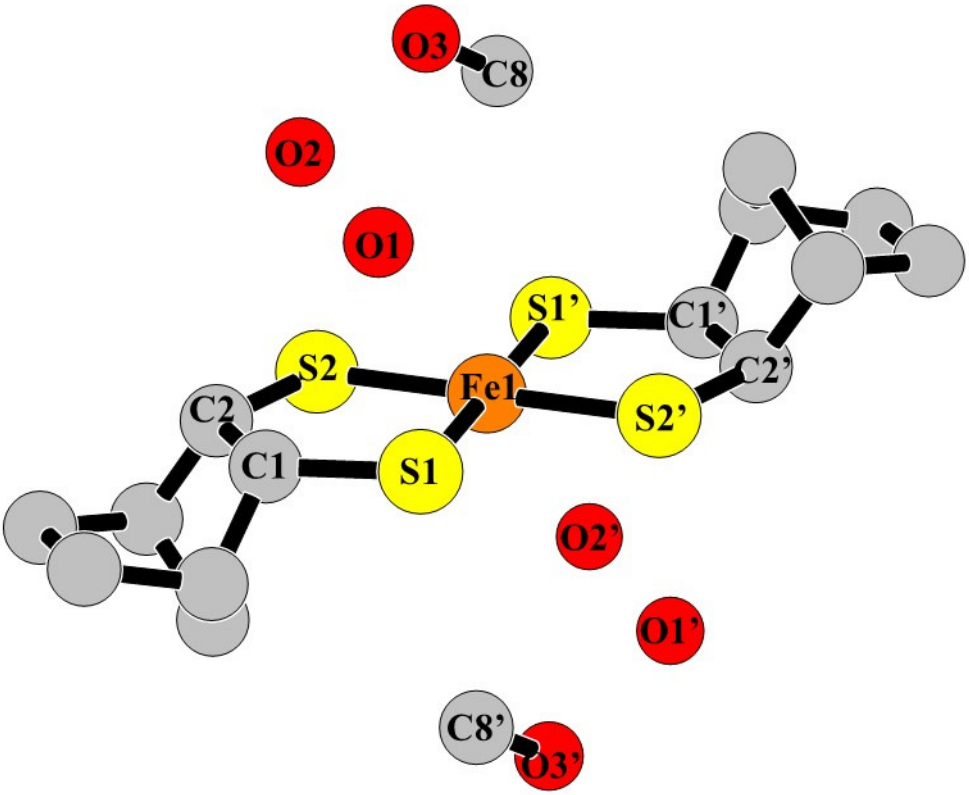

Figure 4.11: Fe^{II}-S4 unit of $[Ph_4P]_2[Fe^{II}(ndt)_2]\bullet2CH_3OH\bullet4H_2O$ [H-atoms omitted for clarity]

Table 4.4: Selected Crystallographic Data for $[Ph_4P]_2[Fe^{II}(ndt)_2]\bullet(CH_3OH)_2(H_2O)_4$

Bond Lengths (Å)		Bond Angles (°)
Fe(1) – S(1): 2.208(5)	S(1) – O(1): 3.290(1)	S(1) – Fe(1) – S(2): 90.03(9)
Fe(1) – S(2): 2.220(2)	S(2) – O(2): 3.290(3)	S(2) – Fe(1) – S(1'): 89.97(2)
Fe(1) – S(1'): 2.208(5)	C(1) – S(1): 1.835(7)	S(1') – Fe(1) – S(2'): 90.03(9)
Fe(1) – S(2'): 2.220(2)	C(2) – S(2): 1.845(7)	S(2') – Fe(1) – S(1): 89.97(2)

Other structurally similar compounds to this are $[Fe^{II}(o\text{-xylyl dithiol})]^{2-}$ and $[Fe^{III}_2(edt)_4]^{2-}$. A comparison of crystallographic features (Table 4.5) reveal that with edt the complex exhibits a dimeric structure but with the *o*-xylyl dithiol it has a monomeric structure. For $[Fe^{III}_2(edt)_4]^{2-}$, the Fe2S2 core is planar with Fe^{III} center having a trigonal bipyramid structure.[36] On the other hand, for $[Fe^{II}(o\text{-xylyl dithiol})]^{2-}$, the Fe^{II} center has a tetrahedral coordination environment.[43]

Table 4.5: Comparison of Selected Crystallographic Data of $[Fe^{II}(o\text{-xylyl dithiol})]^{2-}$, $[Fe^{II}_2(edt)_4]^{2-}$, & $[Fe^{II}(ndt)_2]^{2-}$

Parameter	$[Fe^{II}(o\text{-xylyl dithiol})]^{2-}$	$[Fe^{II}_2(edt)_4]^{2-}$	$[Fe^{II}(ndt)_2]^{2-}$
Fe – S(avg) (Å)	2.356	2.254	2.214
S – Fe – S' (avg)	104°	90° (equatorial) 99° & 142° (axial)	90°

The $[Ph_4P]_2[Ni^{II}(ndt)_2]$ and $[Ph_4P]_2[Pt^{II}(ndt)_2]$ compounds show a structural similarity akin to $[Ph_4P]_2[Fe^{II}(ndt)_2]$ (Figure 4.12). The M^{II} unit is at a crystallographically imposed center of inversion with the two norbornyl rings in an *anti* fashion. For the Ni^{II} compound, starting from a different geometry (tetrahedral as in $[Ni^{II}Cl_2Br_2]^{2-}$), a *syn* configuration of the two norbornyl rings can be achieved.[44] The structure has H_2O/CH_3OH molecules H-bonded to the S-atoms. The same solvent molecule disorder as observed for $[Ph_4P]_2[Fe^{II}(ndt)_2]$, is present here also (Figure 4.12).

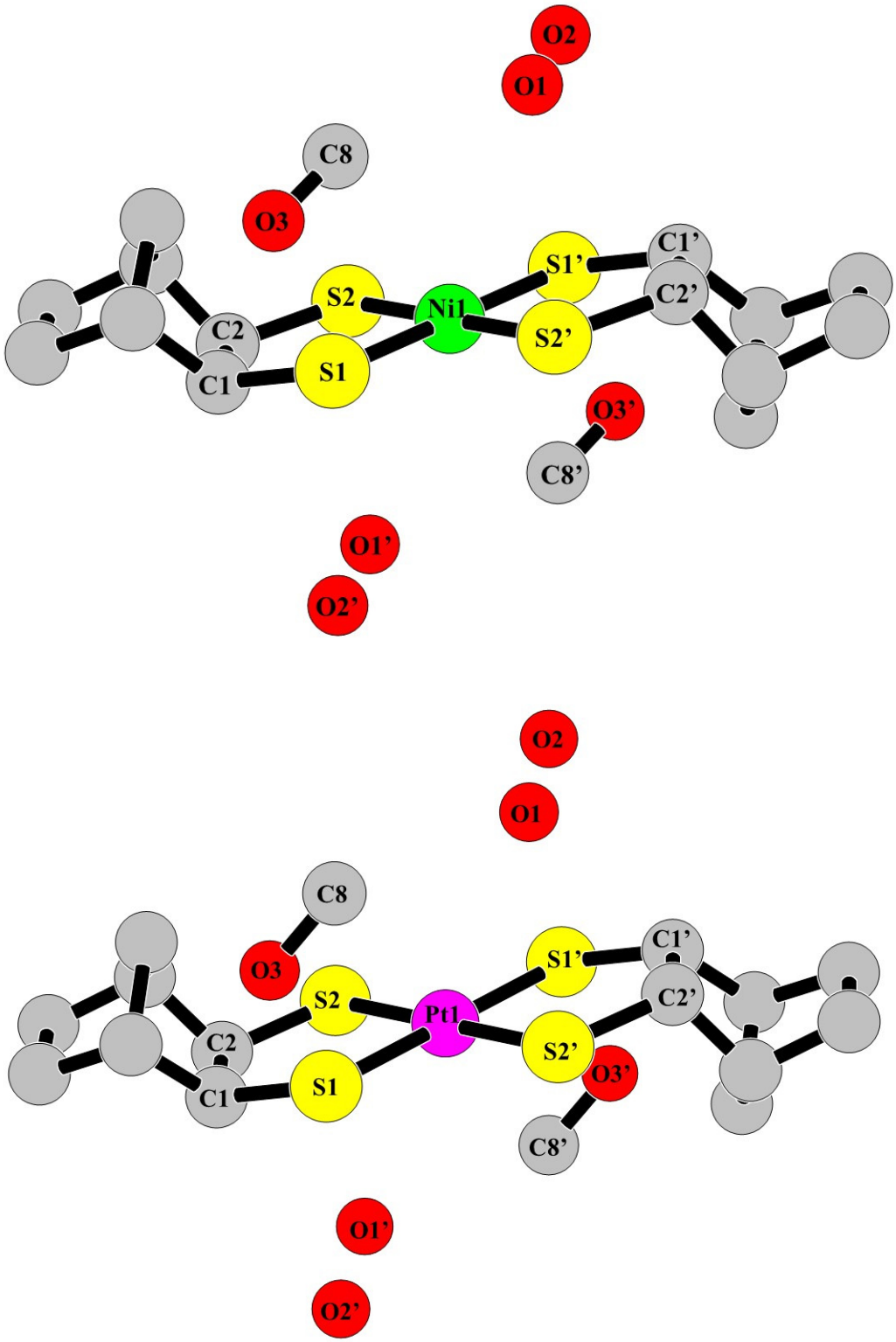

Figure 4.12: M^{II}-S4 unit of $[Ph_4P]_2[Ni^{II}(ndt)_2]\cdot 2CH_3OH\cdot 4H_2O$ (upper) & $[Ph_4P]_2[Pt^{II}(ndt)_2]\cdot 2CH_3OH\cdot 4H_2O$ (lower) [H-atoms omitted for clarity]

Comparing Ni^{II} & Pt^{II} compounds (Table 4.6), it can be seen that the bond angles (S-M^{II}-S') are very close to one another. The M^{II}-S bond distances are greater for the Pt^{II} compound, as expected. There is not much difference either with the H-bonding of the solvent molecules with the S-atoms of the norbornyl moiety. It can be safely concluded that the H-bonding is independent of the nature of the metal.

Table 4.6: Comparison of Selected Crystallographic Data of $[Ph_4P]_2[Ni^{II}(ndt)_2]\bullet(CH_3OH)_2(H_2O)_4$ & $[Ph_4P]_2[Pt^{II}(ndt)_2]\bullet(CH_3OH)_2(H_2O)_4$

Parameters		$[Ph_4P]_2[Ni^{II}(ndt)_2]$	$[Ph_4P]_2[Pt^{II}(ndt)_2]$
M^{II} – S(1)	Å	2.169(5)	2.292(3)
M^{II} – S(2)	Å	2.180(2)	2.297(7)
S(1') – O(1)	Å	4.726(8)	4.772(1)
S(1') – O(2)	Å	3.416(1)	3.320(4)
S(2') – O(1)	Å	3.249(3)	3.281(2)
S(2') – O(2)	Å	4.215(5)	4.172(6)
S(1') – O(3)	Å	5.447(6)	5.584(3)
S(2') – O(3)	Å	3.141(8)	3.079(6)
S(1) – S(2)	Å	3.110(1)	3.211(1)
S(1) – M^{II} – S(2')	o	91.31(5)	88.83(5)
S(2') – M^{II} – S(1')	o	88.19(2)	91.17(2)

Comparing other monomeric compounds of the type $[Ni^{II}(S\text{-}S)_2]^{2-}$, (Table 4.7)[23,24,39,44], it can be found that the Ni^{II}-S bond distances and S-Ni-S' bond angles of the $[Ph_4P]_2[Ni^{II}(ndt)_2]$ compound falls in the same range. The Ni^{II}-S4 unit is square planar in each case. H-bonding to the S-atom of the ligand by the solvent molecules (ranging from water to lower alcohols) is found for all the compounds.

Table 4.7: Comparison of Selected Crystallographic Data of Ni^{II}-S4 Unit

Parameters		anti-$[Ni^{II}(ndt)_2]^{2-}$	syn-$[Ni^{II}(ndt)_2]^{2-}$	$[Ni^{II}(edt)_2]^{2-}$		$[Ni^{II}(cdt)_2]^{2-}$
Ni^{II} – S(1)	Å	2.169	2.177	2.191	2.201	2.187
Ni^{II} – S(2)	Å	2.180	2.178	2.198	2.188	2.196
S(1) – Ni^{II} – S(2')	o	91.31	87.5	91.31	91.00	91.50
S(2') – Ni^{II} – S(1')	o	88.69	92.5	88.69	89.00	89.50

In contrast to the Fe^{II}, Ni^{II} and Pt^{II} counterparts, the Co^{II} compound exhibits a highly distorted tetrahedral (almost approaching D_{2d} symmetry) tetrathiolate environment (Figure 4.13). The Co^{II}-S bond distances are ~0.04 Å different from each other. The two Co^{II}-S bonds from one norbornyl entity are at almost right angle to each other, which is ~30° deviation from the ideal 120°. The bond angle between the two Co^{II}-S bonds from two different norbornyl entity are ~120°, which is ~10° deviation to the ideal tetrahedral bond angle of 109.5°. The structural feature that is similar with the aforesaid counterparts is the H-bonding of the solvent molecules (both H_2O and CH_3OH). The same sort of solvent disorder is also present.

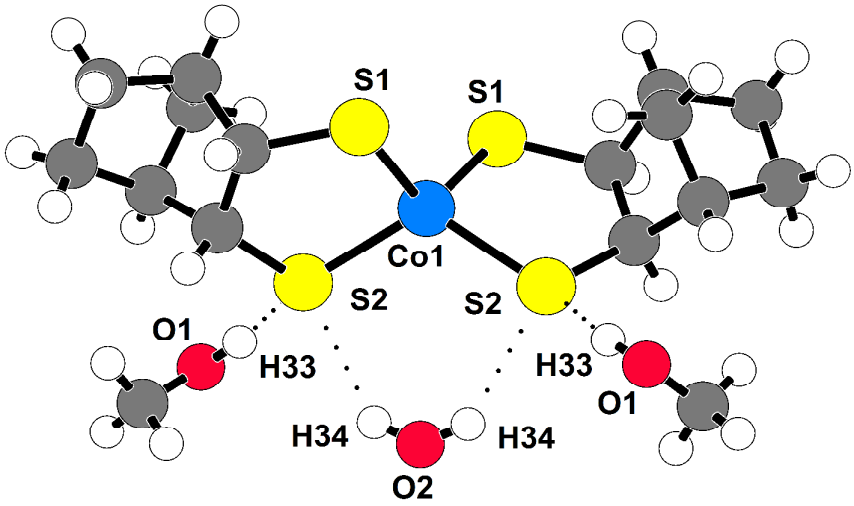

Figure 4.13: Co^{II}-S4 unit of $[Ph_4P]_2[Co^{II}(ndt)_2]\bullet 2CH_3OH\bullet H_2O$

Previously, another group member, Dr. Stephen Fox[33], has shown that this compound can generate idealized square planar geometry under the same reaction conditions akin to the Fe^{II}, Ni^{II} and Pt^{II} counterparts. Interestingly, Cotton and coworkers[jacs 1965, 87, 4189] have reported square planar $[Co^{II}(edt)_2]^{2-}$ complex, while Holm and cis oworkers reported the $[Co^{II/III}(edt)_2]^{2-/1-}$ complex as a mixed valence compound[45]. The $[Co^{II}(edt)_2]^{2-}$ unit is tetrahedral, while the $[Co^{III}(edt)_2]^{-}$ unit is square

planar. Comparing the tetrahedral $[Co^{II}(ndt)_2]^{2-}$ unit with the corresponding $[Co^{II}(edt)_2]^{2-}$ unit, it is seen that both the units approach D_{2d} symmetry. The Co^{II}-S bond distances and S-Co^{II}-S' bond angles are comparable (Table 4.8). Interestingly, Fox reports that the square planar $[Co^{III}(edt)_2]^{-}$ unit when reduced under elevated temperature condition generates a tetrahedral isomer of $[Co^{II}(edt)_2]^{2-}$ unit.

Table 4.8: Comparison of Selected Crystallographic Data of $[Co^{II}(ndt)_2]^{2-}$ & $[Co^{II}(edt)_2]^{2-}$

Parameters		$[Co^{II}(ndt)_2]^{2-}$	$[Co^{II}(edt)_2]^{2-}$
M^{II} – S(1)	Å	2.252(6)	2.287
M^{II} – S(2)	Å	2.292(2)	2.291
M^{II} – S(3)	Å	2.252(1)	2.279
M^{II} – S(4)	Å	2.292(5)	2.280
S(2) – M^{II} – S(1)	o	90.55(3)	90.75
S(1) – M^{II} – S(3)	o	114.58(2)	120.80
S(3) – M^{II} – S(4)	o	90.55(8)	91.83
S(4) – M^{II} – S(2)	o	115.82(9)	118.90

Table 4.9: Crystallographic Parameters for $[M(ndt)_2]^{2-}$ Complexes [M = Fe(II), Co(II), Ni(II), Pt(II)]

	$[PPh_4]_2$ $[Fe^{II}(ndt)_2]$	$[PPh_4]_2$ $[Co^{II}(ndt)_2]$	$[PPh_4]_2$ $[Ni^{II}(ndt)_2]$	$[PPh_4]_2$ $[Pt^{II}(ndt)_2]$
Empirical Formula	$C_{62}H_{60}FeP_2S_4$	$C_{62}H_{60}CoP_2S_4$	$C_{62}H_{60}NiP_2S_4$	$C_{62}H_{60}PtP_2S_4$
Formula Weight	1050	1051	1051	1119
Crystal System	triclinic	monoclinic	triclinic	triclinic
Space Group	*P*-1	*C*2/c	*P*-1	*P*-1
a (Å)	10.9834(4)	26.0011(8)	10.9849(6)	11.0106(3)
b (Å)	12.6473(5)	12.73061(16)	12.5902(9)	12.7899(4)
c (Å)	12.8919(4)	21.9104(6)	12.8609(12)	12.8788(4)
α (°)	115.595(4)	90	115.210(8)	115.755(3)
β (°)	96.531(3)	130.359(5)	96.755(6)	96.266(2)
γ (°)	108.622(3)	90	108.927(5)	108.639(3)
Z	1	4	1	1
Cell Volume ($Å^3$)	1462.66(9)	5526.4(2)	1452.68(18)	1481.01(8)
Crystal Color	red	green	red	red
Crystal Dimensions (mm)	0.3 x 0.3 x 0.2	0.4 x 0.3 x 0.2	0.3 x 0.2 x 0.2	0.5 x 0.3 x 0.2
Crystal Morphology	prism	prism	prism	prism
Calc. Density ($g\ cm^{-3}$)	1.19(3)	1.26(3)	1.20(2)	1.25(8)
F_{000}	619.9	2371.7	613.9	621.7
μ (mm^{-1})	0.507	0.565	0.581	0.594
R_{obs}	0.044(1)	0.033(0)	0.041(0)	0.0397(0)
Temperature (K)	100(1)	100(1)	100(1)	100(1)
θ range (°)	3.07 – 34.14	3.14 – 30.08	3.42 – 37.66	3.10 – 35.08
Radiation (Mo Kα)	0.71073	0.71073	0.71073	0.71073

4.4.4 Electron Absorption Spectra of Metal-ndt Complexes

For $[PPh_4]_2[Fe^{II}(ndt)_2]$ compound, the electron absorption spectra (Figure 4.14) shows that the species in solution maybe of Fe^{III} nature. Previously, Dr. Fox noted this instability[33] and Holm and coworkers demonstrated this solution chemistry behavior in detail with the edt analogue[25]. The electron absorption spectra in different solvents closely resemble that of the oxalyl dithiol and edt analogues of the Fe^{III} (Table 4.10).

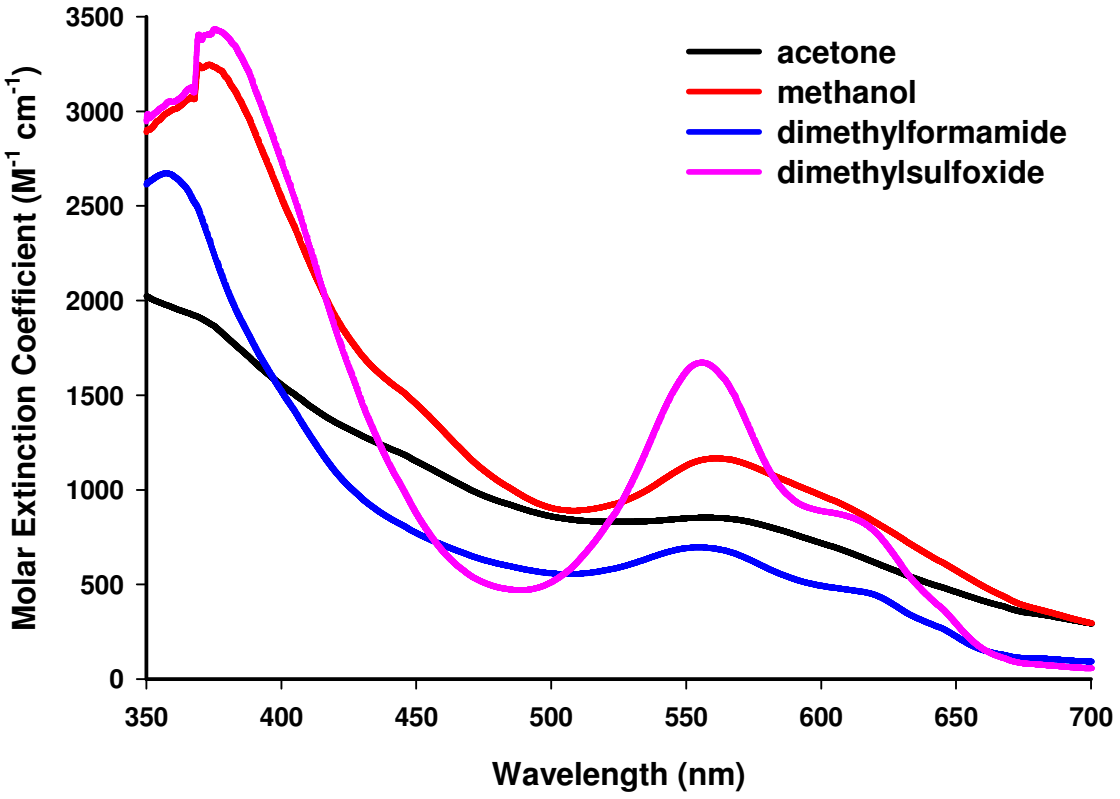

Figure 4.14: Electron Absorption Spectra of "$[Fe^{II}(ndt)_2]^{2-}$" Compound

Table 4.10: Comparison of Electron Absorption Features of $[Fe^{III}(o\text{-xylyl dithiol})]^{2-}$, $[Fe^{III}_2(edt)_4]^{2-}$ & "$[Fe^{II}(ndt)_2]^{2-}$" in DMF

Compound	λ_{max} (ε_M; M^{-1} cm^{-1})			
$[Fe^{II}(o\text{-xylyl dithiol})]^{2-}$	354 (8300)	~450 (sh)	486 (6420)	~640 (1600)
$[Fe^{III}_2(edt)_4]^{2-}$	363 (23,100)	535 (6170)	580 (sh)	
"$[Fe^{II}(ndt)_2]^{2-}$"	358 (2666)	555 (700)		616 (448)

Electron absorption spectra of both the $[Co^{II}(ndt)_2]^{2-}$ and $[Co^{III}(ndt)_2]^{-}$ species were reported by Dr. Fox[33]. The band position at the border of the UV and visible wavelength ranges (~400 nm) blue shifts from the Co^{II} to Co^{III} compound; the charge transfer band in the visible region red shifts from the Co^{II} to Co^{III} compound. In the present study, only the electron absorption spectrum of the $[Co^{III}(ndt)_2]^{-}$ species was observed (750 nm).

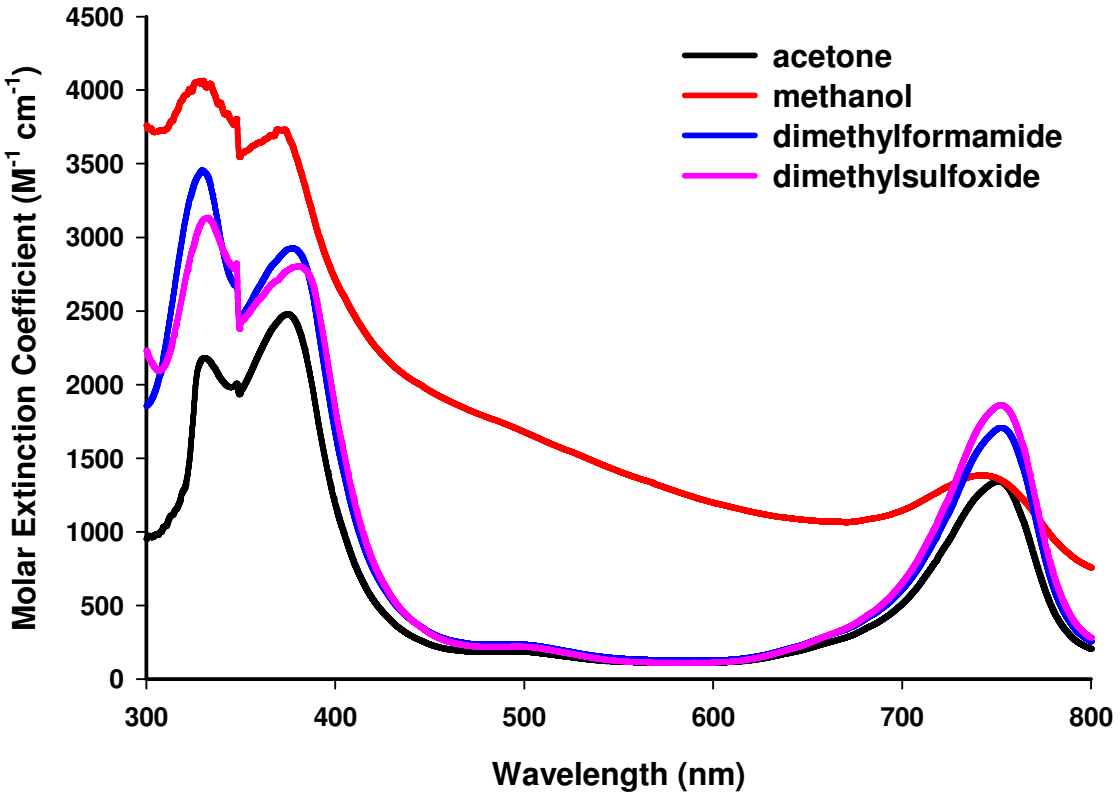

Figure 4.15: Electron Absorption Spectra of $[Co^{III}(ndt)_2]^-$ Compound

With the electron absorption spectra edt analogues being recorded in acetonitrile, no comparative study can be presented.

For the Ni^{II} compounds, the electron absorption spectra in various solvents (Figure 4.12) indicate that the $[Ni(ndt)_2]^{2-}$ compound may have been oxidized. With the electron absorption spectra edt analogues being recorded in other solvents, no comparative study can be presented. The characteristic peaks[28] of $[Ni(ndt)_2]^{2-}$ compound are conspicuous in their absence.

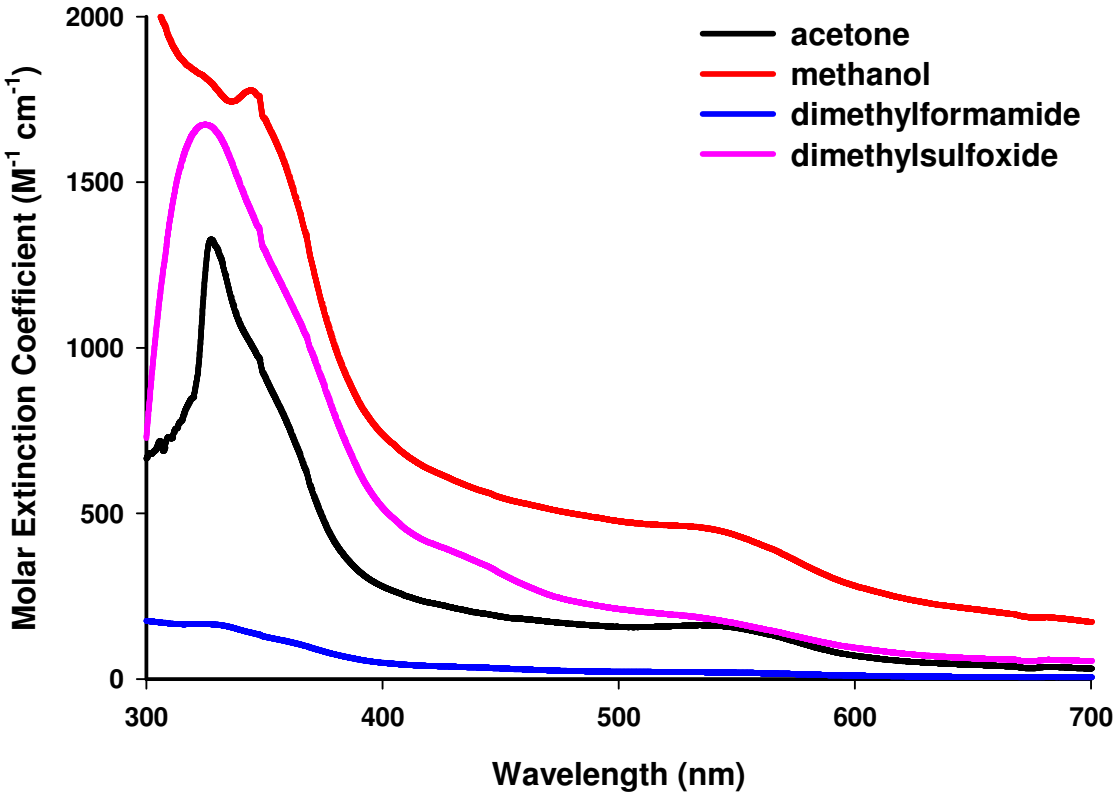

Figure 4.16: Electron Absorption Spectrum of "$[Ni^{II}(ndt)_2]^{2-}$" Compound

4.4.5 Electrochemical Study of Metal-ndt Complexes

Cyclic voltammetry study of the $[Ph_4P]_2[Ni^{II}(ndt)_2]$ compound shows two reversible waves (Figure 4.13). The peak at $E_{½}$ at -754 mV corresponds to $Ni^{2+/3+}$ redox couple, while the $E_{½}$ at -402 mV corresponds to $Ni^{+/2+}$ redox couple. The $E_{½}$ value for the $Ni^{2+/3+}$ redox couple falls in the range with other structurally similar compounds (Table 4.11).[23,24,27] The reversibility of the redox process indicates the viability as a biomimetic model.

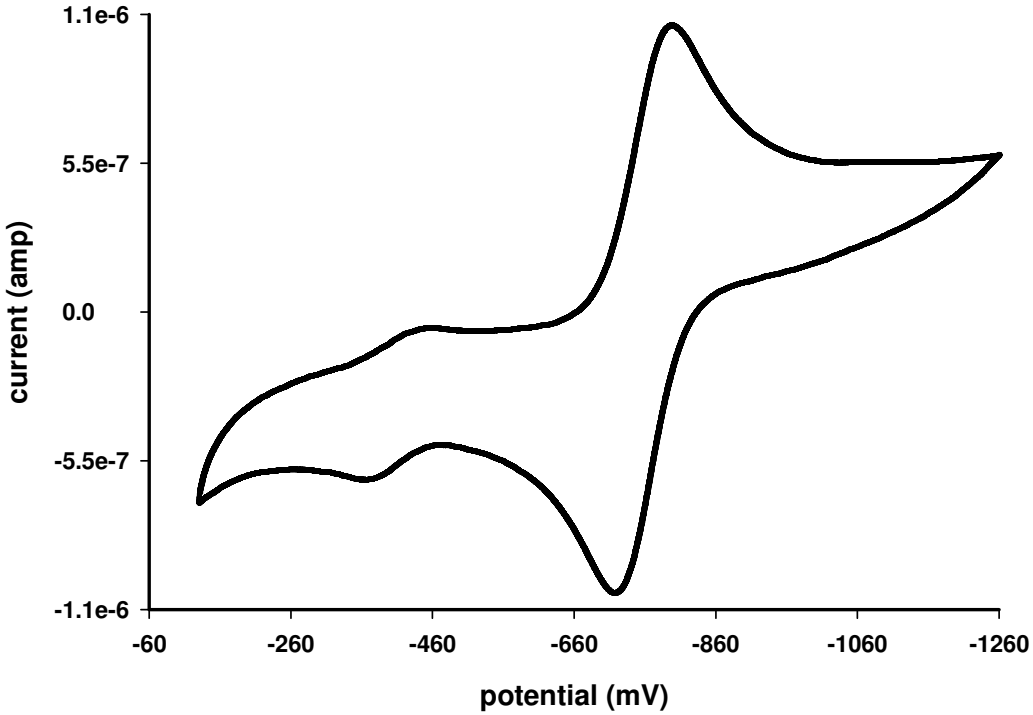

Figure 4.17: Cyclic Voltamogram of $[Ph_4P]_2[Ni^{II}(ndt)_2]$ in DMF

Table 4.11: Comparison of $E_{½}$ Values for the $Ni^{2+/3+}$ Redox Couple

Compound	$[Ni^{II}(edt)_2]^{2-}$	$[Ni^{II}(bdt)_2]^{2-}$	$[Ni^{II}(cdt)_2]^{2-}$	$[Ni^{II}(ndt)_2]^{2-}$
$E_{½}$ (mV)	-680	-750	-694	-754

4.5 Conclusions

A steric and robust alkane dithiol was synthesized. The corresponding dithiolate reacts with late transition metals (Fe, Co, Ni, Pt) to form metal thiolate coordination compounds with square planar and tetrahedral geometries.

Considering all the $[M^{II}(ndt)_2]^{2-}$ structures, the extensive H-bonding of the solvent molecules with the thiolate S-atoms have biomimetic modeling implication for the active site of some metalloenzymes. As delineated in the introduction, the first coordination sphere is heavily surrounded by water molecules being hydrogen bonded to the various residues of the polypeptide.

The Ni^{II} compound exhibited reversible electrochemical behavior. This is important because it shows that the model has potential to serve as biomimetic model to study catalytic cycles with suitable substrates.

4.6 References

(1) Holm, R. H.; Kennepohl, P.; Solomon, E. I. *Chem. Rev.* **1996**, *96*, 2239.

(2) Fontecilla-Camps, J. C.; Amara, P.; Cavazza, C.; Nicolet, Y.; Volbeda, A. *Nature* **2009**, *460*, 814.

(3) Ibers, J. A.; Holm, R. H. *Science* **1980**, *209*, 223.

(4) Krebs, B.; Henkel, G. *Angew. Chem. Int. Ed.* **1991**, *30*, 769.

(5) Kim, J.; Woo, D.; Rees, D. C. *Biochem.* **1993**, *32*, 7104.

(6) Burgess, B. K. *Chem. Rev.* **1990**, *90*, 1377.

(7) Burgess, B. K.; Lowe, D. J. *Chem. Rev.* **1996**, *96*, 2983.

(8) Lee, S. C.; Holm, R. H. *Chem. Rev.* **2004**, *104*, 1135.

(9) Evans, D. J. *Coord. Chem. Rev.* **2005**, *249*, 1582.

(10) Dobbek, H.; Svetlitchnyi, V.; Gremer, L.; Huber, R.; Meyer, O. *Science* **2001**, *293*, 1281.

(11) Kovacs, J. A. *Chem. Rev.* **2004**, *104*, 825.

(12) Miyanaga, A.; Fushinobu, S.; Ito, K.; Wakagi, T. *Biochem. Biophys. Res. Commun.* **2001**, *288*, 1169.

(13) Tsujimura, M.; Dohmae, N.; Odaka, M.; Chijimatsu, M.; Takio, K.; Yohda, M.; Hoshino, M.; Nagashima, S.; Endo, I. *J. Biol. Chem.* **1997**, *272*, 29454.

(14) Endo, I.; Nojiri, M.; Tsujimura, M.; Nakasako, M.; Nagashima, S.; Yohda, M.; Odaka, M. *J. Inorg. Biochem.* **2001**, *83*, 247.

(15) Schlapfer, C. W.; Nakamoto, K. *Inorg. Chem.* **1975**, *14*, 1338.

(16) Lalitha, S.; Chandramouli, G. V. R.; Manoharan, P. T. *Inorg. Chem.* **1988**, *27*, 1492.

(17) Mrkvova, K.; Kamanicek, J.; Sindelar, Z.; Kvitek, L.; Mrozinski, J.; Nahorska, M.; Zak, Z. *Trans. Met. Chem.* **2004**, *29*, 238.

(18) Ray, K.; Begum, A.; Weyhermuller, T.; Piligkos, S.; von Slageren, J.; Neese, F.; Wieghardt, K. *J. Am. Chem. Soc.* **2005**, *127*, 4403.

(19) Cerdeira, A. C.; Simao, D.; Santos, I. C.; Machado, A.; Pereira, L. C. J.; Warenborgh, J. C.; Henriques, R. T.; Almeida, M. *Inorg. Chim. Acta.* **2008**, *361*, 3836.

(20) Coucouvanis, D.; Paital, A. R.; Zhang, Q.; Lehnert, N.; Ahlrichs, R.; Fink, K.; Fenske, D.; Powell, A. K.; Lan, Y. *Inorg. Chem.* **2009**, *48*, 8830.

(21) Benedito, F. L.; Petrenko, T.; Bill, E.; Weyhermuller, T.; Wieghardt, K. *Inorg. Chem.* **2009**, *48*, 10913.

(22) Leussing, D. L.; Alberts, G. S. *J. Am. Chem. Soc.* **1960**, *82*, 4458.

(23) Baidya, N.; Mascharak, P. K.; Stephan, D. W.; Campagna, C. F. *Inorg. Chim. Acta.* **1990**, *177*, 233.

(24) Yamamura, T.; Arai, H.; Kurihara, H.; Kuroda, R. *Chem. Lett.* **1990**, 1975.

(25) Mukherjee, R. N.; Rao, C. P.; Holm, R. H. *Inorg. Chem.* **1986**, *25*, 2979.

(26) Rao, C. P.; Dorfman, J. R.; Holm, R. H. *Inorg. Chem.* **1986**, *25*, 428.

(27) Snyder, B. S.; Rao, C. P.; Holm, R. H. *Aust. J. Chem.* **1986**, *39*, 963.

(28) Fox, S.; Wang, Y.; Silver, A.; Millar, M. *J. Am. Chem. Soc.* **1990**, *112*, 3218.

(29) Shields, T. C.; Kurtz, A. N. *J. Am. Chem. Soc.* **1969**, *91*, 5415.

(30) Bartlett, P. D.; Ghosh, T. *J. Org. Chem.* **1987**, *52*, 4937.

(31) Hou, Y.; Abu-Yousef, I. A.; Harpp, D. N. *Tet. Lett.* **2000**, *41*, 7809.

(32) Ishii, A.; Suzuki, M.; Yamashita, R. *Tetrahedron* **2006**, *62*, 5441.

(33) Fox, S., Stony Brook University, 1990.

(34) Poulain, S.; Julien, S.; Dunach, E. *Tet. Lett.* **2005**, *46*, 7077.

(35) Cotton, F. A.; Weaver, D. L. *J. Am. Chem. Soc.* **1965**, *87*, 4189.

(36) Snow, M. R.; Ibers, J. A. *Inorg. Chem.* **1973**, *12*, 249.

(37) Herskovitz, T.; DePamphilis, B. V.; Gillum, W. O.; Holm, R. H. *Inorg. Chem.* **1975**, *14*, 1426.

(38) Rosenfield, S. G.; Armstrong, W. H.; Mascharak, P. K. *Inorg. Chem.* **1986**, *25*, 3014.

(39) Yamamura, T.; Kurihara, H.; Nakamura, N.; Kuroda, R.; Asakura, K. *Chem. Lett.* **1990**, 101.

(40) Tremel, W.; Krebs, B.; Henkel, G. *J. Chem. Soc. Chem. Commun.* **1986**, 1527.

(41) Tremel, W.; Kriege, M.; Krebs, B.; Henkel, G. *Inorg. Chem.* **1988**, *27*, 3886.

(42) Tatsumi, K.; Matsubara, I.; Inoue, Y.; Nakamura, A.; Miki, K.; Kasai, N. *J. Am. Chem. Soc.* **1989**, *111*, 7766.

(43) Lane, R. W.; Ibers, J. A.; Frankel, R. B.; Papaefthymiou, G. C.; Holm, R. H. *J. Am. Chem. Soc.* **1977**, *99*, 84.

(44) Kockerling, M.; Henkel, G. *Inorg. Chem. Commun.* **2000**, *3*, 117.

(45) Dorfman, J. R.; Rao, C. P.; Holm, R. H. *Inorg. Chem.* **1985**, *24*, 453.

Bibliography

Chapter 1

(1) Heinekey, D. M. *J. Organomet. Chem.* **2009**, *694*, 2671.

(2) Fontecilla-Camps, J. C.; Volveda, A.; Cavazza, C.; Nicolet, Y. *Chem. Rev.* **2007**, *107*, 4273.

(3) Vignais, P. M.; Billoud, B. *Chem. Rev.* **2007**, *107*, 4206.

(4) Shima, S.; Pilak, P.; Vogt, S.; Schick, M.; Stagni, M. S.; Meyer-Klaucke, W.; Warkentin, E.; Thauer, R. K.; Ermler, U. *Science* **2008**, *321*, 572.

(5) Frey, M. *ChemBioChem* **2002**, *3*, 153.

(6) Kubas, G. J. *Chem. Rev.* **2007**, *107*, 4152.

(7) Thauer, R. K. *Microbiol.* **1998**, *144*, 2377.

(8) Yoshida, K.-i.; Kimura, H. *Biochim. Biophys. Acta.* **1985**, *842*, 62.

(9) Darensbourg, M. Y.; Lyon, E. J.; Smee, J. J. *Coord. Chem. Rev.* **2000**, *206-207*, 533.

(10) Volveda, A.; Marie-Helenw, C.; Piras, C.; Hatchikian, E. C.; Frey, M.; Fontecilla-Camps, J. C. *Nature* **1995**, *373*, 580.

(11) Volveda, A.; Garcin, E.; Piras, C.; De Lacey, A. L.; Fernandez, V. M.; Hatchikian, E. C.; Frey, M.; Fontecilla-Camps, J. C. *J. Am. Chem. Soc.* **1996**, *118*, 12989.

(12) Ogata, H.; Hirota, H.; Nakahara, N.; Komori, K.; Shibata, S.; Kato, K.; Kano, K.; Higuchi, Y. *Structure* **2005**, *13*, 1635.

(13) Nicolet, Y.; Piras, C.; Legrand, P.; Hatchikian, E. C.; Fontecilla-Camps, J. C. *Structure* **1999**, *7*, 13.

(14) Osterloh, F.; Saak, W.; Haase, D.; Pohl, S. *Chem. Commun.* **1997**, 979.

(15) Osterloh, F.; Saak, W.; Pohl, S. *J. Am. Chem. Soc.* **1997**, *119*, 5648.

(16) Marr, A. C.; Spencer, D. J. E.; Schroder, M. *Coord. Chem. Rev.* **2001**, *219-221*, 1055.

(17) Verhagen, J. A. W.; Lutz, M.; Spek, A. L.; Bouwman, E. *Eur. J. Inorg. Chem.* **2003**, 3968.

(18) Wang, Q.; Barclay, J. E.; Blake, A. J.; Davies, E. S.; Evans, D. J.; Marr, A. C.; McInnes, E. J. L.; McMaster, J.; Wilson, C.; Schroder, M. *Chem. Eur. J.* **2004**, *10*, 3384.

(19) Bouwman, E.; Reedijk, J. *Coord. Chem. Rev.* **2005**, *249*, 1555.

(20) Tard, C.; Pickett, C. J. *Chem. Rev.* **2009**, *109*, 2245.

(21) Lai, C.-H.; Reibenspies, J. H.; Darensbourg, M. Y. *Angew. Chem. Int. Ed.* **1996**, *35*, 2390.

(22) Zhu, W.; Marr, A. C.; Wang, Q.; Neese, F.; Spencer, D. J. E.; Blake, A. J.; Cooke, P. A.; Wilson, C.; Schroder, M. *Proc. Natl. Acad. Sci.* **2005**, *102*, 18280.

(23) Li, Z.; Ohki, Y.; Tatsumi, K. *J. Am. Chem. Soc.* **2005**, *127*, 8950.

(24) Jiang, J.; Maruani, M.; Solaimanzadeh, J.; Lo, W.; Koch, S. A.; Millar, M. M. *Inorg. Chem.* **2009**, *48*, 6359.

(25) Buter, J.; Kellogg, R. M. *Org. Synth. Coll.* **1993**, *8*, 150.

(26) de Lacey, A. L.; Hatchikian, E. C.; Volveda, A.; Frey, M.; Fontecilla-Camps, J. C.; Fernandez, V. M. *J. Am. Chem. Soc.* **1997**, *119*, 7181.

(27) Smee, J. J.; Miller, M. L.; Grapperhaus, C. A.; Reibenspies, J. H.; Darensbourg, M. Y. *Inorg. Chem.* **2001**, *40*, 3601.

(28) Kruger, H. J.; Peng, G.; Holm, R. H. *Inorg. Chem.* **1991**, *30*, 734.

(29) Farrugia, L. J. *J. Appl. Cryst.* **2012**, *45*, 849.

(30) Hieber, W.; Wirsching, A. *Z. Annorg. Allgem. Chem.* **1940**, *245*, 35.

(31) Roundhill, D. M. *Inorg. Chem.* **1980**, *19*, 557.

(32) Herskovitz, T.; DePamphilis, B. V.; Gillum, W. O.; Holm, R. H. *Inorg. Chem.* **1975**, *14*, 1426.

(33) Mukherjee, R. N.; Rao, C. P.; Holm, R. H. *Inorg. Chem.* **1986**, *25*, 2979.

(34) Rao, C. P.; Dorfman, J. R.; Holm, R. H. *Inorg. Chem.* **1986**, *25*, 428.

(35) Snyder, B. S.; Rao, C. P.; Holm, R. H. *Aust. J. Chem.* **1986**, *39*, 963.

(36) Baidya, N.; Mascharak, P. K.; Stephan, D. W.; Campagna, C. F. *Inorg. Chim. Acta.* **1990**, *177*, 233.

(37) Jiang, J.; Acunzo, A.; Koch, S. A. *J. Am. Chem. Soc.* **2001**, *123*, 12109.

(38) Jiang, J.; Koch, S. A. *Angew. Chem. Int. Ed.* **2001**, *40*, 2629.

(39) Jiang, J.; Koch, S. A. *Inorg. Chem.* **2002**, *41*, 158.

(40) Nakamoto, K. *In Infrared and Raman Spectroscopy of Inorganic and Coordination Compounds*; John Wiley & Sons: New York, **1986**.

(41) Van Der Spek, T. M.; Arendsen, A. F.; Happe, R. P.; Yun, S.; Bagley, K. A.; Stufkens, D. J.; R.;, H. W.; Albracht, S. P. J. *Eur. J. Biochem.* **1996**, *237*, 629.

(42) Amarante, D., Stony Brook Unversity, **2011**.

Chapter 2

(1) Kiley, P. J.; Beinert, H. *Curr. Opin. Microbiol.* **2003**, *6*, 181.

(2) Lippard, S. J. *Acc. Chem. Res.* **1973**, *6*, 282.

(3) Watenpaugh, K. D.; Sieker, L. C.; Herriot, J. R.; Jensen, L. H. *Acta. Cryst. B.* **1973**, *B29*, 943.

(4) Sieker, L. C.; Stenkamp, R. E.; Jensen, L. H.; Prickril, B.; LeGall, J. *FEBS Lett.* **1986**, *208*, 73.

(5) Lane, R. W.; Ibers, J. A.; Frankel, R. B.; Papaefthymiou, G. C.; Holm, R. H. *J. Am. Chem. Soc.* **1977**, *99*, 84.

(6) Lane, R. W.; Ibers, J. A.; Frankel, R. B.; Holm, R. H. *Proc. Natl. Acad. Sci.* **1975**, *72*, 2868.

(7) Holah, D. G.; Coucouvanis, D. *J. Am. Chem. Soc.* **1975**, *97*, 6917.

(8) Swenson, D.; Baenzinger, N. C.; Coucouvanis, D. *J. Am. Chem. Soc.* **1978**, *100*, 1932.

(9) Millar, M.; Lee, J. F.; Koch, S. A.; Fikar, R. *Inorg. Chem.* **1982**, *21*, 4106.

(10) Millar, M.; Koch, S. A.; Fikar, R. *Inorg. Chim. Acta.* **1984**, *88*, L15.

(11) Silver, A.; Koch, S. A.; Millar, M. *Inorg. Chim. Acta.* **1993**, *205*, 9.

(12) Nguyen, T.; Panda, A.; Olmstead, M. M.; Richards, A. F.; Stender, M.; Brynda, M.; Power, P. P. *J. Am. Chem. Soc.* **2005**, *127*, 8545.

(13) MacDonnell, F. M.; Ruhlandt-Senge, K.; Ellison, J. J.; Holm, R. H.; Power, P. P. *Inorg. Chem.* **1995**, *34*, 1815.

(14) Rees, D. C.; Howard, J. B. *Science* **2003**, *300*, 929.

(15) McRee, D. E.; Richardson, D. C.; Richardson, J. S.; Siegel, L. M. *J. Biol. Chem.* **1986**, *261*, 10277.

(16) Moulis, J.-C.; Sieker, L. C.; Wilson, K. S.; Dauter, Z. *Prot. Sci.* **1996**, *5*, 1765.

(17) Strop, P.; Takahara, P. M.; Chiu, H.-J.; Angove, H. C.; Burgess, B. K.; Rees, D. C. *Biochem.* **2001**, *40*, 651.

(18) Rao, P. V.; Holm, R. H. *Chem. Rev.* **2004**, *104*, 527.

(19) Herskovitz, T.; Averill, B. A.; Holm, R. H.; Ibers, J. A.; Phillips, W. D.; Weiher, J. F. *Proc. Natl. Acad. Sci.* **1972**, *69*, 2437.

(20) Averill, B. A.; Herskovitz, T.; Holm, R. H.; Ibers, J. A. *J. Am. Chem. Soc.* **1973**, *95*, 3523.

(21) Bobrik, M. A.; Que Jr., L.; Holm, R. H. *J. Am. Chem. Soc.* **1974**, *96*, 285.

(22) Holm, R. H.; Phillips, W. D.; Averill, B. A.; Mayerle, J. J.; Herskovitz, T. *J. Am. Chem. Soc.* **1974**, *96*, 2109.

(23) DePamphilis, B. V.; Averill, B. A.; Herskovitz, T.; Que Jr., L.; Holm, R. H. *J. Am. Chem. Soc.* **1974**, *96*, 4159.

(24) Que Jr., L.; Bobrik, M. A.; Ibers, J. A.; Holm, R. H. *J. Am. Chem. Soc.* **1974**, *96*, 4168.

(25) Lawson Daku, L. M.; Pecaut, J.; Lenormand-Foucaut, A.; Vieux-Melchoir, B.; Ivenson, P.; Jordanov, J. *Inorg. Chem.* **2003**, *42*, 6824.

(26) Ueyama, N.; Yamada, Y.; Okamura, T.; Kimura, S.; Nakamura, A. *Inorg. Chem.* **1996**, *35*, 6473.

(27) Tanaka, K.; Tanaka, T.; Kawafune, I. *Inorg. Chem.* **1984**, *23*, 518.

(28) Ohno, R.; Ueyama, N.; Nakamura, A. *Chem. Lett.* **1989**, 399.

(29) Blonk, H. L.; Kievit, O.; Roth, E. K. H.; Jordanov, J.; van der Linden, J. G. M.; Steggerda, J. J. *Inorg. Chem.* **1991**, *30*, 3231.

(30) O'Sullivan, T.; Millar, M. M. *J. Am. Chem. Soc.* **1985**, *107*, 4096.

(31) Ohki, Y.; Tanifuji, K.; Yamada, N.; Imada, M.; Tajima, T.; Tatsumi, K. *Proc. Natl. Acad. Sci.* **2011**, *108*, 12635.

(32) Tanifuji, K.; Yamada, N.; Tajima, T.; Sasamori, T.; Tokitoh, N.; Matsuo, T.; Tamao, K.; Ohki, Y.; Tatsumi, K. *Inorg. Chem.* **2014**, *53*, 4000.

(33) Olmstead, M. M.; Power, P. P. *J. Organomet. Chem.* **1991**, *408*, 1.

(34) Ruhlandt-Senge, K.; Power, P. P. *Bull. Soc. Chim. Fr.* **1992**, *129*, 594.

(35) Ellison, J. J.; Power, P. P. *J. Organomet. Chem.* **1996**, *1996*, 263.

(36) Sigel, G. A.; Power, P. P. *Inorg. Chem.* **1987**, *26*, 2819.

(37) Schiemenz, B.; Power, P. P. *Organomet.* **1996**, *15*, 958.

(38) Corson, B. B.; Ipatieff, V. N. *J. Am. Chem. Soc.* **1937**, *59*, 645.

(39) Pearson, D. E.; Frazer, M. G.; Frazer, V. S.; Washburn, L. C. *Synthesis* **1976**, *138*, 621.

(40) Reid, J. R.; Dufresne, R. F.; Richard, F.; Chapman, J. J. *Org. Synth. Coll.* **1997**, *74*, 217.

(41) Roger, M.; Barros, N.; Arliguie, T.; Thuery, P.; Maron, L.; Ephritikhine, M. *J. Am. Chem. Soc.* **2006**, *128*, 8790.

(42) Blower, P. J.; Dilworth, J. R.; Hutchinson, J.; Nicholson, T.; Zubieta, J. A. *J. Chem. Soc. Dalton Trans.* **1985**, 2639.

(43) Blower, P. J.; Dilworth, J. R.; Hutchinson, J.; Zubieta, J. A. *J. Chem. Soc. Dalton Trans.* **1985**, 1533.

(44) Koch, S. A.; Fikar, R.; Millar, M.; O'Sullivan, T. *Inorg. Chem.* **1984**, *23*, 122.

(45) Wong, G. B.; Bobrik, M. A.; Holm, R. H. *Inorg. Chem.* **1978**, *17*, 578.

(46) Mague, J. T.; Linhardt, L.; Fink, M. J. *Acta. Cryst. E.* **2008**, *E64*, o335.

(47) Kohler, E. P.; Blanchard Jr, L. W. *J. Am. Chem. Soc.* **1935**, *54*, 367.

(48) Bishop, P. T.; Dilworth, J. R.; Zubieta, J. A. *J. Chem. Soc. Dalton Trans.* **1985**, 257.

(49) Newman, M. S.; Karnes, H. A. *J. Org. Chem.* **1966**, *31*, 3980.

(50) Koch, S. A.; Maelia, L. E.; Millar, M. *J. Am. Chem. Soc.* **1983**, *105*, 5944.

(51) Hagen, K. S.; Holm, R. H. *Inorg. Chem.* **1984**, *23*, 418.

(52) Rosenfield, S. G.; Armstrong, W. H.; Mascharak, P. K. *Inorg. Chem.* **1986**, *25*, 3014.

(53) Ragsdale, S. W.; Ljungdahl, L. G. *J. Bacteriol.* **1984**, *157*, 1.

Chapter 3

(1) Johnson, L. K.; Killian, C. M.; Brookhart, M. *J. Am. Chem. Soc.* **1995**, *117*, 6414.

(2) Ittel, S. D.; Johnson, L. K.; Brookhart, M. *Chem. Rev.* **2000**, *100*, 1169.

(3) Schmid, M.; Eberhardt, R.; Klinga, M.; Leskela, M.; Rieger, B. *Organomet.* **2001**, *20*, 2321.

(4) Schmid, M.; Eberhardt, R.; Kukral, J.; Rieger, B. *Z. Naturforsch.* **2002**, *57b*, 1141.

(5) Gibson, V. C.; Tomov, A.; Wass, D. F.; White, A. P. J.; Williams, D. J. *J. Chem. Soc. Dalton Trans.* **2002**, 2261.

(6) Small, B. L.; Brookhart, M.; Bennett, A. M. A. *J. Am. Chem. Soc.* **1998**, *120*, 4049.

(7) Britsovek, G. J. P.; Bruce, M.; Gibson, V. C.; Kimberley, B. S.; Maddox, P. J.; Mastroianni, S.; McTavish, S. J.; Redshaw, C.; Solan, G. A.; Stromberg, S.; White, A. P. J.; Williams, D. J. *J. Am. Chem. Soc.* **1999**, *121*, 8728.

(8) Gibson, V. C.; Redshaw, C.; Solan, G. A. *Chem. Rev.* **2007**, *107*, 1745.

(9) Chen, J.; Huang, Y.; Li, Z.; Zhang, Z.; Wei, C.; Lan, T.; Zhang, W. *J. Mol. Cat. A: Chem.* **2006**, *259*, 133.

(10) Huang, J.; Chen, J.; Chi, L.; Wei, C.; Zhang, Z.; Li, Z.; Li, A.; Zhang, L. *J. Appl. Polym. Sci.* **2009**, *112*, 1486.

(11) Corson, B. B.; Ipatieff, V. N. *J. Am. Chem. Soc.* **1937**, *59*, 645.

(12) Powell, G.; Johnson, F. R. *Org. Synth. Coll.* **1943**, *2*, 449.

(13) Bartlett, P. D.; Roha, M.; Stiles, R. M. *J. Am. Chem. Soc.* **1954**, *76*, 2349.

(14) Clark, G. R.; Nielson, A. J.; Richard, C. E. F. *J. Chem. Soc. Dalton Trans.* **1996**, 4265.

(15) Grubert, L.; Jacobi, D.; Buck, K.; Abraham, W.; Mugge, C.; Krause, E. *Eur. J. Org. Chem.* **2001**, 3921.

(16) El-Ayaan, U.; Abdel-Aziz, A. A. *Eur. J. Med. Chem.* **2005**, *40*, 1214.

(17) Helldorfer, M.; Backhaus, J.; Milius, W.; Alt, H. G. *J. Mol. Cat. A: Chem.* **2003**, *193*, 59.

(18) Long, Z.; Wu, B.; Yang, P.; Li, G.; Liu, Y.; Yang, X.-J. *J. Organomet. Chem.* **2009**, *694*, 3793.

(19) Farrugia, L. J. *J. Appl. Cryst.* **2012**, *45*, 849.

(20) Heropoulos, G. A.; Georgakopoulos, S.; Steele, B. R. *Tet. Lett.* **2005**, *46*, 2469.

(21) Suzuki, H.; Manabe, H.; Inouye, M. *Chem. Lett.* **1985**, 1671.

(22) Osuka, A.; Shimizu, H.; Suzuki, H. *Chem. Lett.* **1983**, 1373.

(23) Yang, K.; Lachiotte, R. J.; Eisenberg, R. *Organomet.* **1997**, *16*, 5234.

(24) Kohler, E. P.; Blanchard Jr, L. W. *J. Am. Chem. Soc.* **1935**, *54*, 367.

(25) Rosa, V.; Carabiniero, S. A.; Aviles, T.; Gomes, P. T.; Welter, R.; Campos, J. M.; Ribiero, M. R. *J. Organomet. Chem.* **2008**, *693*, 769.

(26) Trotter, J. *Acta. Cryst.* **1959**, *12*, 605.

(27) De Ridder, D. J. A.; Schenk, H. *Acta. Cryst. C.* **1993**, *C49*, 1970.

(28) Pohl, E.; Herbst-Irmer, R.; Kohler, K.; Roesky, H. W.; Sheldrick, G. M. *Acta. Cryst. C.* **1993**, *C49*, 2141.

(29) Ugono, O.; Cowin, S.; Beatty, A. M. *Acta. Cryst. E.* **2010**, *E66*, 01777.

Chapter 4

(1) Holm, R. H.; Kennepohl, P.; Solomon, E. I. *Chem. Rev.* **1996**, *96*, 2239.

(2) Fontecilla-Camps, J. C.; Amara, P.; Cavazza, C.; Nicolet, Y.; Volbeda, A. *Nature* **2009**, *460*, 814.

(3) Ibers, J. A.; Holm, R. H. *Science* **1980**, *209*, 223.

(4) Krebs, B.; Henkel, G. *Angew. Chem. Int. Ed.* **1991**, *30*, 769.

(5) Kim, J.; Woo, D.; Rees, D. C. *Biochem.* **1993**, *32*, 7104.

(6) Burgess, B. K. *Chem. Rev.* **1990**, *90*, 1377.

(7) Burgess, B. K.; Lowe, D. J. *Chem. Rev.* **1996**, *96*, 2983.

(8) Lee, S. C.; Holm, R. H. *Chem. Rev.* **2004**, *104*, 1135.

(9) Evans, D. J. *Coord. Chem. Rev.* **2005**, *249*, 1582.

(10) Dobbek, H.; Svetlitchnyi, V.; Gremer, L.; Huber, R.; Meyer, O. *Science* **2001**, *293*, 1281.

(11) Kovacs, J. A. *Chem. Rev.* **2004**, *104*, 825.

(12) Miyanaga, A.; Fushinobu, S.; Ito, K.; Wakagi, T. *Biochem. Biophys. Res. Commun.* **2001**, *288*, 1169.

(13) Tsujimura, M.; Dohmae, N.; Odaka, M.; Chijimatsu, M.; Takio, K.; Yohda, M.; Hoshino, M.; Nagashima, S.; Endo, I. *J. Biol. Chem.* **1997**, *272*, 29454.

(14) Endo, I.; Nojiri, M.; Tsujimura, M.; Nakasako, M.; Nagashima, S.; Yohda, M.; Odaka, M. *J. Inorg. Biochem.* **2001**, *83*, 247.

(15) Schlapfer, C. W.; Nakamoto, K. *Inorg. Chem.* **1975**, *14*, 1338.

(16) Lalitha, S.; Chandramouli, G. V. R.; Manoharan, P. T. *Inorg. Chem.* **1988**, *27*, 1492.

(17) Mrkvova, K.; Kamanicek, J.; Sindelar, Z.; Kvitek, L.; Mrozinski, J.; Nahorska, M.; Zak, Z. *Trans. Met. Chem.* **2004**, *29*, 238.

(18) Ray, K.; Begum, A.; Weyhermuller, T.; Piligkos, S.; von Slageren, J.; Neese, F.; Wieghardt, K. *J. Am. Chem. Soc.* **2005**, *127*, 4403.

(19) Cerdeira, A. C.; Simao, D.; Santos, I. C.; Machado, A.; Pereira, L. C. J.; Warenborgh, J. C.; Henriques, R. T.; Almeida, M. *Inorg. Chim. Acta.* **2008**, *361*, 3836.

(20) Coucouvanis, D.; Paital, A. R.; Zhang, Q.; Lehnert, N.; Ahlrichs, R.; Fink, K.; Fenske, D.; Powell, A. K.; Lan, Y. *Inorg. Chem.* **2009**, *48*, 8830.

(21) Benedito, F. L.; Petrenko, T.; Bill, E.; Weyhermuller, T.; Wieghardt, K. *Inorg. Chem.* **2009**, *48*, 10913.

(22) Leussing, D. L.; Alberts, G. S. *J. Am. Chem. Soc.* **1960**, *82*, 4458.

(23) Baidya, N.; Mascharak, P. K.; Stephan, D. W.; Campagna, C. F. *Inorg. Chim. Acta.* **1990**, *177*, 233.

(24) Yamamura, T.; Arai, H.; Kurihara, H.; Kuroda, R. *Chem. Lett.* **1990**, 1975.

(25) Mukherjee, R. N.; Rao, C. P.; Holm, R. H. *Inorg. Chem.* **1986**, *25*, 2979.

(26) Rao, C. P.; Dorfman, J. R.; Holm, R. H. *Inorg. Chem.* **1986**, *25*, 428.

(27) Snyder, B. S.; Rao, C. P.; Holm, R. H. *Aust. J. Chem.* **1986**, *39*, 963.

(28) Fox, S.; Wang, Y.; Silver, A.; Millar, M. *J. Am. Chem. Soc.* **1990**, *112*, 3218.

(29) Shields, T. C.; Kurtz, A. N. *J. Am. Chem. Soc.* **1969**, *91*, 5415.

(30) Bartlett, P. D.; Ghosh, T. *J. Org. Chem.* **1987**, *52*, 4937.

(31) Hou, Y.; Abu-Yousef, I. A.; Harpp, D. N. *Tet. Lett.* **2000**, *41*, 7809.

(32) Ishii, A.; Suzuki, M.; Yamashita, R. *Tetrahedron* **2006**, *62*, 5441.

(33) Fox, S., Stony Brook University, 1990.

(34) Poulain, S.; Julien, S.; Dunach, E. *Tet. Lett.* **2005**, *46*, 7077.

(35) Cotton, F. A.; Weaver, D. L. *J. Am. Chem. Soc.* **1965**, *87*, 4189.

(36) Snow, M. R.; Ibers, J. A. *Inorg. Chem.* **1973**, *12*, 249.

(37) Herskovitz, T.; DePamphilis, B. V.; Gillum, W. O.; Holm, R. H. *Inorg. Chem.* **1975**, *14*, 1426.

(38) Rosenfield, S. G.; Armstrong, W. H.; Mascharak, P. K. *Inorg. Chem.* **1986**, *25*, 3014.

(39) Yamamura, T.; Kurihara, H.; Nakamura, N.; Kuroda, R.; Asakura, K. *Chem. Lett.* **1990**, 101.

(40) Tremel, W.; Krebs, B.; Henkel, G. *J. Chem. Soc. Chem. Commun.* **1986**, 1527.

(41) Tremel, W.; Kriege, M.; Krebs, B.; Henkel, G. *Inorg. Chem.* **1988**, *27*, 3886.

(42) Tatsumi, K.; Matsubara, I.; Inoue, Y.; Nakamura, A.; Miki, K.; Kasai, N. *J. Am. Chem. Soc.* **1989**, *111*, 7766.

(43) Lane, R. W.; Ibers, J. A.; Frankel, R. B.; Papaefthymiou, G. C.; Holm, R. H. *J. Am. Chem. Soc.* **1977**, *99*, 84.

(44) Kockerling, M.; Henkel, G. *Inorg. Chem. Commun.* **2000**, *3*, 117.

(45) Dorfman, J. R.; Rao, C. P.; Holm, R. H. *Inorg. Chem.* **1985**, *24*, 453.